

UNITED STATES DEPARTMENT OF THE INTERIOR
GEOLOGICAL SURVEY

SYNTHESIS REPORT: ENVIRONMENTAL GEOLOGY OF KODIAK SHELF, ALASKA

By

Monty A. Hampton

U.S. Geological Survey
345 Middlefield Road
Menlo Park, California 94025

U.S. Geological Survey
Open-File Report 82-59

This report is preliminary and
has not been reviewed for conformity with
U.S. Geological Survey editorial standards.
Any use of trade names is for descriptive
purposes only and does not imply endorsement
by the USGS.

INTRODUCTION

Environmental geologic studies of Kodiak Shelf, western Gulf of Alaska, have been conducted in support of the Federal government's outer continental shelf petroleum leasing program (Fig. 1). Geologic and geophysical data were gathered aboard the R/V Sea Souder on four cruises in 1976-1979, and aboard the R/V **S.P. Lee** and NOAA ship Discoverer in 1980. Seismic-reflection surveys were run along 8600 km of trackline using combinations of 30- to 160-kilojoule sparker, 800-joule boomer, and **3.5-** and 12-kilohertz high-resolution systems (Fig. 2), and limited side-scanning sonar and underwater photography and television work was done. Sediment samples were gathered at 203 stations (Fig. 3). High-resolution records were contracted in 1976 and 1977 by the U.S. Geological Survey over about 10,000 km of **trackline**.

The approach to this environmental analysis was through examination of the near-surface geology. Initial fieldwork was a reconnaissance to characterize the regional geology, to identify the types of problems existing on Kodiak Shelf, and generally to delineate areas where such problems occur. Succeeding efforts were more feature-specific, with attention focused on certain problem areas.

INSTRUMENTATION AND PROCEDURES

Navigation

The principal navigation system was a Magnavox integrated satellite-Loran C unit. Dead-reckoning positions were **computed** every two seconds, based on Loran C, the ship's single-axis speed log, and the gyro. The **dead-**reckoning positions were updated with satellite fixes.

Navigational data were automatically recorded on magnetic tape, displayed on a CRT, and typed out on a keyboard printer. Every 15-minutes the positions were plotted on a **1:500,000-scale** chart. For easy reference, a "shot-point" number was given to each 15-minute position on seismic profiling lines. In addition to routine plots, satellite fixes and course changes were plotted. Post-cruise corrections to navigation were made, making use of **satellite-**update information.

Seismic Profiling and Visual Format Systems

Sparker: Sparker data were recorded using a Teledyne system, typically at a power of 40 to 80 kilojoules. Seismic signals were received on a Teledyne **100-element**, single-channel hydrophore, and the record was printed on a Raytheon model 1900 Precision Recorder. Usually, sweep and firing rates were at 2 or 3 seconds. Several different settings were used, but filters generally were adjusted to receive signals between 50 and 200 hertz. Records were annotated at 15-minute intervals with shot-point number, time (Greenwich Mean Time, GMT), and water depth.

Uniboom: The Uniboom system used four EG&G model 234 power sources of 200 joules, each driving hull-mounted plates. The hydrophore was an EG&G model 265. Data were recorded on an EPC 4100 recorder. Sweep and firing rates were

typically at one-half second, and filter settings at about 500 to 1600 hertz. Annotations were made in the same manner as those on the sparker system.

High-resolution: A Raytheon TR-109 3.5-kilohertz seismic system, with a Raytheon 105 PTR transceiver and a **CESP-II correlator**, was used to gather high-resolution shallow-penetration seismic data, as well as bathymetry. The system operated with 12 hull-mounted transducers, and the data were recorded on an EPC 4100 recorder. Sweep and firing rates were at one-half second. Annotations were made in the same manner as those on the **uniboam** system.

Bathymetry: A Raytheon TR-73A transducer and a Raytheon 105 PTR transceiver 12-kilohertz system was used to gather bathymetric data, which were displayed on a digital readout and recorded on magnetic tape. Sweep and firing rates typically were at $\frac{1}{2}$ second, and annotations were made the same as for the other acoustic systems.

Record quality: Four factors that significantly affected quality of the seismic records were 1) the typically **coarse-grained** and hard nature of the unconsolidated surficial sediment, 2) the shallow water depth throughout most of the area, 3) acoustic vibrations from the vessel, and 4) rough seas.

Coarse-grained and hard sediment most severely effected the **Uniboam** and 3.5-kHz records, causing much of the outgoing energy from these high-frequency systems to be reflected directly from the sea bottom with only a minor amount penetrating through to **subbottom** reflectors. Some **Uniboam** records show subtle, irregular traces of **subbottom** reflectors, which can be traced and correlated only with difficulty. Many 3.5-kHz records **show** no sign of **subbottom** reflectors and can be used only as indicators of water depth.

The shallow water depth caused multiples to appear at small distances below the initial sea-bottom reflection, partially or totally obscuring signals from deeper reflectors.

Although these four factors each have a deleterious effect on record quality, it was found by varying ship speeds and filter settings that the nature of the bottom sediment was the main reason for the seismic systems to display "poor" **subbottom** acoustic reflections on the records. Depth of penetration and details in the record consequently varied with type of bottom and water depth. Except for certain parts, the records **allow** adequate **subbottom** interpretation of geology.

Side-scanning sonar: The side-scanning sonar units used were **EG&G** analog and digital models, normally operated at a 125-m scan range and towed above the bottom at 10% of the scale employed. High quality records were generally obtained. Most side-scan sonar surveys were run at a ship speed of 4 to **4- $\frac{1}{2}$ knots**. Normally the **Uniboam** and 3.5-kHz units were run simultaneously with side-scanning sonar for depth control and possible **subbottom** information.

Bottom television and bottom camera: A **Hydro** Products bottom television unit, underwater mercury lights, and a 70-mm camera were mounted in a large frame. Photographic exposures could be made by remote control by the TV-screen

observer. A **multiconductor** cable, leading to the camera and light, was taped at 5-In intervals to the winch cable.

Sampling Devices

Grab samplers: The normal Van Veen grab sampler proved to be too **light** for adequate sampling of the typically sandy-gravelly bottoms. Generally, successful attempts were **obtained** with a heavy modified grab sampler designed by Andy Soutar of Scripps Institution of Oceanography.

A four-legged frame housed two vertical rails along which the grab moves. The top covers could be opened completely for full access. The addition of weight up to **400** pounds on top **of the** grab provided sufficient force for the half-round sides to dig into coarse material during the closing operation. When rock fragments got caught between the jaws of the grab, incomplete closure resulted and part or all of the sample was lost. In general the results were good, and this instrument retrieved samples where other devices failed.

Gravity corer: The gravity corer consisted of a 1500-pound weight to which one to three 3-m, 7.6-cm ID steel core barrels were attached. A clear **polybutyrate** liner was inserted in the barrels, and the sediment was retained by a brass-fingered core catcher.

The cores were cut into 1.5-m sections, and **10-cm** long pieces were cut from the ends of some sections for hydrocarbon gas analysis. The remaining core was x-rayed and then split lengthwise into working and archive halves. From the working half, samples were taken for grain size and physical properties measurements. The archive half was described and photographed. Both sections were put into storage tubes that were capped, taped, **labelled**, and stored under refrigeration.

Sediment Analysis

Subsamples were taken from the upper few centimeters of each grab sample or core, and grain size and compositional measurements were made. **Subsamples** were wet-sieved into gravel (> 2 mm), sand (2 mm- 0.062 mm), and fine (< 0.062 m) fractions. The silt (0.062 mm- 0.004 mm) and clay (< 0.004 mm) fractions were measured from the fine fraction using the pipette **method**. Weight percentages of each fraction were calculated.

Splits of each size fraction were examined visually for compositional estimates. The gravel and sand fractions were **examined** directly **by** eye and with a binocular microscope. The fine fraction was analyzed by mounting grains on a microscope slide, using a mixture of water, glycerin, and malachite green as the mounting medium. Malachite green preferentially stains the clay minerals, facilitating compositional analysis of the fine fraction. The fine fraction was analyzed as a unit; the silt and clay fractions were not separated. The compositional data were tabulated as visual (volume) percentages for individual size classes, **but** recomputed to weight percents in calculating whole-sediment compositions. Textural and compositional data are given in Tables 1 and 2.

Hydrocarbon Gas Analysis

Gases were extracted from samples of sediment cores by a headspace method. Sediment samples were recovered by means of gravity, piston and **vibra-corers**. Each **sample** (~0.5L in volume) was placed in an 0.95L can having two septa-covered entry ports for removal of gas. The can was filled with distilled water that had been purged with helium to remove any dissolved gases. From the can a volume of 100 mL of water was removed, and the can was sealed with a double-friction seal top. The resulting 100 mL headspace was purged with helium through the septa. The can was shaken for ten minutes to extract the gases from the sediment into the helium-filled headspace. Gases recovered were mainly those dissolved in sediment pore water. The amount of pore water was estimated by measuring the weight loss upon drying of a sample taken adjacent to the one used for gas analysis. From the headspace about 5 mL of gas mixture was removed in a gas-tight syringe. Exactly one mL of gas mixture was injected into a gas chromatography equipped with both flame ionization and thermal conductivity detectors. The instrument was calibrated by means of standard mixtures of hydrocarbon gases and CO₂. Calculations of gas concentrations were made from peak height measurements on the resulting chromatograms. Partition coefficients were used to correct for differences in gas **solubilities**, and concentrations are reported as **microliters/liter** (Pi/l) or **nanoliters/liter** (nl/l) of interstitial water. Results obtained by this method are semiquantitative but can be compared because each sample was processed in the same manner.

TECTONIC, STRUCTURAL, AND STRATIGRAPHIC FRAMEWORK

Kodiak Shelf is located on the North America lithospheric plate near its boundary with the Pacific plate. The general tectonic setting is that of a normally convergent margin, as indicated by the presence of a Benioff zone, deep ocean trench, and volcanic arc. The environmental geology of Kodiak shelf is strongly influenced by this setting.

The convergent margin extends westward to the end of the Aleutian islands. But, adjacent to Kodiak Shelf to the northeast, from about Middleton Island to Cross Sound, the margin is obliquely convergent, and then to the east and southeast it becomes a transform **margin** (Fig. 4; see von Huene et al, 1979).

Kodiak Shelf is the outer portion of a forearc area, comprising three major structural basins (Fig. 5; see Fisher, 1979; Fisher and von Huene, 1980). The basins extend beneath the seafloor to a regional unconformity, 1 to 7 km deep. Strata above the unconformity are younger than middle or late Miocene age. A series of uplifts, commonly truncated by erosion, trends along the shelf break and forms the seaward boundaries of the basins.

Major transverse tectonic boundaries cross the shelf, extending from the northeast and southwest ends of the Kodiak islands (Fig. 5; see Fisher, et al., 1981). Several lines of evidence suggest that the **crustal** block between the two boundaries stands higher than the blocks on either side. The boundaries appear to involve mostly vertical displacement but there is no

indication of fault control. The ultimate geologic nature of the boundaries is unknown.

SEISMICITY

The aspects of seismicity that are important for geo-environmental assessment include spatial distribution of **hypocenters**, recurrence intervals of seismic **events**, and ground motion characteristics. These are imprecisely understood at the present time, but some general patterns are emerging from the historic record.

The Gulf of Alaska - Aleutian area is one of the most seismically active on earth, accounting for about 7 percent of the annual world-wide release of seismic energy. Most of this energy release is associated with great earthquakes (larger than magnitude 7.8). Since recording of large earthquakes began in 1902, at least 95 potentially destructive events ($M > 6$) have occurred in the vicinity of Kodiak Shelf. These earthquakes are a consequence of interaction between the North America and Pacific plates; in particular along the shallow portion of the Benioff zone that extends from the Aleutian Trench to beneath the Kodiak islands (Pulpan and Kienle, 1979).

Great earthquakes in the Gulf of Alaska - Aleutian area occur in a spatial-temporal series. Aftershock zones are non-overlapping and define segments of lithosphere that experience separate episodes of major seismic activity (Sykes, 1971). Certain segments that have recently been inactive are identified as seismic gaps, judged most likely for the next great earthquakes. Estimates of recurrence intervals within segments range from 800 years based on long-term geological evidence (Plafker and Rubin, 1967) to 30 years based on the historic record (Sykes, 1971). The Shumagin seismic gap, as proposed by Pulpan and Kienle (1979), may extend to within a few kilometers of the southwest boundary of Kodiak Shelf.

The last great earthquake within the **lithospheric** segment that includes Kodiak Shelf was the 1964 event of magnitude 8.5. The epicenter was in Prince William Sound, a few hundred kilometers to the northeast, but aftershocks covered the entire shelf. Seafloor uplift of 15 m occurred in the central Gulf of Alaska (Malloy and Merrill, 1972) and 7 m on Kodiak Shelf (von Huene et al., 1972).

The historic record shows a cluster of seismic events near the mouth of **Kiliuda** Trough and nearby on southern and middle Albatross Banks (Fig. 6). The southwestern boundary of this zone is about at the same location as one of the transverse tectonic segments described by Fisher et al. (1981, see Fig. 5) and also near the southwestern extent of aftershocks from the 1964 Alaska earthquake. Other **shallow** seismicity on the **shelf** is diffuse and shows no linear trends or alignment along known faults (Pulpan and Kienle, 1979).

SHALLOW STRUCTURES

Shallow folds and faults on Kodiak Shelf trend approximately $N45^{\circ} E$, parallel to the Aleutian Trench, except for a few local divergences (Fig. 7). Structures occur in zones, indicating areal variation in the intensity of related environmental concerns on the shelf.

Faults are discerned in high-resolution seismic profiles by offset of the seafloor, discontinuity of reflectors, **non-stratigraphic** divergences in dip, and occurrence of diffractions. Some faults merge with folds along strike.

A major fault zone extends along the southeast coast of Kodiak Island, both on and offshore (Capps, 1937; Moore, 1967; von Huene et al., 1972), and continues some 600 km to Montague Island in the eastern Gulf. Fault lengths range up to at least 60 km on Kodiak Shelf (Fig. 7), and perhaps up to 140 km (Thrasher, 1979). Faults in this zone are steep and have both **landward** and seaward dips.

A less extensive zone of faults, with associated large folds, occurs near the shelf break along southern and middle Albatross Banks. A similar structural style exists near the shelf break on **Portlock** Bank, close to the boundary of our areal coverage, but faults die out and folds become broad and subdued on the intervening area of northern Albatross Bank.

A transverse zone of folds trends across **Portlock** Bank. These folds are part of a series of structures that **may** form one of the transverse tectonic boundaries described by Fisher et al. (1981).

Several lines of evidence suggest that the major zones of shallow structures are actively forming and related to modern tectonism. Von Huene et al. (1972) compared bathymetric records before and after the 1964 Alaska earthquake and determined that up to 7 m of uplift occurred on middle Albatross Bank. Fault offset in 1964 was documented on and adjacent to Montague Island (**Malloy and Merrill**, 1972) at the northeast extent of the zone that trends along the coast of Kodiak Island. Only indirect evidence, such as sharp bathymetric expression of fault scarps and occurrence of aftershocks, suggests offset on Kodiak Shelf itself.

PHYSIOGRAPHY

The **physiography** of Kodiak Shelf consists of a series of flat **banks**, generally 50 to 100 m deep, cut by transverse troughs up to 200 m deep (Fig. 8). The main elements of the **physiography** have structural and/or erosional origin.

Bathymetric maps have been prepared by **Dunleavy** et al. (1980) and by Turner et al. (1979). These maps **show** low hills and shallow depressions on the banks, as well as closed depressions in the troughs.

Folds along the shelf break commonly have seafloor expression. They have produced a continuous sill across the mouth of Stevenson Trough, but it has been breached in two places, as can be seen on bathymetric **maps**. On the banks, the folds have been eroded to expose bedrock of **middle** or late Miocene

to **Quaternary** age (McClellan et al. , 1980).

The position **of** the shelf break along Kodiak Shelf is fundamentally controlled **by** structure and is highly variable in form and depth. The change in seafloor gradient that defines the shelf break typically occurs on the seaward flank **of** a shelf-edge **anticline**. The precise location of the break commonly is at the edge of a prograding body of sediment building seaward from the fold, with strata conformable to the seafloor (Fig. 9). The shape of the shelf break varies from sharp to broad. Young **anticlines** growing seaward of the main shelf break are forming a new break off **Kiliuda Trough** and southwest middle Albatross Bank, and off **Portlock Bank** (Fig. 10).

Other second-order physiographic features that have environmental significance are bedrock ridges, fault **scarps**, and sand waves. Ridges occur where steeply inclined bedrock crops out at the seafloor and has experienced differential erosion (Fig. 11). Maximum relief of these features is about 5 m.

Fields of large sand waves appear at three locations, in Stevenson Trough, on northern Albatross Bank, and between **Chirikof** and Trinity Islands (Fig. 12). Wave heights reach 15 inters, and wave lengths reach 300 meters. Smaller sandwaves, on the order of a meter high, have been noted on **side-scanning** sonar records but are not considered in this report.

Abrupt **scarps** are abundant in the zones of faults described previously, and occur locally in other places over the shelf. Maximum offset is about 10 m but varies significantly along the **length** of a fault.

The slope of the seafloor is **low** over **much** of Kodiak Shelf, being nearly flat on most parts of the banks, and rarely exceeding 5% on the flanks of troughs (Fig. 13). A notable exception is **Sitkinak Trough**, where gradients reach 20%. The upper continental slope is also relatively steep, with gradients of 10-40% being typical.

STRATIGRAPHY, FACIES, AND SURFICIAL SEDIMENT

Surficial unconsolidated sediment on Kodiak Shelf consists of various proportions of **terrigenous**, volcanic, and **biogenic** debris (**Gershanovich**, 1968; **Bouma** and Hampton, 1976; Hampton, 1981). A thickness map of unconsolidated sediment is shown in Figure 14. The map is of generalized nature because of wide **trackline** spacing and because the quality of seismic reflection records does not **allow** precise measurement of thickness in all places. (See Hampton and **Bouma**, 1978, for a discussion of methods used in constructing the map.) But, it is apparent that unconsolidated sediment forms a thin veneer over much of the shelf, typically less than 100 **ms** of acoustic penetration measured as two-way travel time. (Note that **1 ms** two-way travel time = 1 m thickness for acoustic velocity of 2000 m/sec.) Local closed basins have up to 200 **ms** of **fill**, and sediment thickness in Sitkinak Trough exceeds 400 **ms**.

Sedimentary bedrock crops out over broad areas of the shelf. It is well stratified and folded. Where covered with unconsolidated material, a marked structural discordance typically occurs, and it is the depth to this

unconformity that is given in Figure 14.

A variety of sediment types exists on the shelf (Tables 1 and 2). Distribution is related to physiography and also to stratigraphic units that have been defined on the basis of seismic stratigraphy (Fig. 15, Table 3; see Thrasher, 1979). **Surficial** sediment types have been defined and mapped by performing Q-mode factor analysis on textural and compositional data (Hampton, 1981). Twelve variables were used in the analysis. These particular variables seem to best represent the distinct elements of the seafloor sediment on Kodiak Shelf, as decided after extensive subjective examination of samples. Textural variables include gravel, sand, silt, and clay size fractions. Compositional variables include terrigenous minerals, volcanic ash, **whole** or broken **megafaunal** carbonate shells (all in the coarse fraction and **much** larger than 2 mm), crushed **megafaunal** shells (predominantly in the sand size fraction), fine carbonate (in the silt and clay size fraction), foraminifera shells, clay minerals, and siliceous **microfossil** shells.

Data for each variable were scaled on a range between zero and one. This normalization represents the relative percentage of each measurement in the range between the minimum and maximum values of that variable. Varimax loadings (proportional contributions of each factor to a given sample) were computed for five factors, which account for 97% of the cumulative variance of measurements (Table 4). The factors represent composites of all the original variables, and use of five factors is judged to give the optimum synthesis of the original data. **Communalities** (amount of the sums of squares of the normalized data accounted for by the five factors) of all but 9 samples are high (exceeds 0.80). Four of the samples (61,128,234,236) with **low communalities** represent a sediment type rich in foraminifera. When a **six-factor** model is used, the foraminifera variable dominates the sixth factor. Sample 502 is from the edge of **Shelikof** Strait and probably represents a different sedimentary environment. The remaining samples that have low **communalities** (D24, D25, D26, D38) show no obvious distinguishing features and may have experienced sampling or analytical errors.

Samples for which factor 1 has the highest factor loading are shown in Figure 16. Similar maps for the other factors are Figures 17-20. The technique used in preparing these maps was to show a totally blackened circle if the particular factor is clearly dominant in a sample. If other factors are present in significant amounts, arbitrarily defined as a factor loading at least one-half as large as the highest loading **value**, the relative proportions of these factors are scaled as unshaded areas of the circle.

Compositions of the five factors in terms of the relative importance of the twelve original variables are given in Table 5. The values in each column indicate only a relative ranking, and negative numbers simply designate a strong disassociation of a particular variable with a particular factor. Roughly, factor 1 represents coarse terrigenous material, factor 2 is **mud** with abundant clay minerals and significant volcanic ash, carbonate, and siliceous **microfossils**, factor 3 is sand-size volcanic ash, factor 4 is **terrigenous** sand, and factor 5 is **shelly** sand.

The coarse-grained deposits of factor 1 occur most commonly on the banks (Fig. 16) and are associated with seismic stratigraphic units interpreted as

glacial deposits by Thrasher (1979). The fine-grained material of factor 2, in contrast, occurs most commonly in troughs (Fig. 17), largely corresponding to Thrasher's Holocene soft sediment unit. Factor 2 identifies **winnowed** and redistributed debris from the adjacent banks. The ash-rich sediment composing factor 3 is scattered from Stevenson Trough to middle Albatross Bank (Fig. 18) and does not appear to correlate with any particular **physiographic** feature or seismic stratigraphic unit. Its present distribution apparently reflects the original distribution of ash from the 1912 **Katmai** explosion, as the greatest accumulation was in this general area (Wilcox, 1959). The well-sorted sand of factor 4 is widespread (except on middle Albatross Bank) (Fig. 19) and probably is derived from reworking of glacial material, as a basal transgressive sand and/or as a post-transgressive winnowing product. Large sandwaves are formed at places in this unit (Fig. 12) implying strong reworking and sorting. Factor 5 dominates at relatively few stations and is restricted between **Portlock** Bank and northern Albatross Bank (Fig. 20). This **shelly**, sandy material may represent nearshore, transgressive material. The reason for its restricted occurrence is unknown.

Volcanic ash, derived from the 1912 eruption of Katmai volcano on the Alaska Peninsula, is an important constituent of **surficial** sediment (Hampton et al., 1979a). The abundances of volcanic ash, relative to the total sand size and finer terrigenous material, are shown in Figure 21. In general, the ash distribution on the seafloor of Kodiak Shelf shows high concentrations in **Chiniak** Trough and in shallow depressions on the banks. Low concentrations exist on flat parts of the banks. The ash is a significant component of two sediment types, defined by factors 2 and 3. The ash associated with factor 2 tends to be fine grained (silt and clay size), whereas that of factor 3 tends to be coarser (sand size). Perhaps this segregation reflects original atmospheric distribution of ash following the eruption, because the coarser ash (factor 3) occurs where Wilcox (1959) infers the thickest accumulation of ash, and fine ash (factor 2) is most common where accumulation was less. But, the abundance of factor 2 debris in **Kiliuda** Trough also implies **post-depositional** winnowing of fine ash and redeposition in this quiet setting.

Clay minerals are present in small to moderate quantities in all **surficial** sediment types. Composition of the clays was analyzed by Hein et al. (1979), and two major sources were identified: the Copper River about 400 km away in the eastern Gulf of Alaska and local bedrock outcrops on Kodiak Shelf itself. Clay-mineral suites from these two sources are mixed over most of the shelf, but bedrock-derived clays are enriched around outcrops and in nearby shallow depressions on the banks. Microscopic analysis shows that some Katmai ash has been altered to clay, but most is surprisingly fresh.

Bedrock samples, taken as dart cores from areas of seafloor outcrop, are composed of semilithified to **lithified** siltstone and fine-grained sandstone. Grab samples of poorly sorted mixtures of terrigenous and **megafaunal** shell debris were obtained at some areas designated as bedrock outcrop on Figure 15. This implies a thin cover of unconsolidated material, especially in valleys between bedrock ridges (Fig. 11).

SAND WAVES

Three major sand wave fields exist on Kodiak Shelf: in Stevenson Trough, on northern Albatross Bank, and on southern Albatross Bank between Chirikof and the Trinity Islands (Fig. 12). In Stevenson Trough, the waves have heights up to 8 m and lengths up to 300 m (Fig. 22). They face seaward for the most part, except for the waves in the northern part of the field, which face **landward**. Wave crests are straight to slightly sinuous on side-scan monographs. On middle Albatross Bank, the waves are a maximum of 5 m high and face seaward.

The sand waves between Chirikof and the Trinity Islands are up to 15 m high and 300 m long (Fig. 22). Most are sharp-crested, symmetrical features, but landward and seaward-facing waves are present. These waves occur within an acoustically distinct sediment body, overlying bedrock and glacial deposits, that reaches a maximum thickness of about 40 m and pinches out abruptly landward and seaward of the sand waves.

GAS-CHARGED SEDIMENT

One to six sediment samples for gas analysis were taken at various depth intervals in cores from 32 stations in four general areas: 1) Sitkinak Trough, 2) Kiliuda Trough, 3) Chiniak Trough, 4) the continental slope and the Aleutian Trench (Fig. 23; Hampton and Kvenvolden, in press). Kiliuda Trough was examined in greatest detail. Sediment samples for gas analyses could not be collected from the banks adjacent to the troughs because the coarse sediment on the banks resisted coring by the gravity corers.

Gas concentrations are summarized in Table 6. For simplicity, a single value is reported for the concentration of gas at each station. These values were obtained by interpolation or extrapolation of the concentrations observed at various depths in each core and represent the best estimate of the gas concentrations at a one-meter **subbottom** datum. C_1 , C_2 , $C_2:1$, c_3 , and $C_3:1$ and CO_2 are present in almost all samples. higher molecular weight hydrocarbon gases, **isobutane** ($i-C_4$) and **n-butane** ($n-C_4$), were detected in some samples. C_1 and CO_2 are the most abundant gases present; the abundance of other hydrocarbon gases are orders of magnitude lower.

Highest concentrations of C_1 , as well as C_2 and C_3 , are generally found in Kiliuda Trough (Table 6). Variations in concentrations are large over small areas as indicated by the difference in abundance of gas at nearby stations; compare, for example, the concentrations at stations 440 and 442 (Fig. 23, Table 6). Lowest concentrations of C_1 are **generally found** associated with sediment from the continental slope and Aleutian Trench. With the exception of station 225, on the slope south of Middle Albatross Bank, all stations **show** methane concentrations **lower** than 90 pi/l and **usually** less than 20 pi/l (Table 6).

In this work, as in previous studies in the southern Bering Sea (Kvenvolden and Redden, 1980), the eastern Gulf of Alaska (Kvenvolden et al., 1977), Norton Sound (Kvenvolden et al., 1981), and the Aleutian Basin (Cooper et al., 1979), concentrations of c_1 generally increase with depth in the

sediment, whereas the other hydrocarbon gases show no definite trends with depth. The increasing gradient in C₁ concentrations with sediment depth is illustrated in Figure 24 for stations having the highest C₁ concentrations. At these stations, concentrations of C₁ increase sharply with depth and at the one-meter datum level approach or exceed 10³ pi/l*. C₁ concentrations increase with depth three or more orders of magnitude within the sampled interval and approach or reach concentrations that exceed the volatility of C₁ in water which is about 40 x 10³ µl/l at ambient conditions. For example at stations 344, C₁ concentrations increase from 10' to 10⁴ µl/l. Gaps due to gas expansion are visible in some of these cores. In each of the four areas sampled, at least one core has concentrations of C₁ that approach or exceed 500 pi/l at a sediment depth of one-meter. Five cores from Kiliuda Trough have C₁ concentrations that exceed this value (Table 6, Fig. 24). This observation shows that high abundances of C₁ are common on the Kodiak Shelf.

Quantities of hydrocarbon gases larger than C₁, that is, the C₂₊ hydrocarbons, are low; however, the distribution of the gases relative to C₁ is important in assessing whether the source of gas is thermogenic vs biogenic. In all cases here, the abundances of C₂₊ relative to C₁ are small and in the range of values generally expected for gases associated with C₁ that has been derived through dominantly biological processes (Bernard et al., 1976). If the hydrocarbon gases observed in these sediments had been derived mainly through thermogenic processes, the abundances of C₂₊ relative to C₁ would be expected to be much larger (Bernard et al., 1976). Even at stations 224, 225, and 356 where the concentrations of C₂₊ hydrocarbons are anomalously large (Table 6), the ratio of C₂₊ to C₁ are not sufficiently great to indicate the presence of significant amounts of thermogenically derived hydrocarbons.

Further evidence indicating that biological processes are likely responsible for the C₁, at least at stations 439 and 440 in Kiliuda Trough, comes from carbon isotopic abundance measurements (Table 7). δ¹³C₁ values range from -76.9 to -85.5 per mil. These carbon isotopic compositions are clearly in the range for C₁ derived from biological processes and unfractionated by thermal processes (Claypool et al., 1973). Likewise, the δ¹³C of CO₂ ranges from -14.3 to -23.4 per mil, and indicates that this CO₂ is likely generated by biological processes operating on organic matter in the sediments.

The sedimentary environment in the troughs seems very suitable for the production of biogenic gas. For example, the soft sediment fill is typically high in microfossil content (diatoms), indicating that organic-rich material, which could serve as a source for the microbial production of gas, collects in the troughs. In addition, modern sediment accumulation rates are likely to be relatively high, because material from broad areas of the banks is swept into the troughs by ocean currents and storm waves. These high rates of sedimentation would also promote the preservation of organic matter and subsequent generation of biogenic gas.

Although general areas of gas-rich sediment can be defined, the concentrations of gas within these areas are highly variable. Cores taken at small lateral separations (for example, cores 344 and 441; Fig. 23, Table 6)

contain gas ranging in concentration from normal to very high. Tests of a recently developed pressurized core barrel (Denk et al., 1981) show that gas concentrations can vary significantly over small vertical distances. Thus, gas-charging of sediment may be an abruptly variable.

ACOUSTIC ANOMALIES

Seismic reflection records from **uniboom** and minisparker systems show acoustic anomalies at several places on Kodiak Shelf (Fig. 25). Six anomaly types, all defined on the basis of an abrupt departure from normal in strength, continuity, or geometry of acoustic reflectors along a profile, have been observed and mapped on Kodiak Shelf (Figs. 26-31)-

1. Acoustic turbidity or impenetrability below a certain **subbottom** level (Fig. 26). A non-layered gray return is seen on the records within the anomalous zone, with reflectors outside the zone terminating abruptly against it. This type of anomaly occurs exclusively within soft sediment (unit **Qs** of Thrasher, 1979) of **Kiliuda** and **Chiniak** Troughs.

2. Jumpy reflectors, wherein the acoustic signal is discontinuous along certain horizons (Fig. 27). Commonly, where reflections are received from a certain level, lower reflections are attenuated or not recorded at all. Where reflections are not received from the upper level, lower reflections are strong. This alternation over short distances gives a "jumpy" appearance to the seismic signature. Jumpy reflectors occur both on the banks and in the troughs.

3. Stratigraphic intervals that are variably transparent to weakly reflective along their extent (Fig. 28). The interval is wavy and may be discordant with underlying or overlying stratigraphy. Top and bottom boundaries are **subparallel**. This anomaly type has been seen only in **Kiliuda** Trough.

4. Discontinuous sets of reflectors that are variable in the strength of their return (Fig. **29a,b**). Typically, the return alternates between sharp and distinct (normal signature) to murky or transparent intervals.

5. An undulatory to highly irregular basal reflector overlain by a stratigraphic interval with discontinuous reflectors (Fig. 30). The upper surface of the discontinuously reflective interval may cut across higher reflectors, and some reflectors in this interval may cut across **hills** in the basal reflector. The upper surface in some places reaches the seafloor. The basal reflector and the upper boundary to the discontinuous interval appear to be acoustic artifacts rather than real stratigraphy or a buried topographic surface. This anomaly type occurs only on the margin of southern Albatross Bank and **Kiliuda** Trough.

6. Steeply inclined secondary reflectors in otherwise horizontally stratified material, giving a fractured appearance to the stratigraphy (Fig. 31). This anomaly type only occurs on the margin of southern Albatross Bank and **Kiliuda** Trough.

All anomaly types except type 6 are somewhat gradational and cannot always be classified uniquely with certainty. Moreover, subtle deviations

from normal, undisturbed seismic signature occur commonly in the records, and it is a matter of judgment what to identify as a true acoustic anomaly. Only definite examples of acoustic anomalies are mapped in Figure 26.

Acoustic anomalies occur in three primary areas on Kodiak Shelf:
1) along the length of Chiniak Trough and nearby on northern Albatross Bank, 2) on middle Albatross Bank near Kiliuda Trough, and 3) within the recurved area of Kiliuda Trough and nearby on southern Albatross Bank. In the troughs, anomalies occur in soft Holocene sediment fill (e.g., station 440; Fig. 26), but more commonly in harder Pleistocene sediment such as that composing the slopes leading into the trough (Fig. 30). The anomaly occurring on middle Albatross Bank in the vicinity of a gas seep discussed later is in Pleistocene sediment whose depositional history is certainly related to glacial activity, but not enough detail is known to explain this local accumulation of gas. Perhaps this sediment is similar to the organic-rich pre-transgressional sediment believed to be a source of gas in Norton Sound (Kvenvolden et al. , 1981).

In Chinak Trough, the anomalies are mostly local occurrences of jumpy and discontinuous reflectors, with one zone of acoustic turbidity near the mouth of the trough. On middle Albatross Bank is a broad area of jumpy and discontinuous reflectors. The recurved area of Kiliuda Trough and nearby southern Albatross Bank shows a variety of anomaly types. The typical sequence is fractured appearance (type 6) on southern Albatross Bank, with undulatory reflector-discontinuous interval (type 5) on the sloping margin of Kiliuda Trough and extending some distance under the soft sediment fill, followed by an acoustically turbid zone (type 1) within the soft sediment fill in the deepest part of the trough, and followed by a transparent zone (type 3) on the northern slope of the trough.

An acoustic anomaly in the water column, probably representing gas seepage from the seafloor, was found in 12-kilohertz seismic reflection records at 57°01.1'N, 152°10.3'W on middle Albatross Bank (Fig. 32a). Attempts to retrieve sediment cores near the seep were unsuccessful because the sediment is stiff and coarse grained. This seep occurs at the top of a low hill, along the extension of a fault mapped by Thrasher (1979). Subseafloor acoustic anomalies in the form of jumpy reflectors (type 2) appear in the vicinity of the seep (Fig. 32b). This apparent gas seep is the only one that we have observed in our records, but others have been noted on the shelf (B. W. Turner, personal communication). The origin of gas in the seep, whether biogenic or thermogenic is uncertain.

The acoustically turbid type of anomaly (type 1) seen in seismic profiles of the soft sediment fill at and near station 440 (Fig. 26) and the jumpy reflectors in the sediment near the probable gas seep (Fig. 29) are similar to gas-associated anomalies reported elsewhere (Schubel, 1974; Nelson et al., 1978) and are explainable by the known acoustic behavior of sediment that contains bubble-phase gas (Hampton and Anderson, 1974; Holmes and Thor, 1979). Particularly characteristic is the weakness or lack of acoustic penetration through gassy layers. Indeed, gas-charged cores have been collected where of these types of acoustic anomalies occur on Kodiak Shelf, although correspondence between gas-charged cores and anomalies is not one-to-one.

The other acoustic anomaly types have not been reported elsewhere and are not readily explainable by acoustic theory. Acoustic energy readily penetrates deeply in these areas, but the fact that gas-charged sediment cores were recovered in some of these anomalies supports the hypothesis that they are caused by the presence of high gas concentrations in the sediment, although other origins cannot be totally discounted.

SEDIMENT SLIDES

Sediment slides in the area of Kodiak Shelf have been identified in seismic reflection profiles, and the distribution of slides is shown in Figure 33. The presence of slides is inferred with various degrees of confidence from several diagnostic features including abrupt **scarps**, acoustic indications of a **subbottom** slide surface, offset and rotated bodies of sediment, discontinuous or distorted bedding, and **hummocky** seafloor topography. These features appear in many combinations. In Figure 33, those occurrences showing convincing morphologic features of slides are designated by solid lines. Slide surfaces and **headwall** scarps are typically **visable**, as are slide masses delineated by offset and rotated bedding (e.g., Fig. 34). Occurrences identified by dashed lines in Figure 34 are areas of **hummocky** seafloor, commonly with distorted subbottom reflectors but no other features of slides (Fig. 35). Heights of the hummocks range from a few meters to several tens of meters. These occurrences are less certain indicators of slides, and some may be depositional or tectonic structures.

Indications of slides are rare on Kodiak Shelf, whereas they are abundant on the adjacent upper continental slope. The two possible slides identified on the shelf are in Stevenson Trough and appear as small hummocks on the seafloor. Self and Mahmood (1977) report slides on the flanks of unidentified troughs southwest of Kodiak Island and south of Sitkinak Island, but exact locations are not given. Steep slopes occur in this area (Fig. 13), but our records do not reveal slides.

Two kinds of slides have been described on the upper continental slope (Hampton and Bouma, 1977). Large slides cover areas exceeding 100 km² in some places and involve thicknesses of slumped material of a few hundred meters. Slide surfaces are curved, and these slides have the general appearance of large rotational slumps according to the classification scheme of Varnes (1978) (Fig. 34). Smaller slides cover small areas and typically **appear** on single profile lines. Thicknesses are on the order of a few tens of **meters**, and slide surfaces appear to be planar. These slides fit the general description of translational slides according to **Varnes'** terminology (Fig. 36).

The distribution of large slides is uneven along the upper continental slope. They are abundant off southern and middle Albatross Bank and off **Portlock** Bank but have not been found off northern Albatross Bank. (The slides identified off northern Albatross Bank in Figure 33 are small. **Small** slides occur in other areas, also). The occurrence of large slides shows a relation to structural and tectonic elements of the region. Near-surface folds and faults are actively **growing**, with **consequent** slope steepening, and the shelf-break arch is well **developed** (Fig. 37a,b). Recent epicenters are

concentrated near the large slides adjacent to southern and middle Albatross Banks (Fig. 6). In contrast, gentle folding, low seafloor inclinations, and a subdued shelf-break arch characterize the area where large slides are absent (Fig. 38). Recent epicenters are sparse.

A quantitative evaluation by Hampton et al. (1978) of two specific large slumps indicates that steep slopes, removal of lateral ground support by faulting, and earthquake accelerations are the most likely environmental forces to activate these failures. Magnitudes of these forces are probably less in the area off northern Albatross Bank, implying a variation of the intensity of tectonism along the shelf break. Future generation of large slumps can be expected on the upper continental slope in the areas of intense tectonism.

Small slides on the continental slope occur both in tectonically active and inactive areas. The slides noted off northern Albatross Bank are of that variety (Fig. 36). The planar slide surface and wide areal distribution suggests stratigraphic control (weak sediment layers). But, earthquakes may trigger these slides.

The scarcity of slides on Kodiak Shelf probably is accounted for by the presence of relatively strong sediment on sloping portions of the seafloor and the low seafloor slopes in general (Fig. 13). This is in strong contrast to the nearby northeastern Gulf of Alaska where large slumps occur on slopes less than 1° in fine-grained, underconsolidated sediment derived from coastal glaciers and the Copper River (Carlson and Molnia, 1977; Molnia et al., 1977). Analysis shows that in this area, low strength due to rapid sedimentation rates and consequent underconsolidation, earthquake acceleration, wave loading, and perhaps bubble-phase gas are the important environmental driving forces (Hampton et al., 1978). The weakest sediment on Kodiak Shelf (sediment type Qs, Fig. 15), which commonly shows evidence of gas-charging and is exposed to strong earthquake forces, is not prone to sliding. This sediment is present mainly on nearly flat seafloor, but is also stable in most relatively steep areas such as Sitkinak Trough. Other forms of sediment instability such as liquefaction and consolidation subsidence are possible in the soft sediment, but indications of these phenomena could be subtle and have not been detected.

SEDIMENTARY PROCESSES AND HISTORY

The sedimentary processes and history of Kodiak Shelf can be deduced from available data. The bedrock probably was eroded during Pleistocene time. The coarse-grained unconsolidated sediment that covers bedrock, to judge from sediment texture and the inferred regional history, was deposited by Pleistocene glacial processes (Karlstrom, 1964; University of Alaska, 1974). Thrasher (1979) has delineated glacial ground-, lateral-, and end-moraine deposits.

The glacial deposits were reworked during the Holocene transgression. As evidence, some seismic records show probable glacial deposits, with an irregular upper surface that has been partially planed off at the present

seafloor, to have low areas filled with acoustically more transparent material that is horizontally stratified. **Along** trough margins these strata become inclined toward the trough axes (Fig. 39). This situation implies that glacial deposits have been redistributed, with **infilling** of low areas and construction of progradational sedimentary wedges laterally into troughs. Also, the bank sediment containing large amounts of finely broken shell material (factor 5), which **now** exists far from shore in water depths of 70-100 m, probably was produced by nearshore wave action during the transgression. Carbon-14 age dates of two samples gave 3850 \pm 50 yrs. **B.P.** (station 90) and 2130 yrs. **B.P.** (station 138).

The influx of modern sediment is **low**, because no large rivers drain onto Kodiak Shelf. The Copper River and local submarine outcrops provide minor **epiclastic** material. Occasional strong volcanic eruptions such as the Katmai event in 1912 are a relatively major source of sediment (volcanic **ash**), although the absolute amount is minor. **Biogenic** sources provide some siliceous and carbonate shell debris.

The present-day sedimentary setting is therefore one of reworking of predominantly **pre-Holocene** deposits. Currents impinge on the seafloor from the southwestward-flowing Alaska current and from large storm waves (see **Muench** and **Schmacher**, 1980). Fine sediment is winnowed from the **surficial** deposits on the banks, and its fate is determined by the pattern of ocean currents and by physiography. A minor amount is redeposited on the banks in broad, shallow depressions where thin, **surficial** layers of ash- and clay-rich material have been sampled (e.g., stations 91 and 115; see also **Hampton** et al., 1979a). A **much** greater amount is deposited in troughs. **Kiliuda** and **Chiniak** Troughs in particular are floored by **fine-grained**, ash-rich sediment. These troughs have sills across their mouths and are quiet depositional settings. Sitkinak Trough contains thick accumulations of terrigenous muddy sediment that may be derived mainly as first-cycle input from **Shelikof** Strait, or it may be reworked Kodiak **Shelf** debris.

The sedimentary environment in Stevenson Trough is distinct from the others. The presence of sand (factor 4) that has been molded into large, predominantly seaward-facing sand waves suggests strong bottom currents. But, it is uncertain whether these currents are active at present or mainly during the Holocene transgression. A layer of Katmai ash, buried about 10 cm beneath the surface of a clean sand deposit (factor 4) at station 56 in **the bedform** field shows that some modern transport of sand is taking place, but , oceanographic studies (**Muench** and **Schumacher**, 1980) have not revealed abnormally strong currents in Stevenson Trough. Strong currents have not been measured near the other **major** fields of large sand waves, either.

ENVIRONMENTAL ASSESSMENT

Geologic processes pose several environmental conditions of concern to resource development on Kodiak Shelf. Some processes may affect the operation and safety of offshore engineering activities. For example, seismic events may severely disrupt petroleum exploration and production operations on drilling platforms. Other geologic processes in turn **may** be affected by

resource development, with deleterious environmental consequences. For example, incorporation of spilled contaminants into bottom sediment may affect benthic life.

Environmental geologic concerns on Kodiak Shelf are broadly related to tectonic and sedimentary processes. Most processes affect broad areas, and their origin or occurrence at a specific location can have both local and widespread consequences. The following analysis is on a regional, rather than tract-by-tract basis.

Seismic-Tectonic Effects

The tectonic setting of Kodiak Shelf creates many potential environmental hazards. Convergence of the Pacific and North America plates generates large-magnitude earthquakes that make the entire shelf subject to seismic shaking. But, **seismicity** and structural deformation are spatially variable across the region, posing different sets of concerns from place-to-place. **Zonation** of seismicity has been postulated, with identification of a seismic gap near Kodiak Shelf where the potential for a major earthquake is great. Folding and faulting are more severe along sections of the shelf break and near Kodiak Island than at other places, and postulated transverse tectonic boundaries may indicate other areas of concentrated deformation.

The minimum estimated recurrence interval of 30 years for a major earthquake could be exceeded by the lifetime of an oil-producing province, because the last major event to affect Kodiak Shelf was in 1964. So, although earthquakes cannot be predicted with confidence, seismic hazards are a valid concern for offshore development. Strong ground shaking, fault rupture, sediment displacement, and tectonic deformation of the seafloor have all occurred on or adjacent to Kodiak Shelf and can be expected in the future.

Kodiak Shelf might be affected seismically by major events in either of two regional zones; that involved with the 1964 Alaska earthquake or that identified as the **Shumagin** seismic gap. The 1964 earthquake had aftershocks across the entire Kodiak **Shelf**, and seafloor deformation or ground shaking of the magnitude associated with this event could affect operation of **bottom-**founded installations such as drilling platforms. A major event in the **Shumagin** seismic gap may not have epicenters located on Kodiak Shelf, if present theory is correct (e.g., Sykes, 1971; **Pulpan** and **Kienle**, 1979), but significant ground shaking could be generated at least in the southwest part of the area.

Another area of seismic concern is near the mouth of **Kiliuda** Trough and adjacent sections of southern and middle Albatross Banks, where several moderate earthquakes have occurred (Fig. 6). This area displays a much higher rate of strain release than elsewhere on Kodiak Shelf, and seismic reflection records show evidence of folding, faulting, seafloor deformation, and sediment sliding (**Pulpan** and **Kienle**, 1979; Hampton et al., 1979). The shelf-break area of **Portlock** Bank shows similar structural features (Fig. 37), suggesting similar tectonic behavior, but the historic record shows no concentration of seismic activity there (Fig. 6).

The area along the shelf break on northern Albatross Bank, judging from structural and seismic evidence, appears to be less active and therefore less prone to local tectonic hazards than the two adjacent zones of strong deformation described above (Fig. 38). Regional **seismicity** could still produce significant ground shaking there, of course.

Displacement of the seafloor can result from movement along shallow **faults**, causing damage to installations that span them. Present-day **seismicity** does not indicate any clear linear seismic trends that define active faults (Pulpan and Kienle, 1979). But, offset in 1964 along faults within the zone extending along and offshore of Kodiak Island has been documented in places and inferred in others (Malloy and Merrill, 1972; von Huene, 1972), raising special concern for proper routing of pipeline corridors across the zone. Another significant fault zone exists along the shelf break of southern and middle Albatross Bank, and other individual examples have been noted across the shelf (Fig. 7). Faulting and tectonic deformation of the seafloor can generate tsunamis, which can devastate coastal areas as happened on Kodiak Island in 1964 (Kachadoorian and Plafker, 1967).

Large volcanic eruptions have spread blankets of ash across Kodiak Shelf from time-to-time; the Katmai event in 1912 being an example (Wilcox, 1959). The most severe volcanic hazards are local and would not have an affect on Kodiak Shelf, because the nearest volcanoes are about 200 km away on the Alaska Peninsula. But, the abrasive action of ash particles and acid rains associated with eruptions can be a nuisance to offshore operations.

Sediment

The sedimentary environment of Kodiak Shelf has many unusual features of practical significance. Semilithified to lithified bedrock is exposed over large areas, and a diverse suite of unconsolidated sediment is present including **coarse-grained** material nearly lacking **mud**, volcanic ash, clean sand, and normal terrigenous mud. Furthermore, input of modern sediment is small, and ocean currents impinging on the seafloor can be strong in places but are insignificant in others. Broad areas are being reworked whereas others serve as quiet repositories for winnowed debris.

Sedimentary bedrock appears to provide strong foundation material at the seafloor over broad expanses of Kodiak Shelf, although **geotechnical** data are lacking. Resistance to trenching and pile driving might be significant, and problems with emplacement of engineering structures might be encountered on bedrock ridges, due to rough topography.

Accumulations of unconsolidated sediment on Kodiak Shelf are generally thin, and in many places firm bedrock is within reach of **subbottom** structural foundations. The banks appear overall to be composed of strong, stable material, and foundation problems should be minimal. Boulders in unconsolidated debris might interfere with drilling and setting of casings, however.

The localized concentrations of fine sediment in some of the troughs might have engineering importance, although the deposits typically are only a

few tens of meters thick. Accumulations in Chiniak, Kiliuda, and perhaps Amatuli Troughs might be composed of volcanic ash grains and siliceous microfaunal tests throughout much of their thickness. The ash particles are plate- to rod-shaped and some are highly vesicular. Siliceous shells are hollow and fragile. Individual grains are therefore weak, and the deposits have high void ratios. Grain crushing and rearrangement during loading might result in substantial consolidation. Also, liquefaction, with associated strength loss and subsidence, is a possibility during earthquakes. Similar problems might be encountered with the fine-grained sediment in Sitkinak Trough, but the higher percentage of terrigenous material suggests greater stability. The large thickness of unconsolidated sediment in Sitkinak Trough might necessitate different foundation design than in areas of less fine sediment accumulation. The sandy material in Stevenson Trough and other places on the shelf appears to be a type that would be stable under loading, but its engineering properties have not been studied in detail.

The volcanic ash recovered in sediment samples is relatively fresh, as has also been reported for buried ash deposits in the Gulf of Alaska (Scheidegger and Kulm, 1975). So, the sediment stability problems commonly encountered in terrestrial ash deposits that have been altered to clay are unlikely to be met on Kodiak Shelf.

The surficial deposits of volcanic ash sampled on the banks are only a few centimeters thick and of no engineering concern.

Strong currents are indicated where large bedforms occur (Fig. 12), although the degree of modern activity compared to times of lower sea level is uncertain. Scour of sediment can cause loss of support and differential settlement at the base of seafloor installations (Posey, 1971; Wilson and Abel, 1973; Palmer, 1976). Also, fluttering due to resonance set up by vortex shedding can occur where pipelines have become suspended as a result of scour. This has been documented in nearby Cook Inlet (Goepfert, 1969). Unsuspected loads can be applied to structures as bedforms migrate past them.

Slope instability does not appear to be a major problem on the shelf, having been reported only from a few areas (Fig. 33; see also Self and Mahmood, 1977). The high degree of stability is related to the restricted occurrence of soft sediment mainly on flat areas of seafloor, whereas slopes are underlain by coarse-grained material. Sitkinak Trough is a notable exception, but no large slides have been specifically located there. Because there is low influx of modern sediment onto the shelf, large accumulations of unstable, underconsolidated sediment like those in the nearby northeastern Gulf of Alaska do not occur (see Carlson and Molnia, 1977).

Sediment slides are abundant on the upper continental slope and will become of prime concern only as development moves beyond the shelf break. However, the distribution of these slides does have important implications regarding tectonic hazards on the shelf. Areas near the shelf break that contain large slides appear to be experiencing modern tectonic deformation, with growth of folds, tilting of the seafloor, and earthquakes occurring there. Geologic structures and seismic activity in shelf break areas that do not contain large slides indicate relatively minor tectonic deformation.

Locations of gas-charged sediment have been identified on Kodiak Shelf, and environmental problems are possible. Most gas appears to be generated by shallow microbial decay, although the gas seep on middle Albatross Bank **may** indicate a deeper thermogenic source. Slope instability, **low** strength, and overpressuring have been found associated with gas-charged sediment (Whelan et al., 1976; Nelson et al., 1978). Direct evidence that similar problems exist on Kodiak Shelf is sparse; the gas seep on middle Albatross Bank suggests overpressuring. Gas-related craters, subsidence, or slope instability have not been noticed (see, for example, Nelson et al., 1979). But, although large blowouts and failures may not have been initiated by natural environmental forces, engineering activities could perhaps trigger them, and special attention is warranted in the specified areas.

Man-induced pollution of Kodiak Shelf waters can have magnified effects at certain places on the seafloor. Sediment particles can serve as carriers of contaminants, and localized concentration and storage are determined by the current patterns and hydraulic sorting processes that control sediment dispersal pathways and the locations of depositional sites. The distribution of benthic fauna should vary spatially with sediment type (although supporting biological data are lacking), so that specific **faunal** populations might be affected more than others by a contamination event. For example, the localized occurrence of Katmai ash in some troughs and in bank depressions implies that these sites are presently repositories for fine-grained sediment. Pollutants that become incorporated into bottom sediment should be swept from other areas into the troughs, and local fauna would be affected. **Also**, it is likely that sediment transport across the shelf break is localized where **physiographic** barriers are absent or have been breached, which could cause disturbance of local populations after a pollution event.

REFERENCES

- Bernard, B.B., Brooks, J.M., and Sackett, W.M., 1976, Natural gas seepage in the Gulf of Mexico. *Earth Planet. Sci. Lett.*, v. 31, p. 48-54.
- Bouma, A.H., and Hampton M.A., 1976, Preliminary report on the surface and shallow subsurface geology of lower Cook Inlet and Kodiak Shelf, Alaska. U.S. Geol. Survey Open-File Report 76-695.
- Capps, S.R., 1937, Kodiak and adjacent islands. *U.S. Geol. Survey Bull.*, no. 880-C, 73 p.
- Carlson, P.R., and Molnia, B.F., 1977, Submarine faults and slides on the continental shelf, northern Gulf of Alaska. *Marine Geotechnology*, v. 2, pⁿ 275-290.
- Claypool, G.E., Presley, B.J., and Kaplan, I.R., 1973, Gas analysis in sediment samples from Legs 10, 11, 13, 13, 14, 18 and 19. In: **J.S. Creager, D.W. Scholl, et al.**, Initial Reports of the Deep Sea Drilling Project, v. 19, Washington, D.C., p. 879-884.
- Cooper, A.K., Scholl, D.W., Marlow, M.S., Childs, J.R., Redden, G.D., Kvenvolden, K.A., and Stevenson, A.J., 1979, Hydrocarbon potential of Aleutian Basin, Bering Sea. *Am. Assoc. Petroleum Geologists Bull.*, v. 63, p* 2070-2087.
- Denk, E.W., Dunlap, W.A., Bryant, W.R., Milberger, L.J., Whellan, T.J., III, 1981, A pressurized core barrel for sampling gas-charged marine sediments. *Proceedings 13th Offshore Technology Conference*, p. 43-52.
- Dunleavy, J.M., Childs, J.R., and von Huene, R., 1980, Bathymetric map of the western Gulf of Alaska. U.S. Geol. Survey Open-File Report 80-1093, 14 sheets.
- Fisher, M.A., 1979, Structure and tectonic setting of continental shelf southwest of Kodiak Island, Alaska. *Amer. Assoc. Petroleum Geologists Bull.*, V. 63, p. 301-310.
- Fisher, M.A., Bruns, T.R., and von Huene, R., 1981, Transverse tectonic, boundaries near Kodiak Island, Alaska. *Geol. Soc. America Bull.* (pt. 1), V. 92, p. 10-18.
- Fisher, M.A., and von Huene, R., 1980, Structure of upper Cenozoic strata beneath Kodiak Shelf, Alaska. *Amer. Assoc. Petroleum Geologists Bull.*, V. 64, p. 1014-1033.
- Gershanovich, D.E., 1968, New data on the **geomorphology** and recent sediments of the Bering Sea and the Gulf of Alaska. *Marine Geology*, v. 6, p. 281-296.

- Goepfert, B.L., 1969, An engineering challenge - Cook Inlet, Alaska. Proceedings 1st Offshore Technology Conference, p. 511-524.
- Hampton, L.D., and Anderson, **A.L.**, 1979, Acoustics and gas in sediments: Applied Research Laboratories (ARL) experience. In: **I.R.** Kaplan (cd.), Natural Gases in Marine Sediments. Plenum Press, New York, N.Y., p 249-274.
- Hampton, M. A., 1981, Grain size and composition of seafloor sediment, Kodiak Shelf, **Alaska**. U.S. Geol. Survey Open-File Report 81-659, 78 p.
- Hampton, M.A., and **Bouma, A.H.**, 1977, Slope instability near the shelf break, Western Gulf of Alaska. Marine **Geotechnology**, v. 2, p. 309-331.
- Hampton, M.A., and **Bouma, A.H.**, 1978, Generalized thickness map of unconsolidated **surficial** sedimentary units, Kodiak Shelf, western Gulf of Alaska. U.S. Geol. Survey Open-File Report 78-729.
- Hampton, M.A., **Bouma, A.H.**, Frost, T.P., and **Colburn, I.P.**, 1979a, Volcanic ash in **surficial** sediments of the Kodiak Shelf - An indicator of sediment dispersal patterns. Marine Geology, v. 29, p. 347-356.
- Hampton, M.A., **Bouma, A.H.**, **Pulpan, H.**, and von **Huene, K.**, 1979b, Geo-environmental assessment of the Kodiak Shelf, western Gulf of Alaska. Proceedings 11th Offshore Technology Conference, p. 365-376.
- Hampton, M.A., **Bouma, A.H.**, **Sangrey, D.A.**, **Carlson, P.R.**, **Molnia, B.F.**, and **Clukey, E.C.**, 1978, Quantitative study of slope instability in the Gulf of Alaska. Proceedings 10th Offshore Technology Conference, p. 2308-2318.
- Hampton, M.A., and **Kvenvolden, K.A.**, in press, Geology and geochemistry of gas-charged sediment on Kodiak Shelf, Alaska: **Gee-Marine Letters**.
- Hein, J.R., **Bouma, A.H.**, Hampton, M.H., and Ross, C.R., 1979, Clay mineralogy, fine-grained sediment dispersal, and inferred current **patterns**, lower Cook Inlet and Kodiak Shelf, Alaska: **Sedimentary Geology**, v. 24, p. 291-306.
- Holmes, M.L., and Thor, D.R., 1979, Distribution of gas-charged sediments in Norton Basin, northern Bering Sea. U.S. Geol. Survey Open-File Report 80-979, 29 p.
- Kachadoorian, R.**, and **Plafker, G.**, 1967, Effects of the earthquake of March 27, 1964 on the communities of Kodiak and nearby islands. U.S. Geol. Survey Professional Paper 542-F.
- Karlstrom, T.N.V.**, 1964, Quaternary geology of the Kenai Lowland and glacial history of the Cook Inlet region, Alaska. U.S. Geol. Survey Professional Paper 443.
- Kvenvolden, K.A.**, and **Redden, G.D.**, 1980, Hydrocarbon gas in sediment from the **shelf, slope, and basin** of the Bering Sea. **Geochim. Cosmochim. Acts**, v. 44, p. 145-150.

- Kvenvolden, K. A., Redden, G. D., and Carlson, P. R., 1977, Hydrocarbon gases in sediments of Eastern Gulf of Alaska. *Am. Assoc. Petroleum Geologists Bull.*, V. 61, p. 806.
- Kvenvolden, K.A., Redden, G.D., Thor, D.R., and Nelson, C.H., 1981, Hydrocarbon gases in near-surface sediment of northern Bering Sea. In: **D.W. Hood and J.A. Calder (eds.)**, *The Eastern Bering Sea Shelf: Oceanography and Resources*. v. 1., U.S. Dept. Commerce, p. 411-424.
- Malloy, R.J., and Merrill, G.F., 1972, Vertical **crustal** movements on the seafloor. In: *The Great Alaska Earthquake of 1964, Oceanography and Coastal Engineering*. Washington, D.C., National Research Council, National Academy of Sciences, p. 252-265.
- McClellan, P.H., **Arnal**, R.E., Barron, J.A., von Huene, R., Fisher, M.A., and Moore, G.W., 1980, Biostratigraphic results of dart-coring in the western Gulf of Alaska, and their tectonic implications: U.S. **Geol. Survey Open-File Report** 80-63.
- Molnia, B.F., **Carlson**, P.R., and Bruns, T.R., 1977, Large submarine slide in Kayak Trough, Gulf of Alaska. *Reviews in Engineering Geology*, v. III, **Geol. Soc. America**, p. 137-148.
- Moore, G.W., 1967, Preliminary geologic map of Kodiak Island and vicinity, Alaska. U.S. **Geol. Survey Open-File Report** 67-271.
- Muench, R.D., and Schumacher, J.D., 1980, Physical oceanographic and meteorologic conditions in the northwest Gulf of Alaska. NOAA Technical Memorandum ERL **PMEL-22**, 147 p.
- Nelson, C.H., Kvenvolden, K.A., and Clukey, E.C., 1978, Thermogenic gases in near-surface sediments in Norton Sound, Alaska. *Proceedings 10th Offshore Technology Conference*, p. 2623-2633.
- Nelson, C.H., Thor, D.R., Sandstrom, M.W., and Kvenvolden, K.A., 1979, Modern biogenic gas-generated craters (sea-floor "pockmarks") on the Bering Shelf, Alaska. **Geol. Soc. America Bull.**, v. 90, p. 1144-1152.
- Palmer, H.D., 1976, Sedimentation and ocean engineering structures. In: **D.J. Stanley and D.J. P. Swift (eds.)**, *Marine Sediment Transport and Environmental Management*. New York John Wiley and Sons, p. 519-534.
- Plafker, G., and Rubin, M., 1967, Vertical tectonic displacements in south-central Alaska during and prior to the great 1964 earthquake. *Jour. Geosci. Osaka City Univ.*, p. 53-72.
- Posey, C.J., 1971, Protection of offshore structures against **underscour**. *Jour. Hydraulics Division, Amer. Soc. Civil Engineers*, No. **Hy7, Proc.** Paper 8230, p. 1011-1016.
- Pulpan, H. and Kienle, J., 1979, Western Gulf of Alaska seismic risk. *Proceedings 11th Offshore Technology Conference*, p. 2209-2218.

- Scheidegger, K.F.** , and **Kulm, L.D.** , 1975, Late Cenozoic volcanism in the Aleutian arc: information from ash layers in the northeastern Gulf of Alaska. **Geol. Soc. America**, v. 86, p. 1407-1412.
- Schubel, J.R.**, 1974, Gas bubbles and the acoustically impenetrable, or turbid, character of some marine sediments. In: **I.R. Kaplan** (cd.), **Natural Gases in Marine Sediments**. New York, Plenum Press, p. 275-298.
- Self, G.W., and **Mahmood, A.**, 1977, Assessment of relative slope stability of Kodiak Shelf, Alaska, using high-resolution acoustic profiling data. **Marine Geotechnology**, v. 2, p. 333-347.
- Sykes, L.R., 1971, Aftershock zones of great earthquakes, seismicity gaps, and earthquake prediction for Alaska and the Aleutians. **Jour. Geophysical Research**, v. 75, p. 8021-8041.
- Thrasher, G.P., 1979, Geologic map of the Kodiak outer continental shelf, western Gulf of Alaska. U.S. **Geol. Survey Open-File Report 79-1267**.
- Turner, B.W., Thrasher, G.P., Shearer, G.B., and **Holden, K.D.**, 1979, Bathymetric maps of the Kodiak and other continental shelf, western Gulf of Alaska. U.S. **Geol. Survey Open-File Report 79-263**, 13 sheets.
- University of Alaska, 1974, **The Western Gulf of Alaska - A summary of available knowledge: Anchorage, Arctic Environmental Information and Data Center**, 599 p.
- Varnes, D.J., 1978, Slope movement types and processes. In: R.L'. Schuster and R.J. Krizek (eds.), **Landslides-Analysis and Control**, Washington, D.C. , National Academy of Sciences, p. 12-33
- von Huene, R., 1972, Structure of the continental margin and tectonism of the eastern Aleutian Trench. **Geol. Soc. America Bull.**, v. 83, p. 3613-3636
- von **Huene, R.**, Fisher, M.A., and **Bruns, T.R.**, 1979, Continental margins of the Gulf of Alaska and late Cenozoic tectonic plate boundaries. In: A. Sisson (cd.), **Proceedings of the Sixth Alaska Geological Society Symposium**. Anchorage, Alaska Geological Society, p. J-1 - J-33.
- Von **Huene, R.**, Hampton, M.A., Fisher, M.A., **Varchol, D.J.**, and **Cochrane, G.R.**, 1980, **Map showing near-surface geologic structures of Kodiak Shelf, Alaska**. U.S. **Geol. Survey Miscellaneous Field Studies Map MF-1200**.
- von **Huene, R.**, Shore, G.G., and **Malloy, R.J.**, 1972, Offshore tectonic features in the affected region. In: **The Great Alaska Earthquake of 1964, Oceanography and Coastal Engineering**. Washington, D.C., National Research Council, National **Academy** of Sciences, p. 266-289.

Table 1. Locations, textures, and compositions of sediment samples.

Sample	North Latitude	West Longitude	Water Depth (m)	Location*	Texture (weight percents)				Composition (weight percents)				
					Coarse	Sand	silt	Clay	Terrig.	Carb.	Ash	Clay	Silic.
1	57°56.54'	150°13.56'	192	StT		98	1	1	100	tr	tr	tr	
50	59°52.50'	151°54.50'	32		58	42	tr	tr	94	6			tr
51	58°12.54'	151°55.74'	60		100				95	5			
52	58°24.42'	151°13.80'	107	StT	70	25	3	2					
53	58°12.56'	150°39.79'	86	PB	100				88	12			
54	58° 73.62'	150°30.26'	175	StT	2	78	14	6	61	14	22	3	tr
55	73°01.86'	150°21.64'	184	StT		83	12	5	27	1	70	2	tr
56	57° 55.56'	150°11.34'	190	StT		99	tr	1	99	tr		1	
57	57° 50.94'	150°03.74'	194	StT	2	76	17	5	48	4	43	4	1
58	57° 46.99'	149°55.40'	232	StT	15	56	22	7	49	tr	41	9	1
59	57° 46.60'	149°29.66'	495	Cs	28	56	10	6	52	1	41	6	
60	57° 45.96'	149°37.41'	444	CS	2	81	10	7	56	tr	36	7	1
61	57° 35.61'	150°24.46'	112	NAB	38	54	5	3	73	17	5	4	1
62	57°39.15'	150°33.49'	102	NAB	12	85	2	1	68	29	2	1	tr
63	57°43.96'	150°39.25'	90	NAB	17	79	3	1	40	58	1	1	tr
64	57°47.50'	150°45.00'	83	NAB	34	62	2	2	51	34	14	1	tr
65	57°51.50'	150°51.50'	77	NAB	32	62	3	3	47	46	5	2	tr
66	57°55.10'	150°59.30'	81	NAB	13	75	8	4	20	64	12	3	1
67	57°59.70'	151°06.40'	82	NAB	21	53	18	8	53	18	17	10	2
68	57°28.15'	151°28.35'	154	CT	1	43	46	10	5	2	86	7	tr
69	57°23.43'	151°11.44'	80	NAB	13	82	2	3	14	5	79	2	tr
70	57°24.08'	150°52.25'	96	NAB	1	97	1	1	94	1	4	1	tr
71	57°20.01'	150°59.08'	95	NAB		96	3	1	61	1	34	1	tr
72	57°24.20'	151°05.10'	92	NAB	tr	94	3	3	6	1	91	2	tr
75	57°45.80'	151°08.05'	70	NAB	10	90			13	87			
76	58°06.20'	151°46.10'	95		tr	96	1	3	12	6	80	2	tr
77	58°11.60'	151°37.00'	38		95	5			94	6			
79	58°13.23'	151°38.07'	68		36	62	tr	2	41	58	1	tr	tr
80	58°01.50'	151°21.63'	181	NAB	32	62	4	2					
81	58°05.21'	151°14.55'	143	NAB/StT		60	30	10	2	1	85	11	

Table 1. (continued)

Sample	North Latitude	West Longitude	Water Depth (m)	Location*	Coarse	Texture (weight percents)			Composition (weight percents)				Silic.
						Sand	Silt	Clay	Terrig.	Carb.	Ash	Clay	
82	58°03.60'	151°15.90'	103	NAB	64	16	15	5	58	18	14	8	2
85	57°45.00'	151°44.00'	55	NAB	28	70	1	1	5	85	10		tr
86	57°41.40'	151°34.70'	61	NAB	36	61	1	2					
87	57°36.45'	151°47.60'	132	CT	4	58	31	7	3	4	80	10	3
88	57°30.00'	151°38.80'	167	CT		22	69	9	6	tr	75	17	2
89	57°28.50'	151°44.50'	70	MAB	68	24	6	2	63	11	25	1	tr
90	57°25.10'	151°51.90'	67	MAB	6	91	1	2	3	93	3	1	tr
91	57°19.29'	152°01.82'	73	MAB	5	91	2	2	3	14	84	1	tr
92	56°56.40'	152°32.90'	167	KT		6	74	20	15	tr	41	29	15
93	56°53.50'	152°41.00'	128	KT		24	62	14	12	1	38	37	12
94	56°48.15'	152°52.75'	63	SAB	87	10	2	1	83	14	1	2	tr
96	56°41.40'	153°05.90'	146	KT		3	61	36	11	tr	52	36	1
97	56°40.10'	153°10.20'	150	KT		1	60	39	5	tr	38	56	1
98	56°38.00'	153°16.00'	145	KT		1	62	37	13	tr	46	41	tr
112													
27 113	56°33.50'	152°27.20'	197	KT	25	70	3	2	94	2	3	1	tr
115	56°57.02'	152°06.28'	76	MAB		92	5	3	2	9	87	2	tr
127	57°11.24'	151°29.59'	69	MAB	17	25	11	7	31	54	10	5	tr
128	58°31.47'	149°21.90'	121	PB	25	45	15	15	37	36	15	11	1
130	58°42.23'	149°03.38'	145	PB		79	11	10	81		15	3	1
131	58°44.99'	148°58.18'	214	AT	3	45	25	27					
132	58°48.16	148°54.71'	236	AT	5	33	32	30	56	tr	26	15	3
134	58°49.42'	149°14.22'	206	AT	20	41	17	22					
135	58°40.39'	149°31.82'	136	PB		77	15	8	78		10	11	1
136	58°34.90'	149°45.19'	125	PB		73	17	10					
137	58°29.46'	150°05.25'	93	PB	10	72	13	5	53	42	6	9	tr
138	58°22.30'	150°24.07'	60	PB	24	70	3	3	41	51	7	1	tr
141	58°13.12'	149°11.85'	120	PB	56	26	11	7	60	13	22	5	tr
200	58°36.79'	151°50.26'	159		48	46	2	4	92	3	2	2	1
201	58°42.24'	152°17.77'	126		54	43	1	2	67	31	tr	2	tr
202	58°46.12'	152°42.85'	190		3	65	13	19	72	3	12	10	3
204	58°51.37'	152°54.13'	164		36	32	19	13	52	tr	34	12	2
205	58°59.89'	153°13.38'	118		35	47	11	7	80	2	12.	5	1
215	57°11.38'	152°25.89'	115	MAB/KT	15	63	14	8					
216	57°06.00'	152°20.60'	96	MAB	1	88	7	4	6	35	56	3	tr

Table 1. (continued)

Sample	North Latitude	West. Longitude	Water Depth (m)	Location*	Texture (weight percents)				Composition (weight percents)				
					Coarse	Sand	silt	clay	Terrig.	Carb.	Ash	Clay	Silic.
217	57°00.00'	152°93.50'	76	MAB	52	44	3	1	49	27	23	1	tr
219	57°42.65'	151°53.60'	79	CT	73	25	1	1	89	10	1		tr
227	57°05.60'	151°14.00'	358	Cs		72	19	9	7	tr	87	6	tr
228	57°07.50'	151°15.40'	185	CT	33	59	5	3	67	28	2	3	tr
229	57°14.20'	151°19.90'	172	CT		55	36	9	6	1	74	17	2
232	57°22.01'	150°35.92'	262	CS	29	69	1	1	98	tr	1	1	tr
233	57°17.60'	150°34.50'	630	CS		23	55	22					
234	57°31.54'	150°49.42'	93	NAB	50	47	2	1	52	2e	19	1	tr
236	58°04.20'	149°28.20'	230	StT		38	4e	14	5	tr	71	23	1
241	57°41.29'	149°39.16'	606	Cs	5	e6	4	5	37		62	1	tr
242	57°31.40'	150°16.00'	300	CS		64	30	6	7	tr	eo	12	1
243	57°48.50'	150°01.10'	190	StT	24	66	7	3	77	2	16	5	tr
244	57°51.70'	149°50.90'	257	StT	1	eo	15	4	17	tr	75	7	1
245	57°57.60'	149°39.70'	135	StT	9	72	6	13	21	33	41	4	1
246	50°12.80'	149°13.40'	134	PB	32	47	13	8	35	29	23	23	tr
28 329	57°38.95'	151°58.03'	218	CT		36	50	14	3	tr	76	20	1
330	58°00.96'	150°50.59'	135	StT	10	78	7	5	50	2e	17	5	tr
336	57°46.60'	149°02.08'	1700	CS		1	50	49	16		40	39	5
340	57°17.48'	150°24.92'	762	CS	2	23	51	24	43	2	34	21	tr
341	56°59.00	152°21.47'	80	MAB	50	43	4	3	50	41	6	3	tr
342	56°55.77	152°15.17'	79	MAB	59	34	4	3	66	5	26	3	tr
343	56°39.37	153°04.72'	155	KT		5	64	31	14	1	66	15	4
344	56°39.47	153°05.63'	160	KT		1	60	39	16	2	23	56	3
345	56°36.11'	153°10.00'	119	KT		65	23	12	69	1	17	12	1
346	56°36.22	153°12.51'	120	KT		67	22	11					
347	56°36.76'	153°17.92'	130	KT		4	67	29	16	tr	36	44	3
348	56°37.66'	153°18.89'	143	UT		3	63	34	12		4e	36	4
349	56°38.24'	153°19.80'	148	KT		1	61	38	3		53	42	2
350	56°46.20'	153°10.00'	154	KT		13	53	34	11		40	37	12
351	56°46.86'	153°11.02'	125	KT	22	32	29	17	52	tr	26	16	6
353	56°39.90'	153°11.08'	148	KT		1	61	3e	6	tr	43	45	6
354	56°37.85'	153°16.05'	143	KT		1	61	38	11	3	60	21	5
355	56°08.53'	153°29.41'	314	StT	10	45	26	19	67	2	21	10	tr
356	56°05.55'	153°31.28'	370	StT	43	49	5	3	93	tr	3'	4	tr
357	56°07.56'	153°38.46'	240	StT		56	30	14	53	1	22	21	3

Table 1. (continued)

Sample	North Latitude	West Longitude	Water Depth (m)	Location*	Texture (weight percents)				Composition (weight percents)				
					Coarse	Sand	Silt	Clay	Terrig.	Carb.	Ash	Clay	Silic.
358	56°47.03'	153°11.70'	122	KT	2	69	16	13	54	tr	30	15	1
359	56°46.47'	153°10.59'	152	KT		49	32	19	37	tr	37	22	4
437	57°01.14'	152°10.31'	72	MAB	80	18	1	1	90	7	2	1	tr
443	56°38.56'	152°57.42'	.82	SAB	71	18	7	4	89	2	5	3	1
444	56°22.91'	153°15.75'	35	SAB	39	59	1	1	96	2	1	1	
446	56°05.88'	153°51.49'	213	S1T	10	76	10	4	86		7	6	1
447	56°20.68'	153°50.84'	94	S1T	9	75	10	6	55	31	8	4	2
448	56°23.19'	154°18.80'	42	SAB		99	tr	1	100		tr	tr	tr
449	56°08.13'	154°17.33'	97	SAB	63	30	4	3	93	1	1	4	1
452	55°59.97'	155°07.08'	67	SAB	1	99			100	tr			
453	56°13.90'	155°09.84'	32	SAB	91	9	tr	tr	96	4	tr	tr	tr
454	56°12.08'	154°42.77'	89	SAB		97	1	2	97	tr	2	1	tr
501	56°29.79'	155°08.57'	30	SAB	73	26	tr	1	71	28	tr	tr	tr
502	56°27.49'	55°48.68'	180	SS		39	42	19	50	18	20	12	1
503	56°17.43'	55°32.91'	50	SAB		99	tr	1	94	6	tr	tr	
504	56°03.09'	55°30.25'	25	SAB	96	4	tr	tr	78	22		tr	
505	55°55.32'	55°18.02'	50	SAB	77	23	tr	tr	95	5	tr	tr	tr
570	58°34.4'	48°44.1'	117	PB	49	39	5	7	62	30	1	3	4
571	58°12.9'	150°39.9'	80	StT	52	46	1	1	4	92	tr	tr	4
575	56°05.9'	154°45.3*	115	SA8		10	46	44	32	12	41	2	14
576	56°08.8'	154°22.4'	134	SAB	tr	82	11	7	91	1	2	5	tr
578	56°39.5'	153°05.2'	154	KT		1	51	48	20	6	47	26	1
579	56°54.9'	152°32.6'	170	KT		2	63	35	35	12	37	15	tr
580	57°05.0'	151°38.4'	119	MAB	71	19	6	4	80	8	10	2	1
581	57°14.4'	151°19.0'	163	CT		67	25	8	2	1	92	5	0
582	57°29.7'	151°38.6'	133	CT		39	45	16	26	6	60	8	0
D1	56°03.4'	154°52.7'	113	SAB		100	tr	tr	100	tr			
D2	56°05.7'	154°55.9'	64	SA8		99	tr	1	99		tr	tr	tr
D3	56°09.1'	155°02.9'	55	SAB		100			100			tr	
D4	58°41.5'	148°45.4'	215	AT	3	49	22	26	73	3	14	9	1
05	58°38.4'	148°53.4'	120	PB	41	46	5	9	78	10	2	3	8
De	58°48.2'	149°08.0'	195	PB	1	23	51	25	65	5	7	15	8
D9	5a 40.1'	149°23.2'	135	PB		75	15	10	69	1	23	7	1
D10	58°36.9'	149°23.2'	126	P8	3	57	21	19	29	11	39	12	8
011	58°33.3'	149°32.6'	120	PB		79	10	11	81	4	11	02	2

Table 1. (continued)

Sample	North Latitude	West Longitude	Water Depth (m)	Location*	Coarse	Texture (weight percents)			Composition (weight percents)				
						Sand	silt	Clay	Terrig.	Ca rb.	Ash	Clay	Silic.
012	58°26.5'	149°21.8'	135	PB	9	70	12	9	45	25	18	4	7
013	58°25.6'	149°51.0'	135	PB	15	66	17	2	45	34	13	4	3
014	58°20.5'	149°36.2'	140	PB		58	31	11	24	9	50	14	1
D16	58°10.7'	150°01.6'	128	PB	37	52	6	5	46	36	6	3	9
D18	58°14.4'	150°51.4'	106	StT	4	93	1"	2	55	27	9	2	8
022	58°02.5'	150°59.4'	97	NAB	40	38	13	9	32	30	23	4	11
024	58°20.3'	151°02.4'	101	StT	86	11	1	2	10	87	1	1	1
D25	58°10.4'	150°59.0'	111	NAB	27	67	3	3	20	50	5	2	22
026	58°05.0'	151°20.8'	139	CT		55	29	16	3	47	34	13	2
D27	57°52.9'	151°22.4'	71	NAB	41	57	tr	2	40	53	3	0	5
D31	57°09.1'	151°21.6'	128	CT	64	31	3	2	69	15	11	1	4
032	57°07.8'	152°15.2'	80	MAB		84	12	4	5	8	76	8	3
033	56°40.7'	152°29.9'	146	KT		1	64	35	6	8	56	26	4
D34	56°46.7'	152°11.7'	102	KT		19	53	28	46	7	21	23	3
035	56°40.6'	152°45.2'	82	SAB	tr	97	2	1	72	23	0	1	3
D36	56°28.6'	152°25.8'	338	CS		56	33	11	42	7	33	12	5
D37	56°26.9'	152°36.0'	179	KT	37	53	1	9	75	7	11	2	5
D38	56°32.4'	153°30.8'	132	KT		15	61	24	27	17	36	18	3
D39	56°29.1'	153°28.0'	88	SAB	25	58	7	10	67	24	1	5	3
D40	56°13.0'	154°11.3'	130	SiT		78	15	7	74	7	2	11	5
D41	56°11.6'	154°20.9'	91	SAB	52	41	4	3	88	5	5	2	0
D42	56°04.9'	154°14.8'	93	SAB	54	37	4	5	86	7	2	3	3

●Refer to Fig. 8. **At**=Amatuli Trough, **PB**=Portlock Bank, **StT**=Stevenson Trough, **NAB**=northern Albatross Bank, **CT**=Chiniak Trough, **MAB**=middle Albatross Bank, **SAB**=southern Albatross Bank, **SiT**=Sitkinak Trough, **CS**=continental slope, **SS**=Shelikof Strait.

Table 2. Descriptions of samples for which detailed analyses were not made

Sample	North Latitude	West Longitude	Water Depth (M)	Location	Seal. Unit	Visual Description
50	59°52.50'	151°54.50'	32			Sandy gravel
95	56°48.10'	153°21.40'	170	KT	Qs	Pebbly sand
99	56°24.50'	152°53.70'	50	SAB	QT	Bedrock (siltstone)
100	56°24.00'	152°53.50'	50	SAB	QT	Bedrock (siltstone)
101	56°23.20'	152°54.10'	49	SAB	QT	Bedrock (silty, fine-grained sandstone)
102	56°23.10'	752°53.90'	45	SAB	QT	Bedrock (siltstone)
103	56°22.70'	152°52.00'	50	SAB	QT	Bedrock (silty, fine-grained sandstone)
104	56°22.00'	152°50.90'	75	SAB	QT	Bedrock (silty, fine-grained sandstone)
106	56°29.60'	152°43.70'	60	SAB	QT	Bedrock (siltstone)
107	56°30.15'	152°44.10'	56	SAB	QT	Bedrock (siltstone)
108	56°30.30'	152°44.90'	56	SAB	QT	Bedrock (siltstone)
110	56°31.40'	152°46.70'	64	SAB	QT	Bedrock (siltstone)
111	56°31.70'	152°47.50'	65	SAB	QT	Bedrock (sandy siltstone)
112	56°32.00'	152°48.50'	70	SAB	QT	Coarse sand with broken shells
114	56°37.60'	152°34.00'	160	KT	Qs	Slightly muddy sand
116	57°12.00'	151°51.10'	75	MAB	QT	Bedrock (pebbly, sandy siltstone)
117	57°10.90'	151°50.70'	54	MAB	QT	Bedrock (pebbly, sandy siltstone)
118	57°11.00'	151°50.00'	54	MAB	QT	Bedrock (sandy siltstone)
119	57°10.60'	151°49.10'	56	MAB	QT	Pebbly sand with broken shells
120	57°10.00'	151°48.40'	60	MAB	QT	Bedrock (sandy siltstone)
121	57°09.25'	151°47.50'	70	MAB	QT	Bedrock (sandy siltstone)
123	57°08.75'	151°46.30'	76	MAB	QT	Bedrock (sandy siltstone)
124	57°08.50'	151°45.60'	78	MAB	QT	Bedrock (fine sandstone)
125	57°08.00'	151°45.00'	80	MAB	QT	Sandy silt
129	58°35.85'	149°14.91'	95	PB	Qgm	Pebbly muddy sand
133	58°54.41'	149°01.95'	250	AT	Qgg	Muddy sand
140	58°22.25'	149°54.26'	83	PB	Qgf	Pebbly sand
142	58°08.66'	149°04.71'	114	PB	QT	Bedrock (muddy sand)
144	58°05.92'	149°01.38'	88	PB	QT	Bedrock (sandy siltstone)
145	58°06.59'	149°02.46'	90	PB	QT	Bedrock (sandy siltstone)
147	58°05.55'	149°00.97'	88	PB	QT	Bedrock (fine-grained sandstone)

31

Table 2. (continued)

148	58°04.96'	148°59.95'	90	PB	QT	Bedrock (sandy siltstone)
149	58°04.64'	148°59.49'	98	PB	QT	Bedrock (sandy siltstone)
220	56°43.80'	151°55.90'	62	MAB	QT	Boulder
231	57°24.90'	151°23.60'	187	CT	Qs	Ash-rich mud
352	56°40.19'	153°10.88'	150	KT	Qs	Ash-rich mud
432	57°25.40'	151°23.50'	175	CT	Qs	Ash-rich mud
433	57°26.71'	151°25.26'	174	CT	Qs	Ash-rich mud
435	57°15.04'	151°17.10'	158	CT	Qgg	Ash-rich mud
439	56°40.51'	153°12.30'	159	KT	Qs	Ash-rich mud
440	56°39.15'	153°06.36'	156	KT	Qs	Ash-rich mud
441	56°39.50'	153°04.62'	164	KT	Qs	Ash-rich mud
442	56°39.15'	153°02.11'	135	KT	Qgm	Ash-rich mud
445	56°11.17'	153°17.28'	1003	SiT		Mud
450	55°56.06'	154°14.13'	390	CS		Mud, with sand layers
451	55°58.50'	154°45.80'	371	CS		

Table 3. Description of sedimentary units (From Thrasher, 1979. Refer to Fig. 15).

Qs: Holocene Soft Sediments. Shallow basins of Holocene sediments that exhibit well-defined, continuous, horizontal reflectors.

Qb: Holocene Bedforms and Sand-Fields. **Mapable** regions of **bedforms** and, where possible, the massive sand unit with which they correlate.

Qu: Holocene and Pleistocene Undifferentiated Deposits. Exhibit **well-**developed, non-horizontal, parallel layering, with occasional indications of internal layering.

Qgm: Pleistocene Glacial Lateral and Terminal Moraines. Fairly linear deposits generally located along the sides and across the mouths of sea valleys. Very little or no acoustic internal structure.

Qgg: Pleistocene Glacial Ground Moraine. **Hummocky** upper surface; no internal structure.

Qgf: Pleistocene Glacial-Fluvial and Glacial-Marine Deposits. Thick deposits exhibiting some discontinuous, **non-parallel**, non-horizontal reflectors.

QT: Plio-Pleistocene Sedimentary Rocks. **Gently** depping, truncated sedimentary rocks that exhibit well-developed parallel internal **reflecotrs.**

T: Tertiary Sedimentary Rocks. No seismically determinable internal structure. Observed only in small outcrops along the landward edge of the mapped area.

Quc: Quaternary Undifferentiated Continental **slope** Deposits. Large seismic vertical exaggeration and steep **slopes** seaward of the continental shelf edge preclude accurate mapping on the continental slope.

Qus: Quaternary Undifferentiated Sediment Basins on the Upper Continental Slope. Exhibit well-defined, near-horizontal, continuous reflectors.

Table 4. Varimax factor loadings for 5 factors used to classify and map unconsolidated seafloor sediment on Kodiak Shelf. Factors are based on 12 textural and compositional variables. Factor-loading values listed in the columns for factors 1-5 are the proportional contributions of each factor to a given sample. Communality is the sum of squares of the 5 factor loadings for a sample and will be unity if 5 factors account for all the information in the sample.

STA.	COMM.	1	2	3	4	5
001	0.9967	0.3287	-0.0013	0.2247	0.9015	0.1597
(354	0.9874	0.2885	0.2226	0.4267	0.7709	0.2829
055	0.9973	0.1359	0.2525	0.8318	0.4467	0.1535
056	0.9967	0.3287	-0.0020	0.2238	0.9016	0.1600
057	0.9946	0.2612	0.2980	0.6222	0.6433	0.1912
058	0.9920	0.4003	0.4472	0.5558	0.5579	0.1077
059	0.9952	0.5444	0.2937	0.5664	0.5277	0.1153
060	0.9952	0.2648	0.2595	0.5537	0.7212	0.1760
061	0.7494	0.6262	0.0995	0.1631	0.5071	0.2522
062	0.9869	0.3824	0.0026	0.2731	0.7856	0.3858
063	0.9597	0.2933	-0.0078	0.2634	0.5619	0.6989
064	0.9562	0.5524	0.0500	0.3250	0.5466	0.4941
065	0.9585	0.5085	0.0502	0.2366	0.5194	0.6096
066	0.9645	0.1841	0.1053	0.3752	0.4129	0.7799
067	0.9844	0.5136	0.4011	0.3172	0.6039	0.3073
068	0.9598	0.0636	0.6032	0.76413	0.0799	0.0279
069	0.9857	(2.1857	0.1659	0.8944	0.3011	0.1821
070	0.9961	0.3323	0.0102	0.2579	0.8900	0.1642
071	0.9986	0.2610	0.0736	0.5494	0.7671	0.1864
072	0.9872	0.0449	0.1652	0.9211	0.2855	0.1671
075	9.9124	0.0713	-0.0651	0.2627	0.3674	0.8361
076	0.9872	0.0699	0.1411	0.8839	0.3649	0.2189
079	0.9575	0.5127	-0.0220	0.2133	0.4536	0.6655
080	0.9789	0.6290	0.0473	0.2052	0.7095	0.1884
081	0.9951	0.0348	0.5262	0.8244	0.1656	0.1002
081	0.9951	0.0348	0.5262	0.8244	c). 1656	0.1002
082	0.9874	0.9064	0.3093	0.0892	0.2222	0.1137
085	0.9156	0.2451	-0.0344	0.3586	0.1909	0.8303
086	0.8703	0.4027	0.0847	0.7407	0.0878	0.3802
087	0.9856	0.0689	0.5122	0.8260	0.1415	0.1273
088	0.8900	0.0500	0.7698	0.5425	0.0127	-0.0209
089	0.9826	0.9141	0.1418	0.2370	0.2592	0.0592
090	0.9075	0.0089	-0.0342	0.2801	0.3179	0.8525
091	0.9888	0.0703	0.1375	0.9153	0.2553	0.2492
092	0.8275	0.0546	0.8922	c). 1484	0.0391	0.0706
093	0.8262	0.0440	0.8621	0.2301	c) 1074	0.1287
094	0.9849	0.9588	c). 0528	-0.0586	0.2397	0.0429
096	0.9548	0.0426	0.9496	0.2244	0.0098	-0.0269
097	0.8847	0.0056	0.9351	0.1011	-0.0026	0.0063
098	0.9347	0.0400	0.9503	0.1702	0.0162	-0.0291
113	0.9978	0.5625	0.0475	0.1758	0.7946	0.1297
115	0.9913	0.0388	0.1755	0.9139	0.2737	0.2209
127	0.9283	0.2858	0.1925	0.3019	0.4721	0.7039
128	0.5004	0.3932	0.3170	0.2063	0.2467	0.3768

Table 4. (continued)

STA .	COMM .	1	2	3	4	5
130	0.9930	0.3289	0.2192	0.2982	0.853(1	0.1428
132	0.9429	0.2948	0.7583	0.1749	0.4976	0.0523
135	0.9891	0.3162	0.2760	0.2577	0.8500	0.1547
137	0.9434	0.2997	0.2099	0.2941	0.6172	0.5848
138	0.9419	0.4466	0.0354	0.3360	0.5529	0.5680
141	0.8416	0.8025	0.2520	0.2118	0.2615	0.1442
216	0.8213	0.0841	0.1525	0.7159	0.2769	0.4492
217	0.9614	0.7762	0.0850	0.3609	0.3271	0.3384
219	0.9858	0.9072	0.0322	-0.0059	0.3899	0.0985
227	0.9940	0.0540	0.3798	0.8823	0.2364	0.1116
228	0.9682	0.6244	0.0835	0.1834	0.6285	0.3778
229	0.9844	0.0486	0.6052	0.7539	0.1885	0.1092
232	0.9979	0.5843	0.0211	0.1479	0.7891	0.1073
234	0.6950	0.6709	0.0554	0.2887	0.2852	0.2778
236	0.9723	0.0371	0.7540	0.6253	0.0966	0.0451
241	0.9894	0.2098	0.1745	0.7796	0.5307	0.1594
242	0.9912	0.0471	0.4849	0.8352	0.2104	0.1096
243	0.9944	0.5443	0.1483	0.3092	0.7484	0.1430
244	0.9950	0.0975	0.3090	0.8584	0.3600	0.1536
245	0.9424	0.2097	0.2824	0.6330	0.4070	0.5023
24G	0.5676	0.4628	0.2825	0.3141	0.2368	0.3448
329	0.9751	0.0328	0.7432	0.6455	0.0642	0.0307
330	0.8658	0.3360	0.1449	0.3974	0.6211	0.4338
33G	0.9129	0.0501	0.9483	0.0903	0.0512	0.0159
340	0.9696	0.2032	0.8786	0.2114	0.3340	0.0129
341	0.9608	0.7327	0.0878	0.1653	0.3712	0.5011
342!	0.9906	0.8582	0.1526	0.2872	0.3768	0.0792
343	0.9520	0.0658	0.9095	0.3457	0.0020	-0.0313
344	0.9157	0.0294	0.9532	-0.0132	0.0695	0.0350
345	0.9882	0.3133	0.4298	0.2822	0.7797	0.1338
347	0.9316	0.0493	0.9548	0.1198	0.0566	0.0032
348	0.9680	0.0451	0.9634	0.1938	0.0183	-0.0035
349	0.9493	0.0120	0.9506	0.2103	-0.0358	-0.0107
350	0.9060	0.0400	0.9310	0.1532	0.0715	0.0955
351	0.9587	0.4668	0.6968	0.2235	0.4417	0.1007
353	0.9464	0.0130	0.9631	0.1328	-0.0129	0.0275
354	0.9747	0.0454	0.9548	0.2467	-0.0060	-0.0025
355	0.9775	0.3957	0.5833	0.2146	0.6550	0.0751
356	0.9945	0.7198	0.1049	0.0890	0.6734	0.0633
357	0.9679	0.2490	0.6180	0.2968	0.6428	0.1508
358	0.9783	0.2631	0.4412	0.4510	0.6961	0.1624
359	0.9718	0.1776	0.7347	0.4005	0.4721	0.1312
443	0.9899	0.9062	0.1450	-0.0192	0.3837	0.0091
444	0.9966	0.6720	0.0255	0.1157	0.7219	0.0986
446	0.9946	0.4214	0.1608	0.2300	0.8471	0.1433
447	0.9364	0.3497	0.1763	0.2988	0.6872	0.4707
448	0.9970	0.3289	-0.0075	0.2247	0.9016	0.1596
449	0.9941	0.8565	13.10GEI	-0.0044	0.4978	0.0360
452	0.9968	13.3374	-0.0149	0.2243	0.8987	0.1573
453	0.9847	0.9477	0.0224	-0.0746	0.2829	-0.0180
454	0.9971	0.3295	0.0161	0.2347	0.8990	0.1579

Table 4. (continued)

STA.	COMM .	1	2	3	4	5
501	0.9738	0.9222	0.0082	0.0164	0.3087	0.1666
502	0.6371	0.1370	0.6510	0.0642	0.4058	0.1602
503	0.9962	0.3142	-0.0005	0.2262	0.8959	0.2089
504	0.9797	0.9770	0.0127	-0.0676	0.1382	0.0363
505	0.9859	0.9071	0.0167	-0.0282	0.4015	0.0273
570	0.9783	0.7541	0.1896	0.0334	0.4537	0.4083
571	0.8465	0.5(357	-0.0059	0.1840	-0.0342	0.7455
575	0.8000	0.0958	0.8657	0.0896	c). 1728	c). 0580
576	0.9950	0.3366	0.1728	0.1855	0.8923	0.1461
578	0.9129	0.0567	0.9439	0.1172	0.0707	0.0041
579	0.8011	0.0971	0.8751	0.0468	0.1535	0.0141
580	0.9817	0.9153	0.1547	0.0294	0.3421	0.0452
581	0.9891	0.0343	0.4184	0.8796	0.1723	0.0977
582	0.9386	0.1254	0.7339	0.5537	0.2725	0.0584
D001	0.9967	0.3293	-0.0152	0.2265	0.9009	0.1587
D002	0.9970	0.3289	-0.0075	0.2247	0.9016	0.1596
D003	0.9967	0.3293	-0.0152	0.2265	0.9009	0.1587
D004	0.9523	0.3372	0.5605	0.1259	0.7049	0.1080
D005	0.9260	0.6769	0.2271	0.0448	0.5978	0.2386
D008	0.9536	0.2452	0.8037	-0.0766	0.4826	0.0934
D009	0.9955	0.3006	0.3155	0.3798	0.7982	0.1553
D010	0.8979	0.1510	0.6405	0.4270	0.4398	0.2984
D011	0.9910	0.3266	0.2242	0.2543	0.8566	0.1886
D012	0.9409	0.2856	0.3284	0.3434	0.6419	0.47013
D013	0.8904	0.3240	0.2916	0.2786	0.5988	0.5139
D014	0.9858	0.1138	0.6138	0.6206	0.4070	0.2129
D016	0.9038	0.5730	0.1934	0.1702	0.4449	0.5579
D018	0.9394	0.2493	0.0710	0.3325	0.7299	0.4785
D022	0.8166	0.5648	0.4028	0.2719	0.2331	0.4552
D024	0.6226	0.6810	-0.0004	0.0588	-0.2454	0.3085
D025	0.6019	0.2517	0.1626	0.1588	0.2624	0.6466
D026	0.6902	-0.0208	0.5739	0.2904	0.2051	0.4s3s
D027	0.9579	0.5413	0.0418	0.1756	0.4006	0.6869
D031	0.9769	0.8845	0.1232	0.1104	0.3681	0.1780
D032	0.9203	0.0425	0.2949	0.8189	0.2825	0.2848
D033	0.9414	0.0093	0.9510	0.1884	-0.0162	0.0329
D034	0.9789	0.1681	0.9089	0.0338	0.3441	0.0706
D035	0.9949	0.2634	0.0159	0.2581	0.8339	0.4041
D036	0.9598	0.2022	0.6394	0.4020	0.5451	0.2265
D037	0.9557	0.6567	0.1974	c), 1683	0.6408	0.2157
D038	0.7172	0.0574	0.8189	0.0795	0.1613	0.1046
D039	0.9728	0.5490	0.2468	0.1199	0.6984	0.3290
D040	0.9767	0.2888	0.2853	0.1809	0.8416	0.2662
D041	0.9934	0.8020	0.090'3	0.0862	0.5744	0.0677
D042	0.9889	0.8104	c). 1468	0.0222	0.5406	0.1335
	% CUM. VAR.	45.791	65.111	76.326	92.208	96.956

Table 5. Factor score matrix.

	1	2	3	4	5
gravel size	0.8262	-0.0345	-0.0289	0.3301	0.1309
sand size	-0.0525	-0.0958	-0.4956	-0.5926	0.4329
silt size	-0.0202	0.6255	-0.0009	0.0026	0.0049
clay size	-0.0188	0.5295	0.1285	-().().573	0.0610
terrigenous	0.5182	0.0743	0.1752	-0.6814	-0.2084
clay min.	0.1388	-0.0147	-0.0224	0.1441	0.2186
vole. ash	0.0932!	0.2429	-0.8172	0.1893	-0.1883
silic.micro.	0.0105I	0.1785	0.0929	0.0074	0.2144
foram.	-0.0147	0.4287	0.0s77	-0.0100	0.0318
large shells	-0.0143	-0.0032	0.0907	0.0866	0.7458
crushed shells	-0.0496	0.1940	0.1245	-0.0373	0.1232
fine carb.	0.1200	0.0076	-0.0325	0.0815	0.2162

Table 6. Concentrations of hydrocarbon gases and CO₂ at 1-m sediment depth.

Sample	Deepest Sample in Core (cm)	Number of Samples	Water Depth [m]	C ₁ (nl/L)	C ₂ (nl/L)	C ₂ :1 (nl/L)	C ₃ (nl/L)	C ₃ :1 (nl/L)	i-C ₄ (nl/L)	n-C ₄ (nl/L)	CO ₂ (nl/L)	Comment (AA - acoustic anomaly)
KILIUDA TROUGH												
343	197	4	153	150	200	20	35	20			1200	AA, Average C ₁
441	214	4	164	800	300	41	90	130	9	2cr	2000	Near AA, High C ₁ (Fig. 2)
440	243	4	156	6000	450	50	160	200	9	25	3300	AA, High C ₁ (Fig. 2)
344	210	4	155	2000	300	20	60	20			2500	Adjacent AA, High C ₁ (Fig. 2)
442	110	3	135	40	91	30	35	110	4	4	70	AA, Low C ₁
439	217	4	159	1100	230	25	60	110	5	13	2000	Possible AA, High C ₁ (Fig. 2)
347	110	3	138	370	200	20	40				1000	AA, Average C ₁
348	210	4	143	710	300	20	60				2600	AA, High C ₁ (Fig. 2)
349	310	5	145	190	2(30)	20	40	-			1800	Edge of AA, Average C ₁
358	160	4	122	8	35	20	10	16			300	Adjacent to fault, Low C ₁
359	66		152	80	15(1)	30	30				500	Adjacent to fault, Average C ₁
CHINIAX TROUGH												
231	81	1	182	>80	~100	~35	~100	~12			~1000	Mid trough, No AA
329	210	4	218	50000	80	20	170	7	7	70	5000	Head of trough, No AA, High C ₁ (Fig. 2)
432	169	4	135	~70	75	20	50	160			200	Mid trough, AA, Low C ₁
433	163	3	174	21	90	45	60	130	6	8	300	Mid trough, Adjacent AA, Low C ₁
435	100	3	158	14	70	160	25	160			160	
SITKINAX TROUGH												
355	358	4	314	5	30	25					700	No AA
356	320	3	370	~8000	~40000		300	75	40	30	~1000	No AA, High C ₁ and C ₂
357	357	3	240	30	100	30	20				600	No AA
CONTINENTAL SLOPE												
226	111	1	370	10	70	40	8	12			15011	Mid Albatross Bank
225	150	2	601	~7000	~12000	?	~300	?	20	?	2000	Mid Albatross Bank, No AA, High C ₁ , (Fig. 2)
224	130	2	992	~90	~1800	~30	~130				701	Mid Albatross Bank
241	10	1	172	9	nd	nd	nd	nd	nd	nd	nd	Slope
239	300	2	975	10 ⁺	140 ⁺	50 ⁺	40 ⁺	0 ⁺	10 ⁺	10 ⁺	700 ⁺	Slope
24r)	220	2	415	7	71	35	20	10			900	Slope
336	130	3	700	15	300	20	30				200	Slope
340	240	4	100	4	60	30	15	30			500	Landward of slope basin
33f3	110	3	586	13	50	25	20	30			600	Slope basin
333	110	3	2787	5	20	25					500	Slope basin
334	121	3	2857	4	25	30	10	50			250	Submarine canyon
332	410	6	3273	6	30	20	10	20			800	Trench slope
331	310	3	4895	9	31	10	5	10			700	Aleutian Trench

nd = not determinable for 1 m sediment depth; ⁺ determined at 150 cm sediment depth; - not measurable

Table 7. Carbon isotopic ($\delta^{13}\text{C}_1$) abundances
 (from Hampton and Kvenvolden, in press)

		CH_4	CO_2
439 G2	100-110	-76.9	-21.8
	207-217	-85.5	-23.1
440 G1	143-151	-80.4	-23.4
	235-243	-83.1	-14.3

PDB = Pee Dee Belemnite standard. Values in this table are reported relative to this standard

FIGURE CAPTIONS

- FIG. 1 - Location map of Kodiak Shelf, western Gulf of Alaska.
- FIG. 2 - **Tracklines** of seismic reflection profiles run by R/V SEA SOUNDER and R/V **S.P. LEE**, 1976-1979.
- FIG. 3 - Station locations.
- FIG. 4 - Lithospheric plate boundaries, Gulf of **Alaska**. (From von Huene et al., 1979).
- FIG. 5 - Locations of deep structural basins and transverse tectonic boundaries. (After Fisher et al., 1981).
- FIG. 6 - Epicenters in the vicinity of Kodiak Shelf. a) magnitudes $M_B > 4$ from 1954-1963, b) magnitudes $M_B > 5$ in the 1964 Alaska earthquake series, c) magnitudes $M_B > 5$ from 1965-1975, d) January-June 1978. Letter code represents **hypocentral** depth range (A: 0-25 km, B: 25-50 km, etc.) **Data** compiled by H. **Pulpan**, University of Alaska.
- FIG. 7 - Shallow **folds** and faults. Modified from von Huene et al. (1980).
- FIG. 8 - Major **physiographic** features.
- FIG. 9 - Sparker seismic reflection profile showing typical geologic nature of the shelf break. Dashed line separates bedrock **anticline** (below) from prograding unconsolidated sediment (above).
- FIG. 10 - Sparker seismic reflection profile showing double shelf breaks.
- Fig. 11 - **Uniboom** seismic reflection profile showing inclined strata and bedrock ridges on the seafloor.
- FIG. **12** - Locations of large sand waves and major sand wave fields.
- FIG. 13 - Seafloor slopes. Coverage extends from 3-mile limit to 1000 m contour. Contours in percent.
- FIG. 14 - Generalized thickness map of **surficial** unconsolidated **sedimentary** units.
- FIG. 15 - **Surficial** sedimentary units (from Thrasher, 1979). See Table 3 for description.
- FIG. 16 - Locations of samples in which factor 1 has highest factor loading.
- FIG. **17** - Locations of samples in which factor 2 has highest factor loading.
- FIG. 18 - Locations of samples in which factor **3** has highest factor loading.
- FIG. 19 - Locations of samples in which factor **4** has highest factor loading.

- FIG. 20 - Locations of samples in which factor 5 has highest factor loading.
- FIG. 21 - Weight percents of volcanic ash in **surficial** sediment samples, relative to total **terrigenous** material (including clay minerals) finer than 2 mm. (Revised from Hampton et al., 1979).
- FIG. **22** - **Uniboom** seismic reflection profiles showing large sand waves. a) seaward-facing sand waves, Stevenson Trough, b) symmetrical and asymmetrical waves, southern Albatross Bank.
- FIG. 23 - Locations of stations where sediment samples were analyzed for hydrocarbon gases and CO₂.
- FIG. 24 - Changes in Cl concentrations with depth at eight stations having the highest Cl concentrations. Compiled by **K.A. Kvenvolden**.
- FIG. 25 - Locations of acoustic anomalies. See text for description of anomaly types.
- FIG. 26 - **Uniboom** seismic reflection profile showing acoustic anomaly type 1 (see text) in center of record, flanked by type 5 on left and type 3 on right.
- FIG. 27 - **Uniboom** seismic reflection profile showing acoustic anomaly type 2 (see text).
- FIG. 28 - **Uniboom** seismic reflection profile showing acoustic anomaly type 3 (see text).
- FIG. 29 - **Uniboom** seismic reflection profile showing acoustic anomaly type 4 (see text). a) sharply discontinuous reflectors with more-or-less transparent intervals, b) discontinuous reflectors with murky intervals.
- FIG. 30 - **Uniboom** seismic reflection profile showing acoustic anomaly type 4 (**see text**).
- FIG. 31 - **Uniboom** seismic reflection profile showing acoustic anomaly type 6 (see text).
- FIG. 32 - Seismic reflection records from Middle Albatross Bank. (a) 12 kilohertz **fathogram** showing probable gas seep from the seafloor. (b) 800 joule **boomer** record along same **trackline** as (a) showing acoustic anomalies within the sediment.
- FIG. 33 - Locations of seismic-reflection profiles showing sediment slides.
- FIG. 34 - Sparker seismic reflection profile showing features indicating sediment slides.
- FIG. 35 - Sparker seismic reflection profile showing **hummocky** seafloor and **lack** of coherent sub-bottom **reflectors**; indicators of possible sediment slides.

FIG. 36 - **Uniboom** seismic reflection profile showing small, shallow sediment slides.

FIG. 37 - Sparker seismic reflection profiles showing similar structural styles near the shelf break of a) southern Albatross Bank and b) **Portlock** Bank, indicating severe tectonic deformation.

FIG. 38 - Sparker seismic reflection profile near the shelf break of northern Albatross Bank showing only relatively minor tectonic deformation.

FIG. 39 - **Uniboom** seismic reflection profile showing glacial deposit with rough, partially truncated high spots, and low areas, **infilled** by probable reworked material.

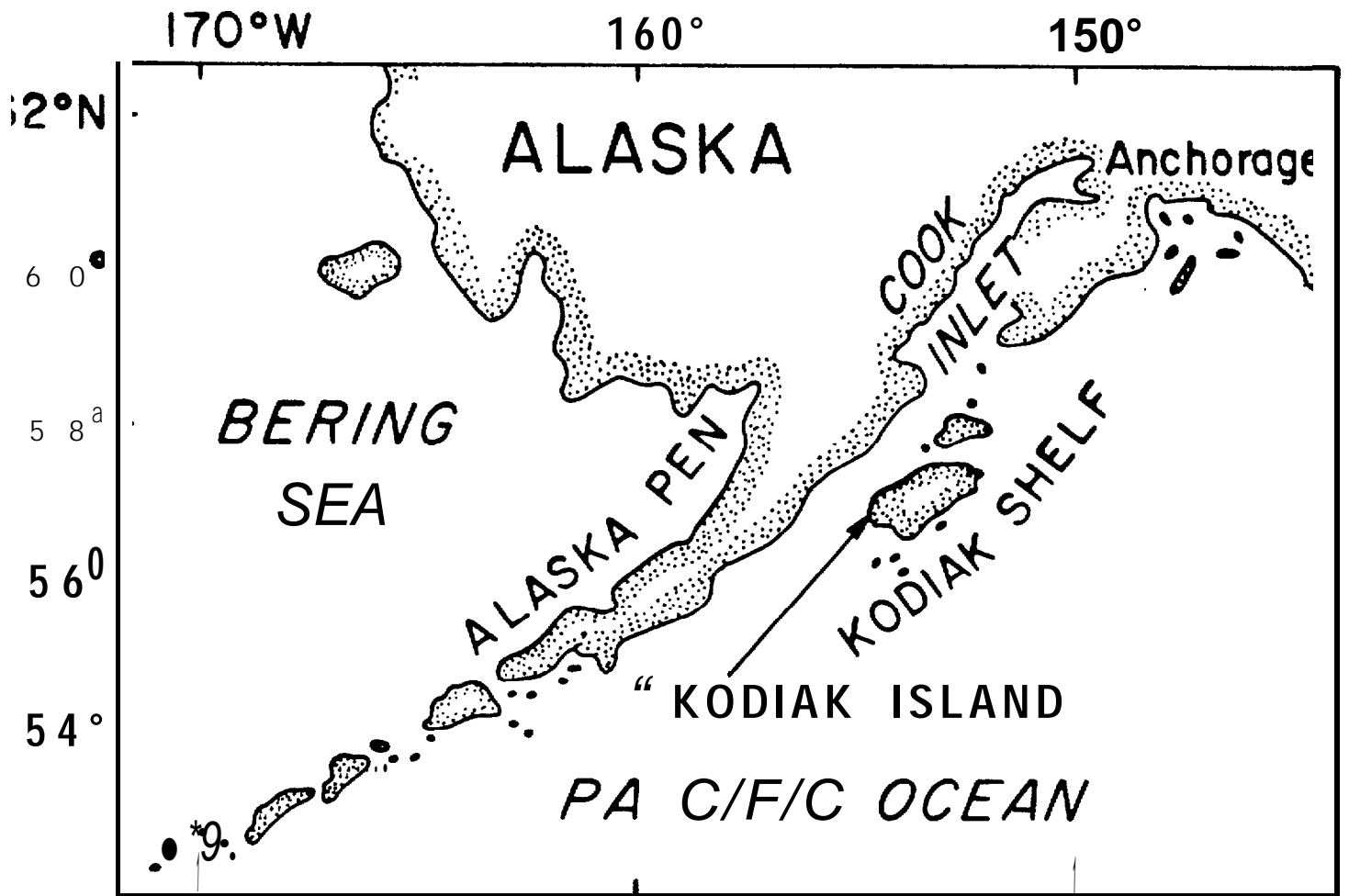


Fig. 1

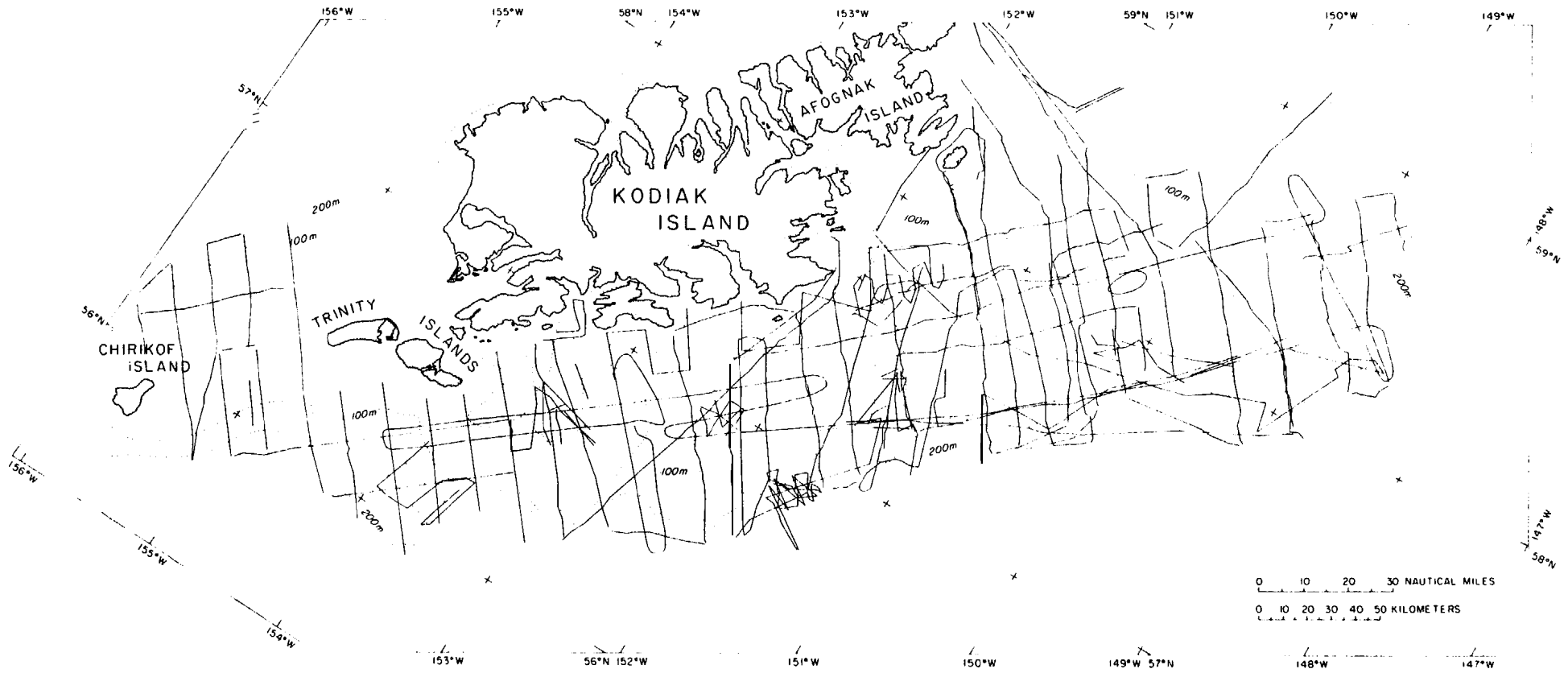


Fig. 2

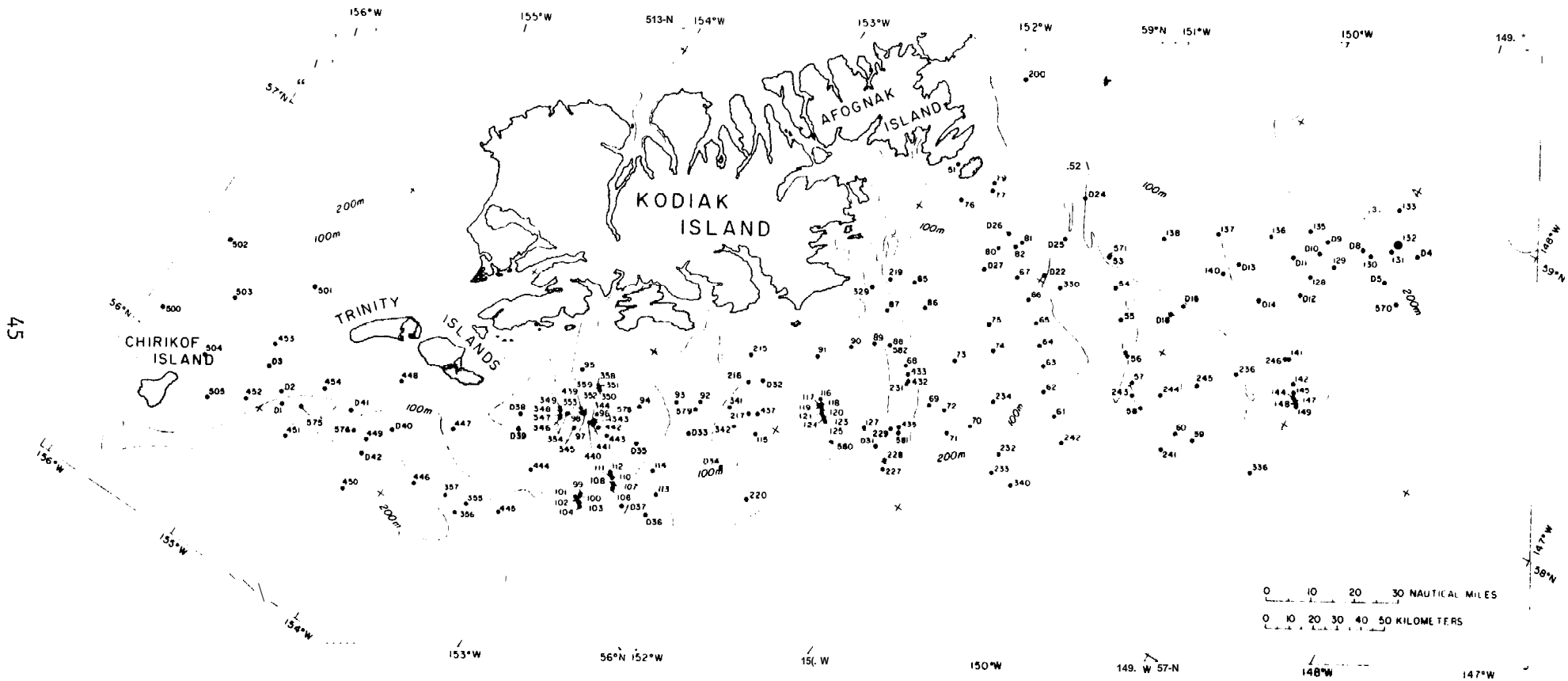


Fig. 3

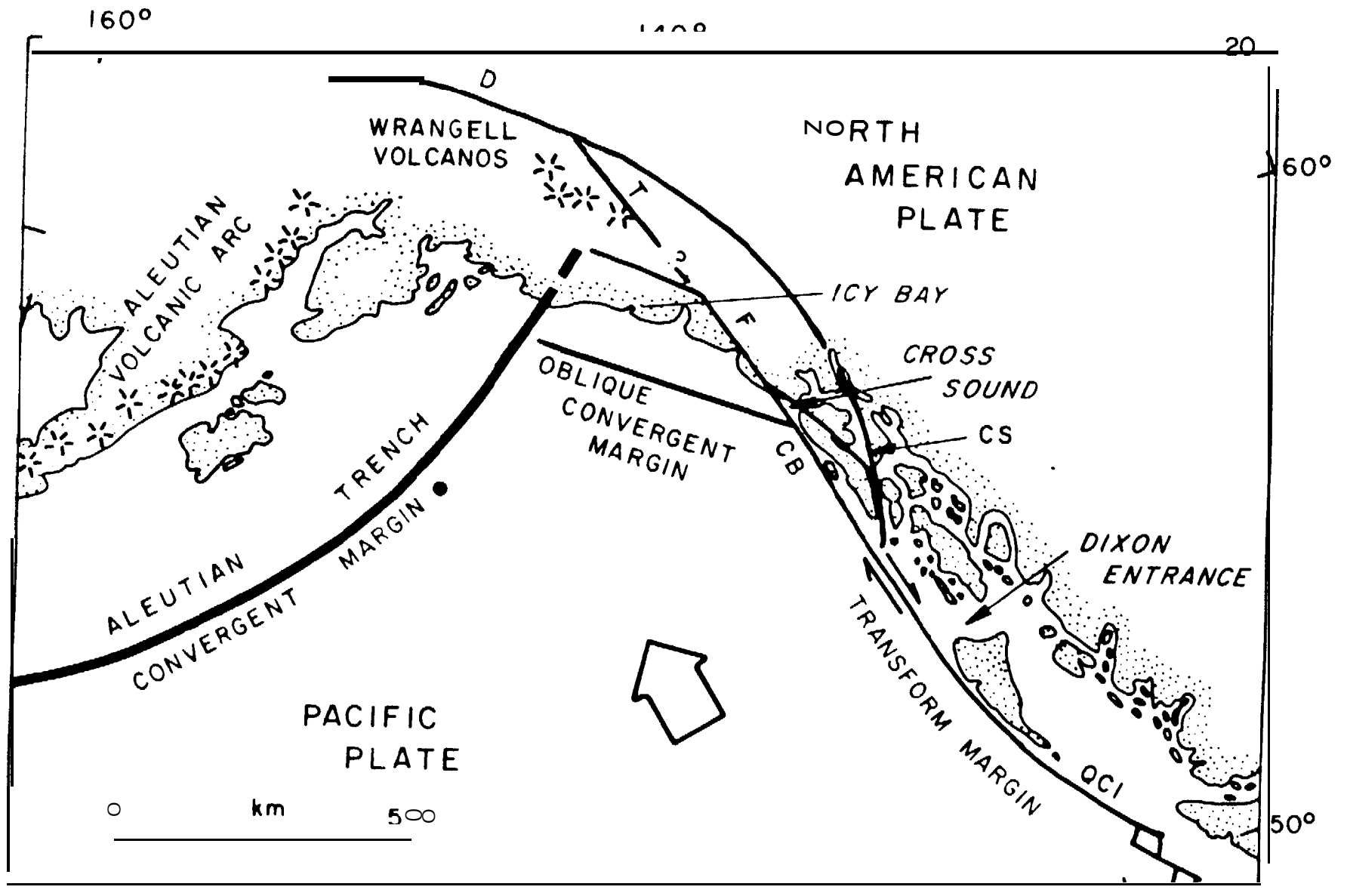


Fig. 4

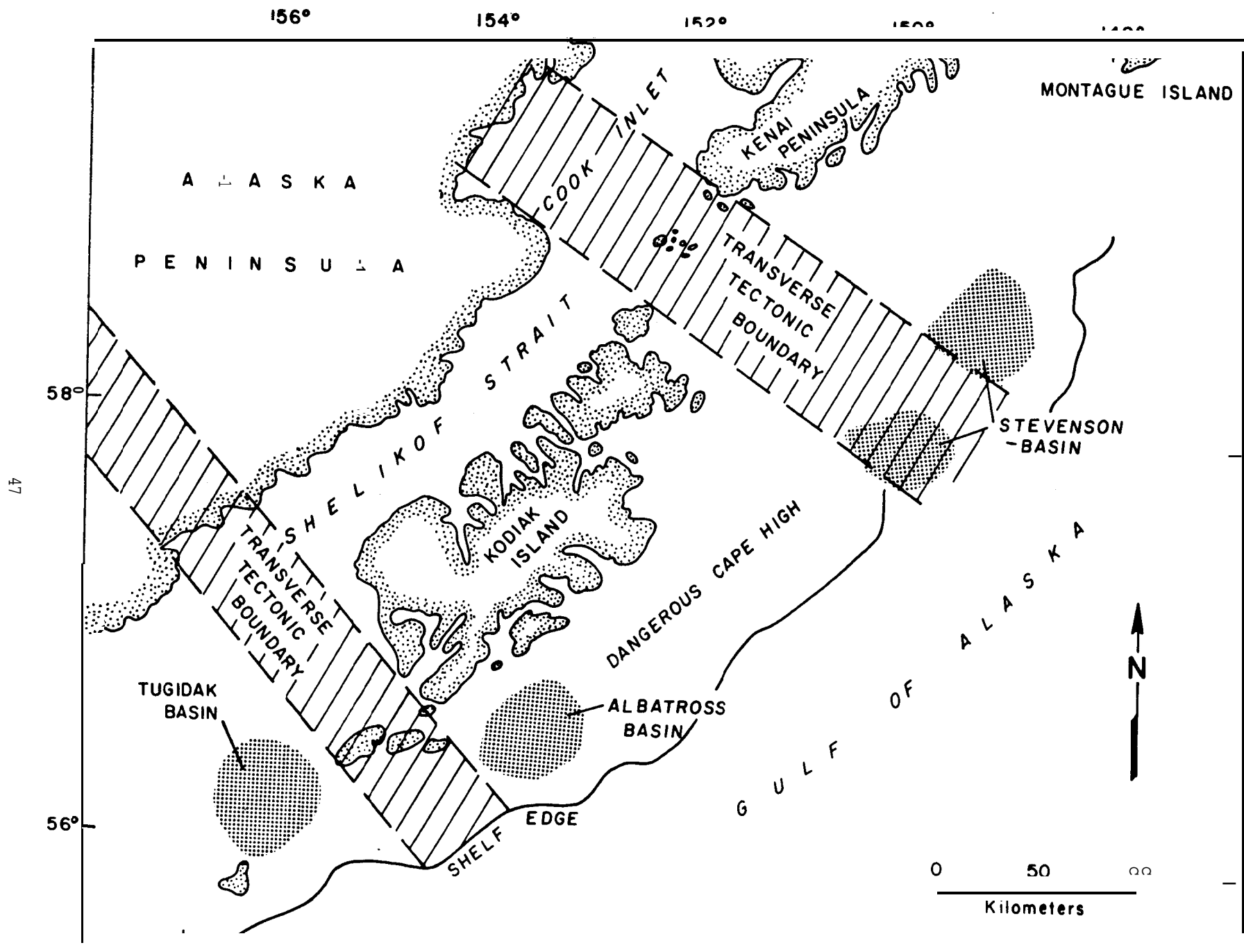
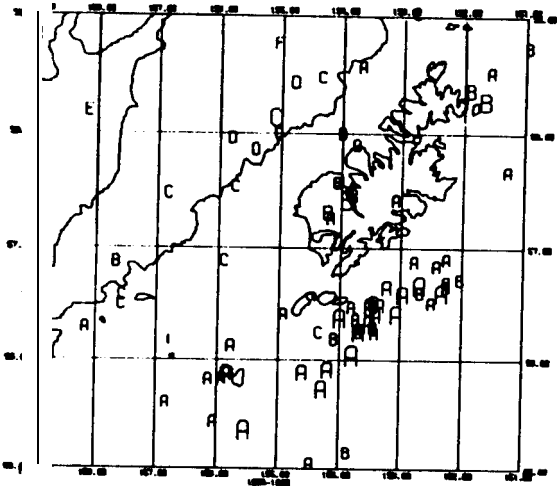
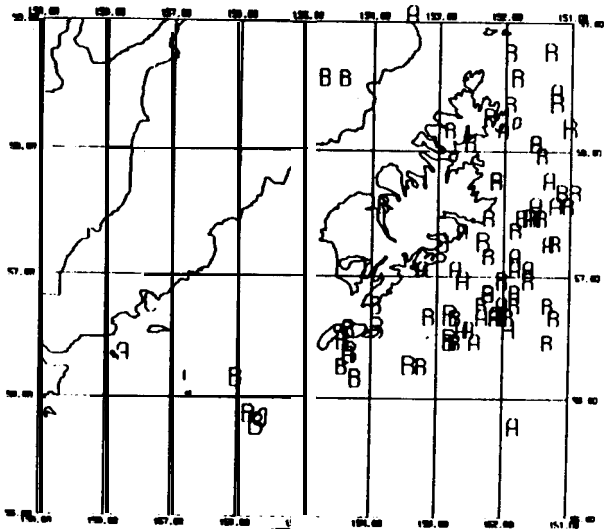


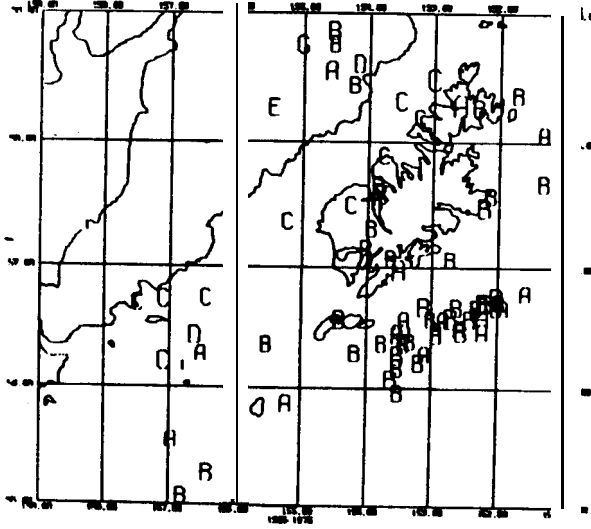
Fig. 5



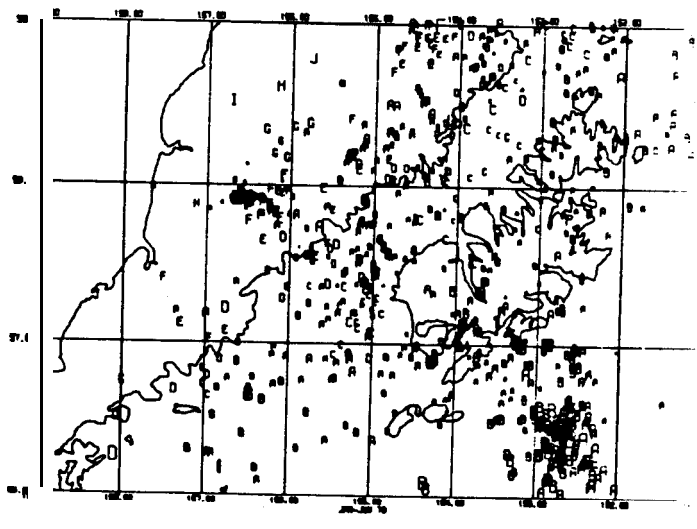
a



b



c



d

Fig. 6

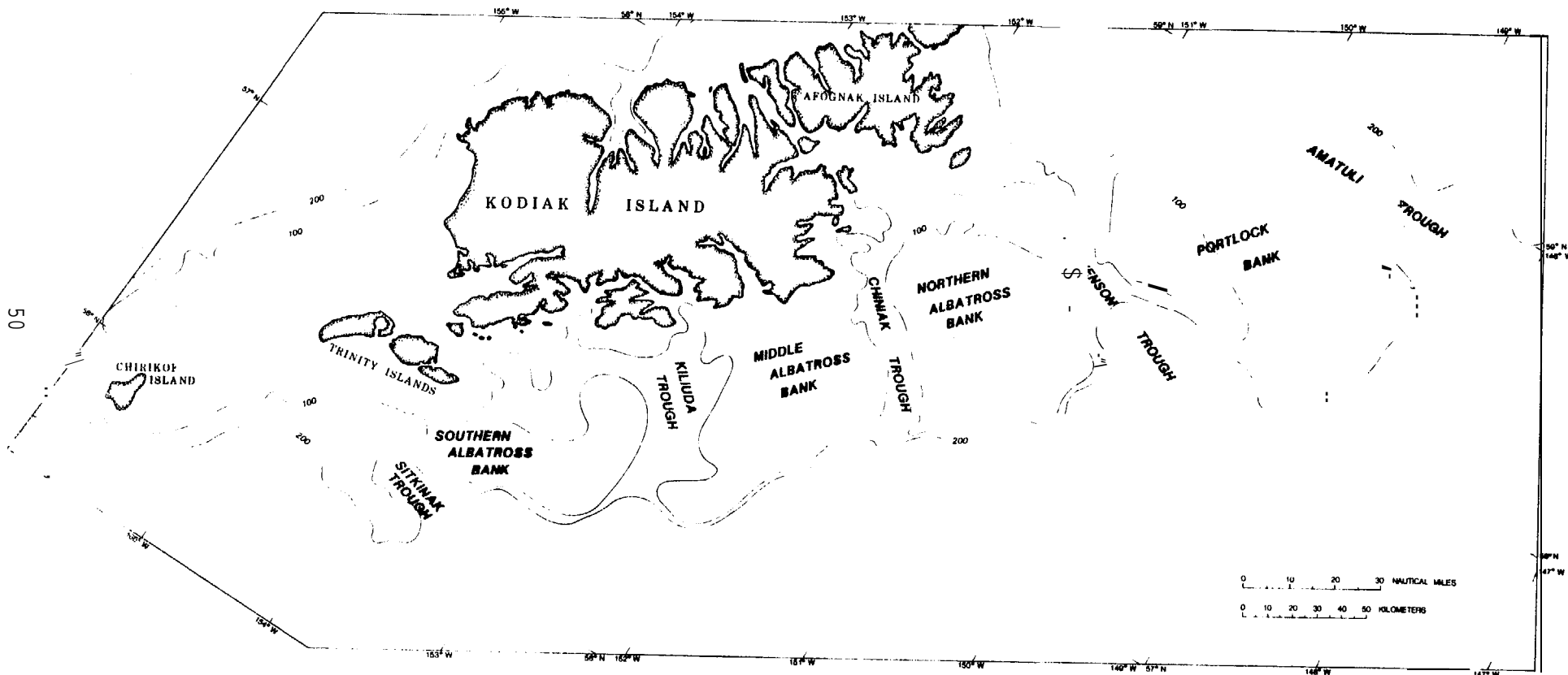


Fig. 8

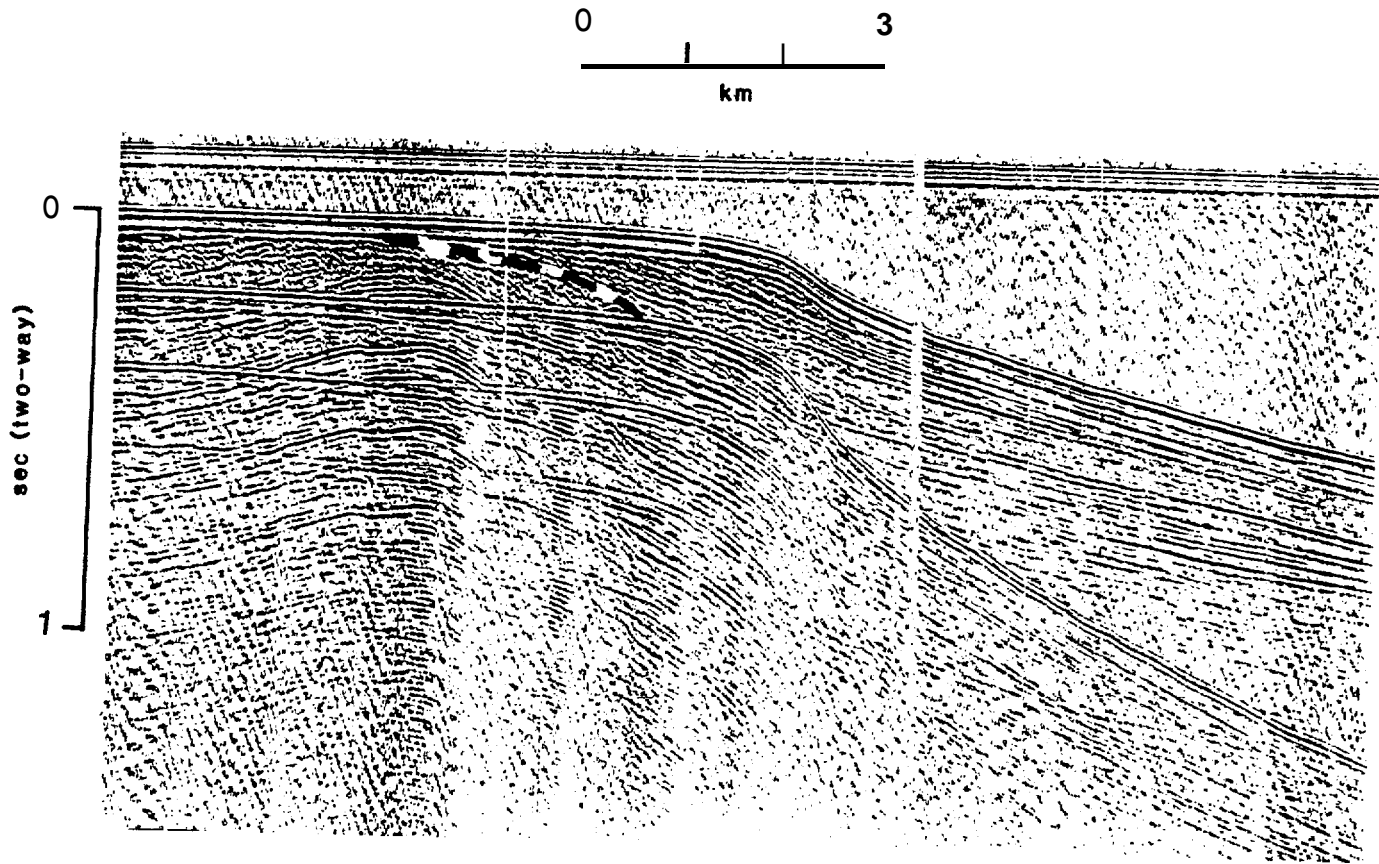


Fig. 9

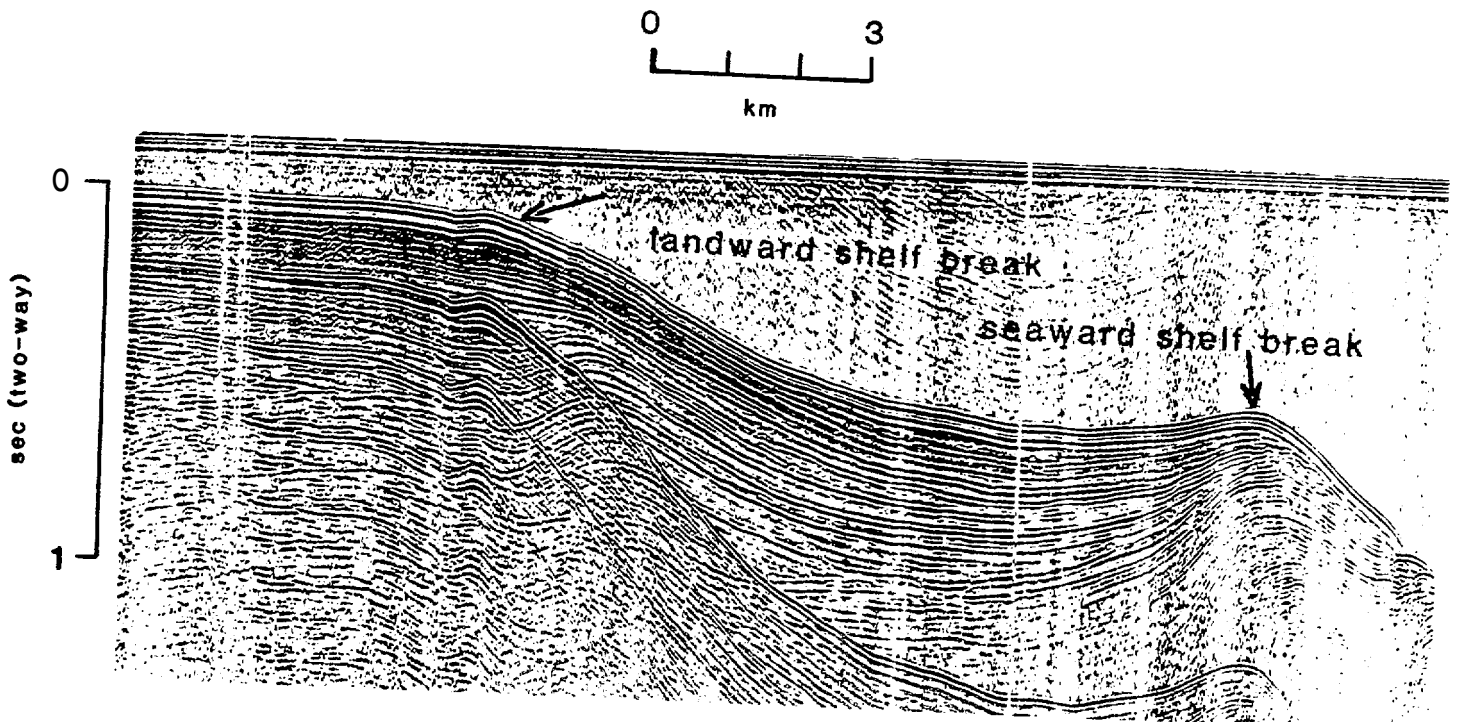


Fig. 10

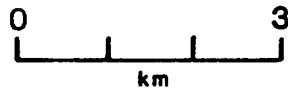


Fig. 11

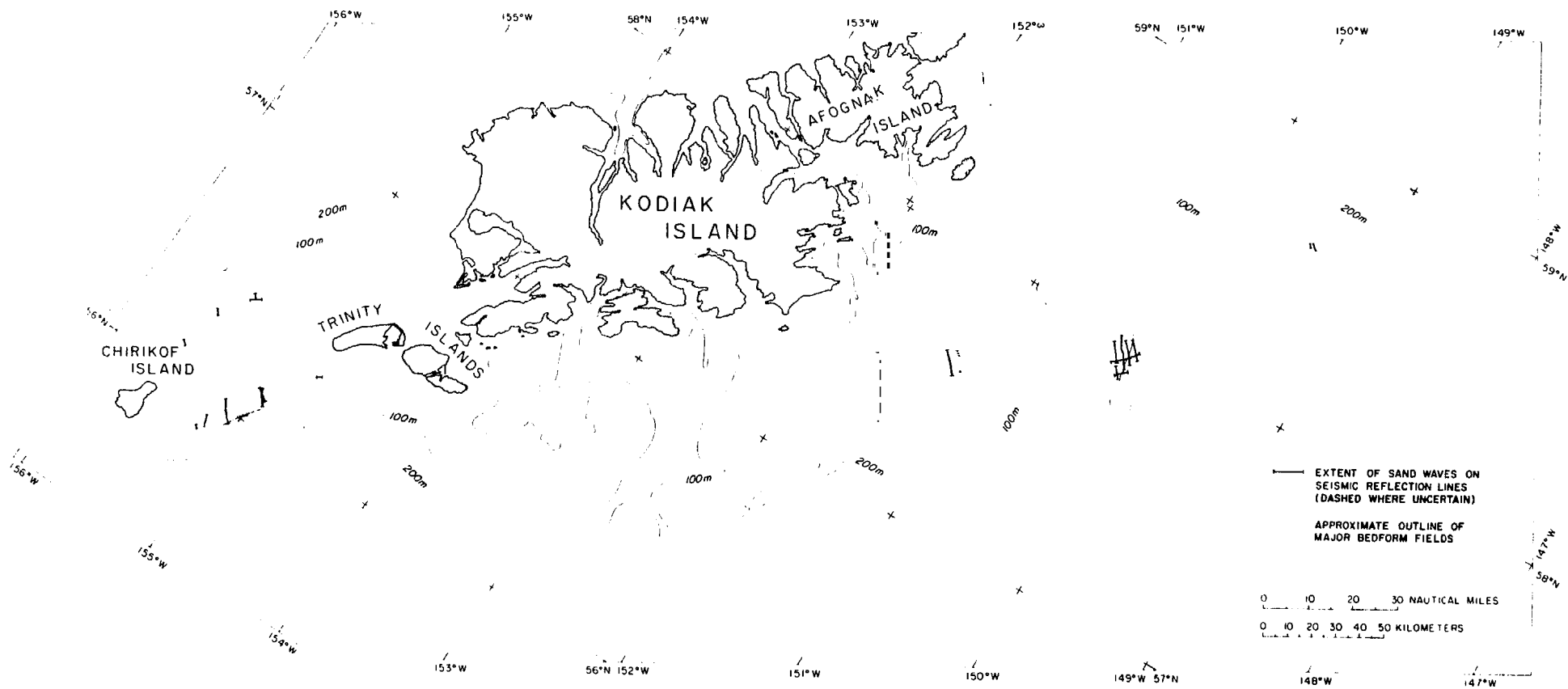


Fig. 12



Fig. 13

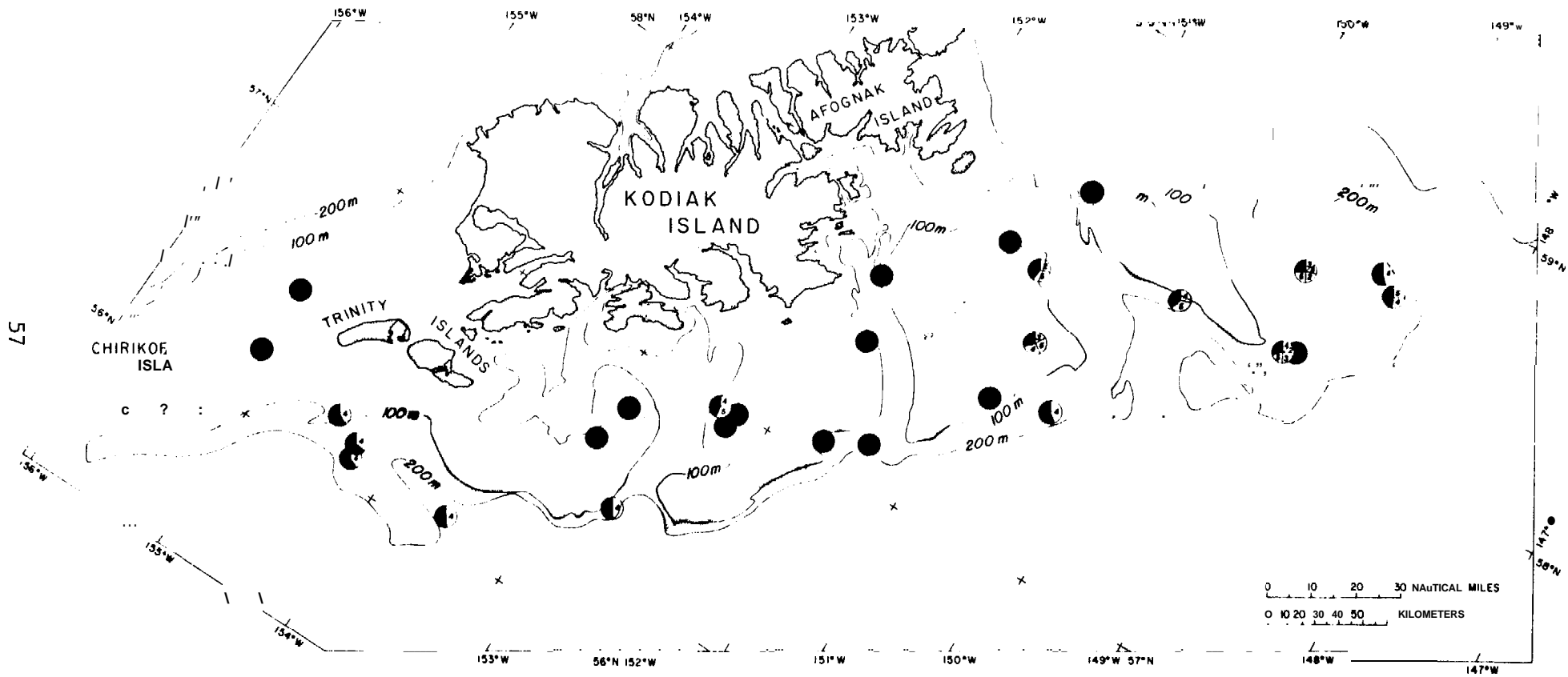


Fig. 16

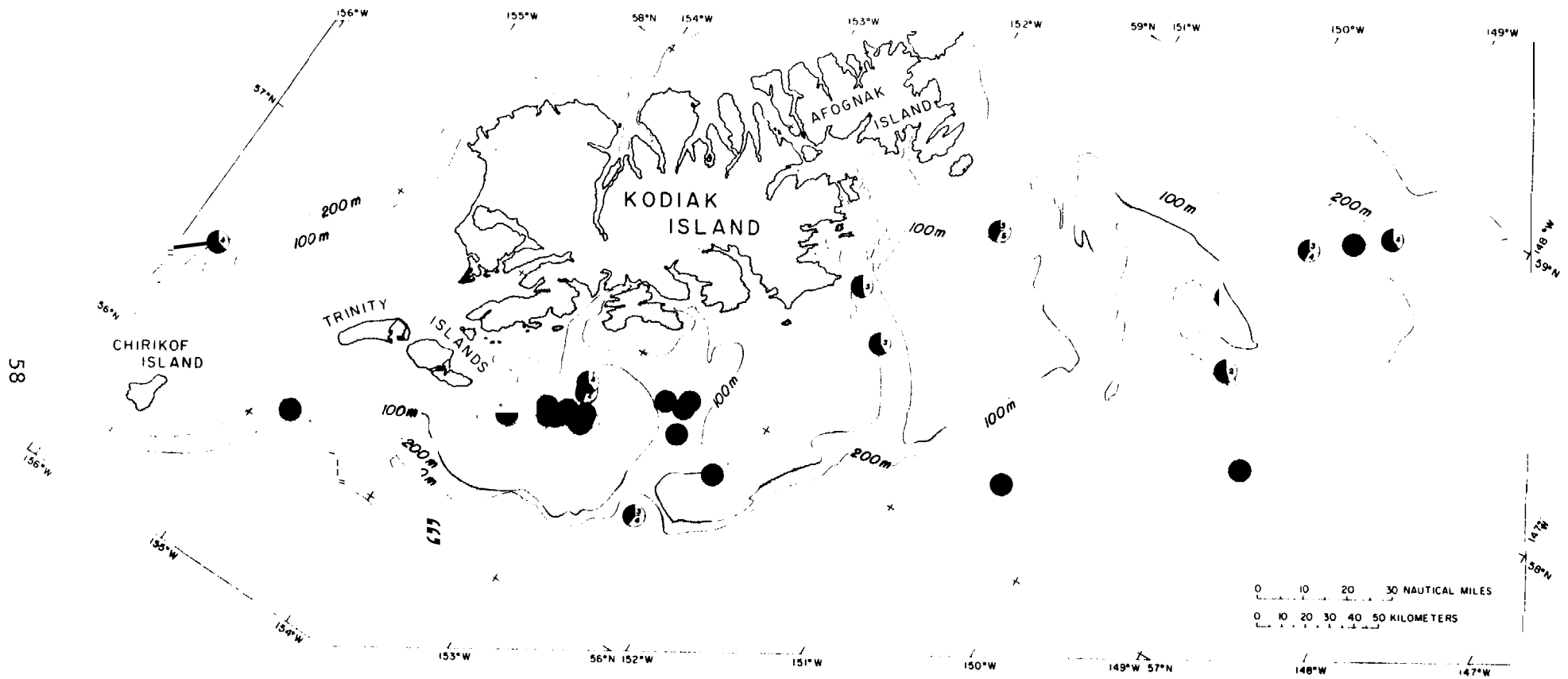


Fig. 17

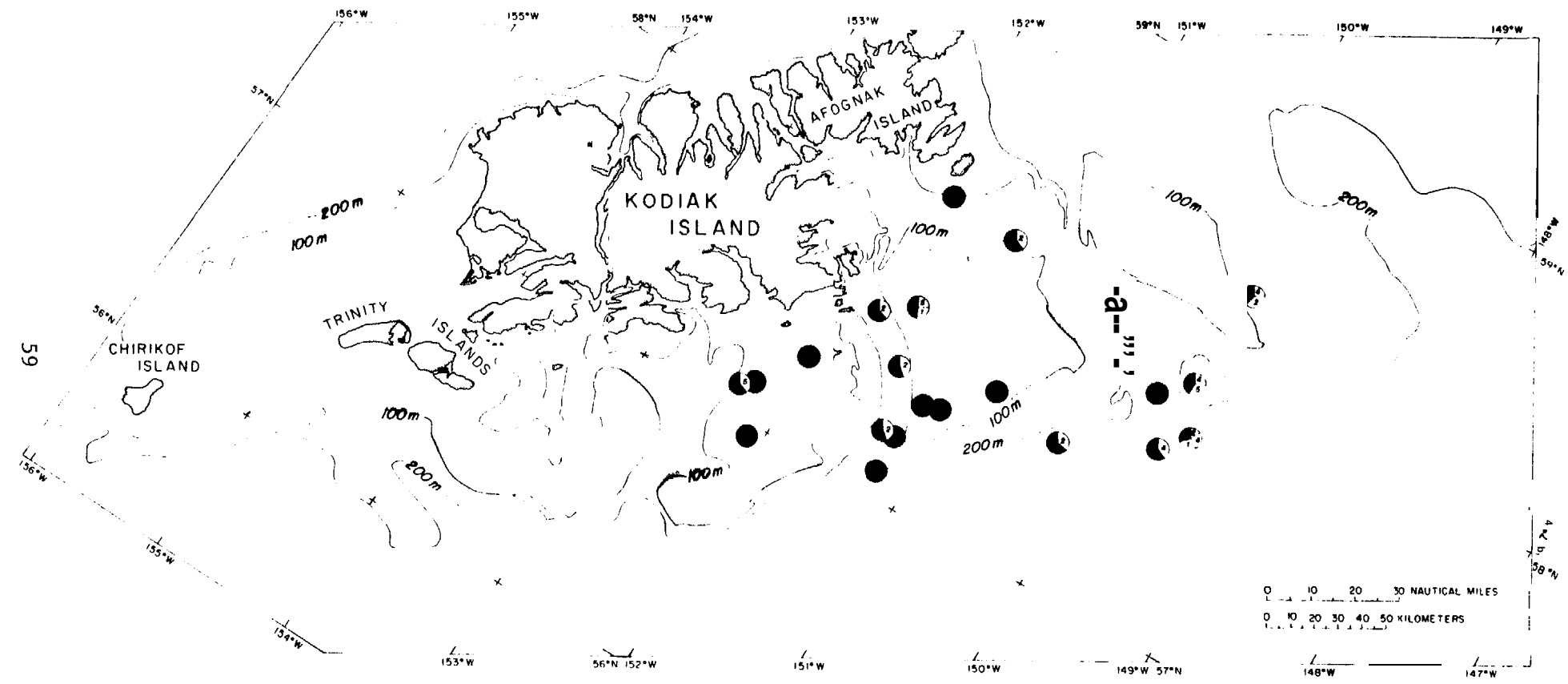


Fig. 8

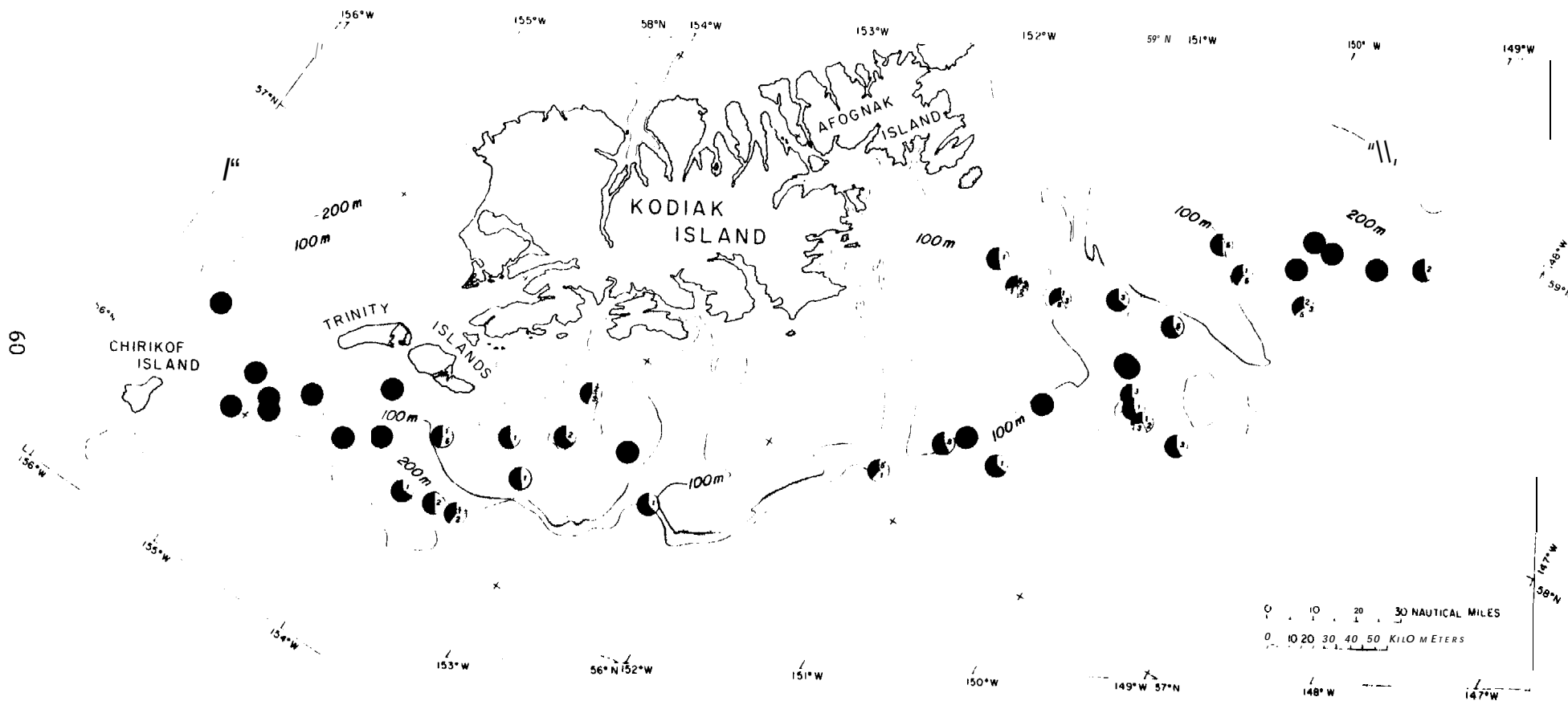


Fig. 19

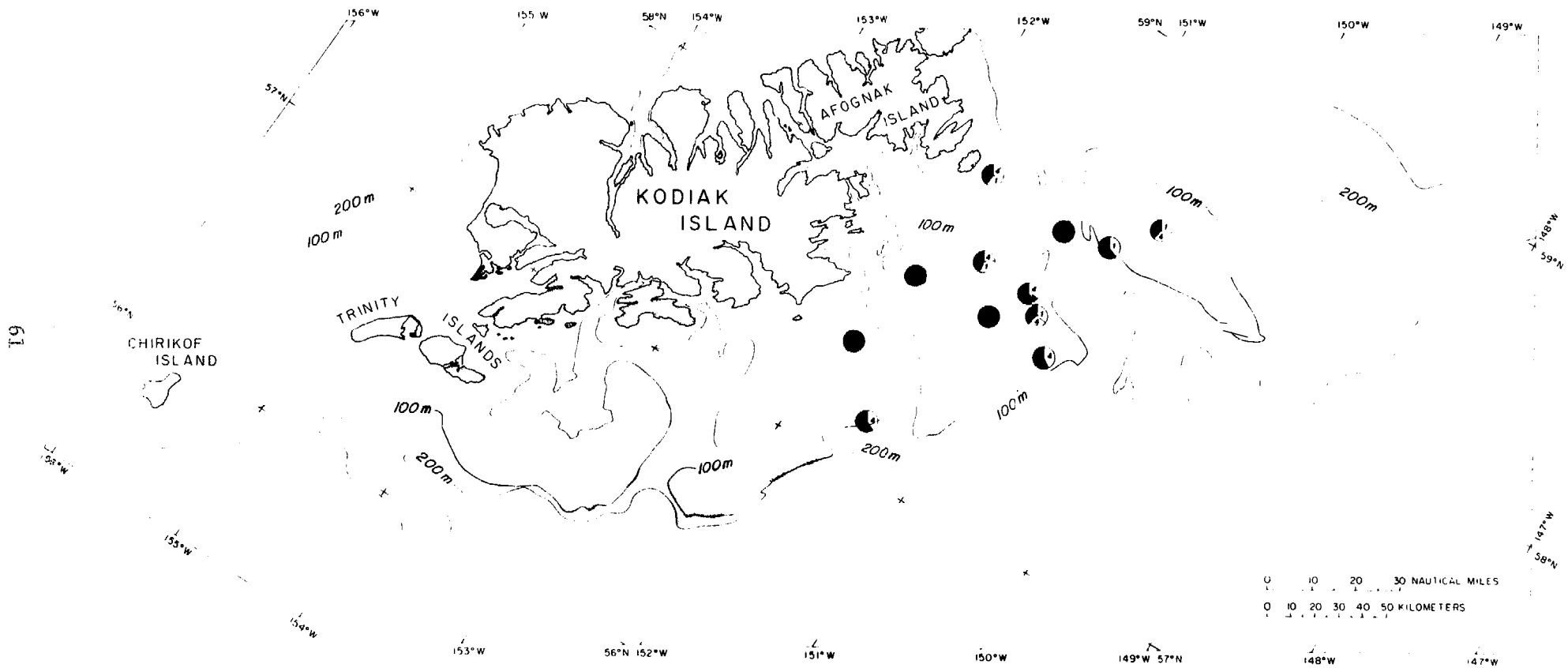


Fig 20

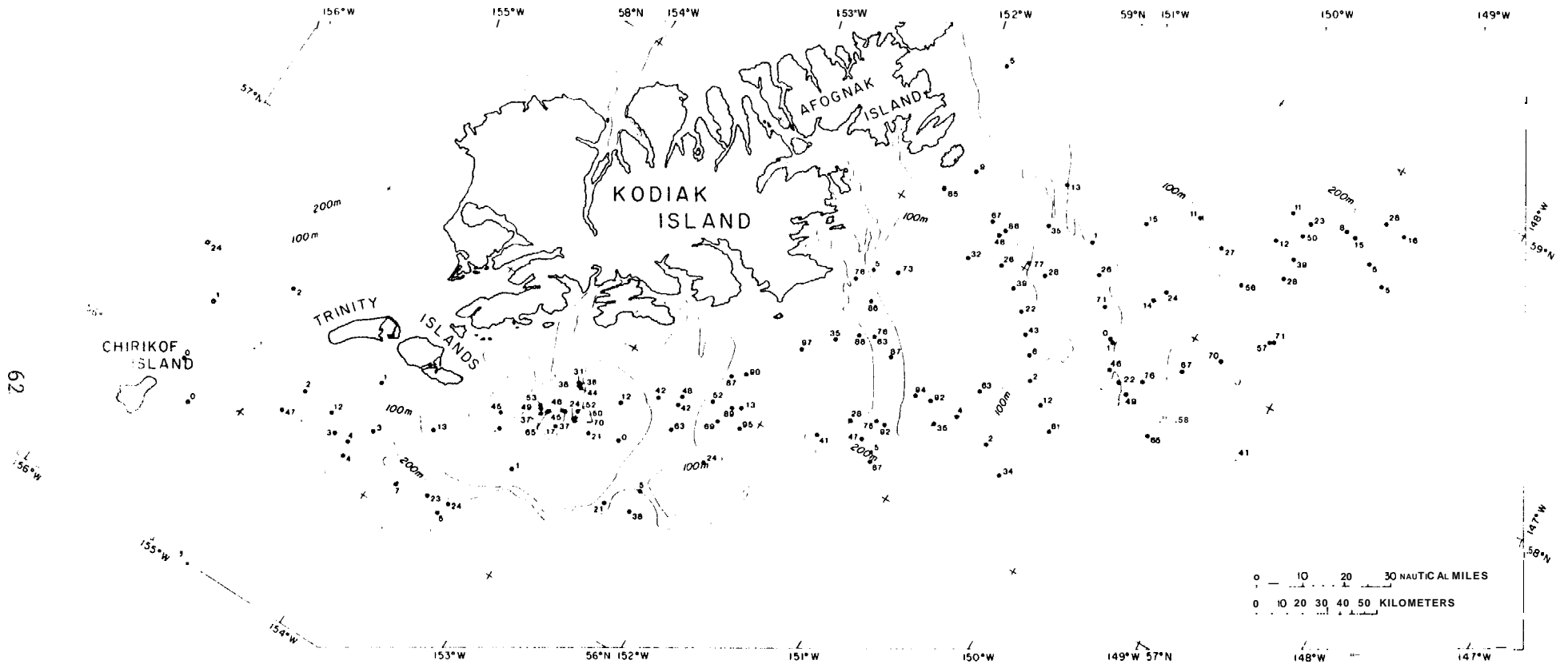
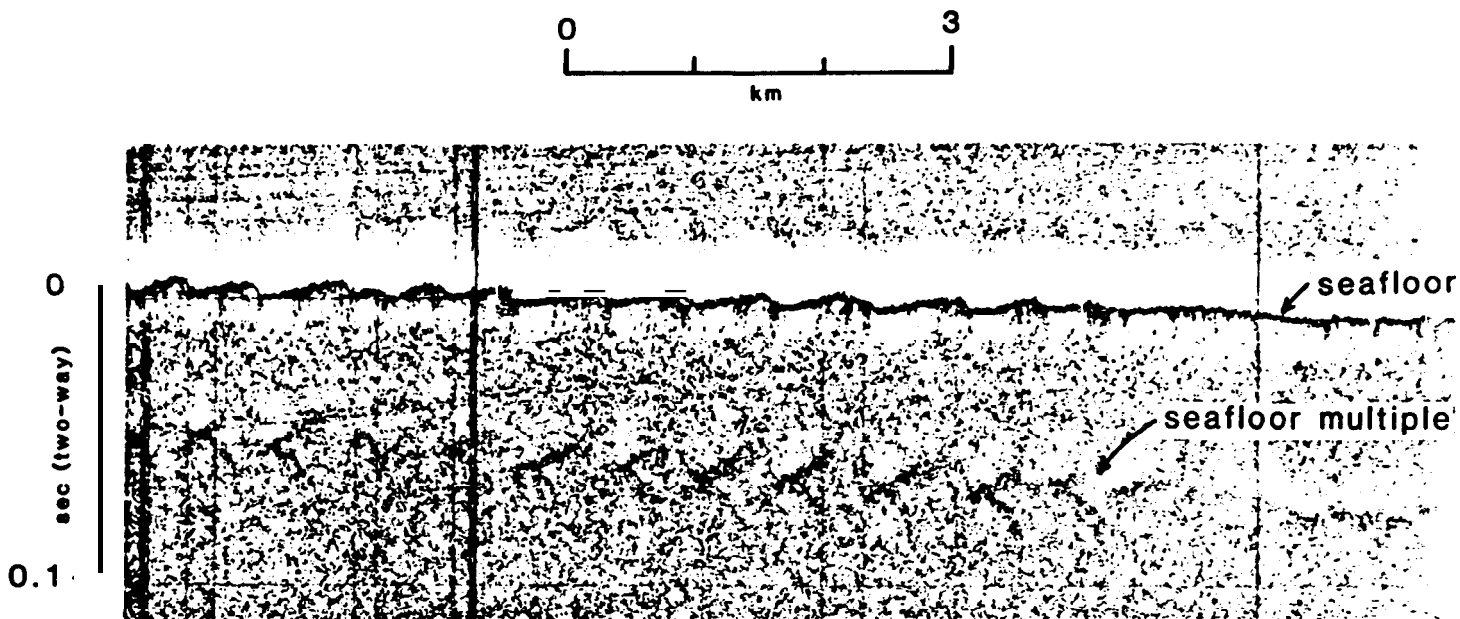
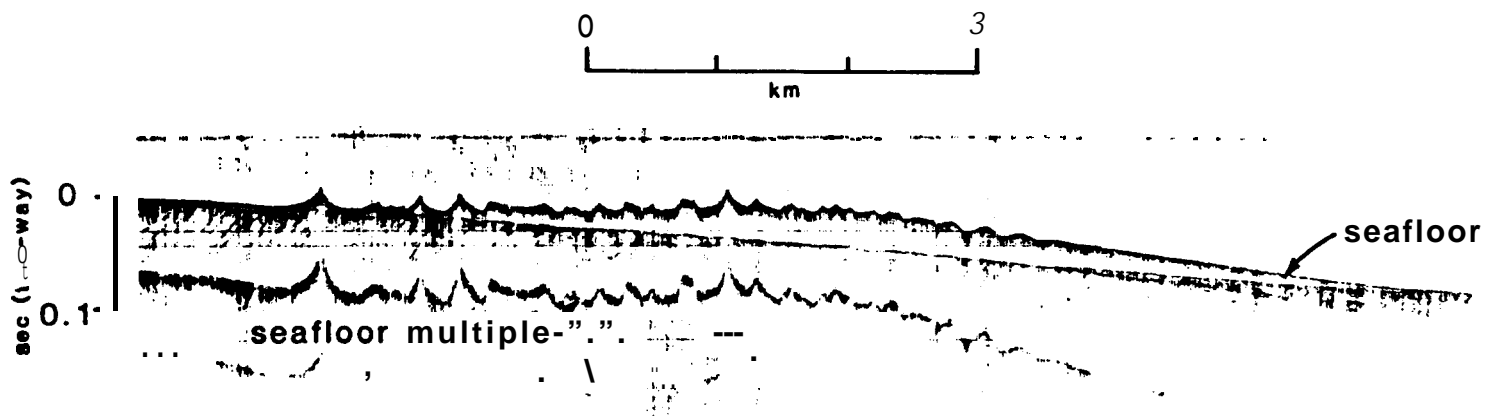


Fig. 21



a



b

Fig. 22

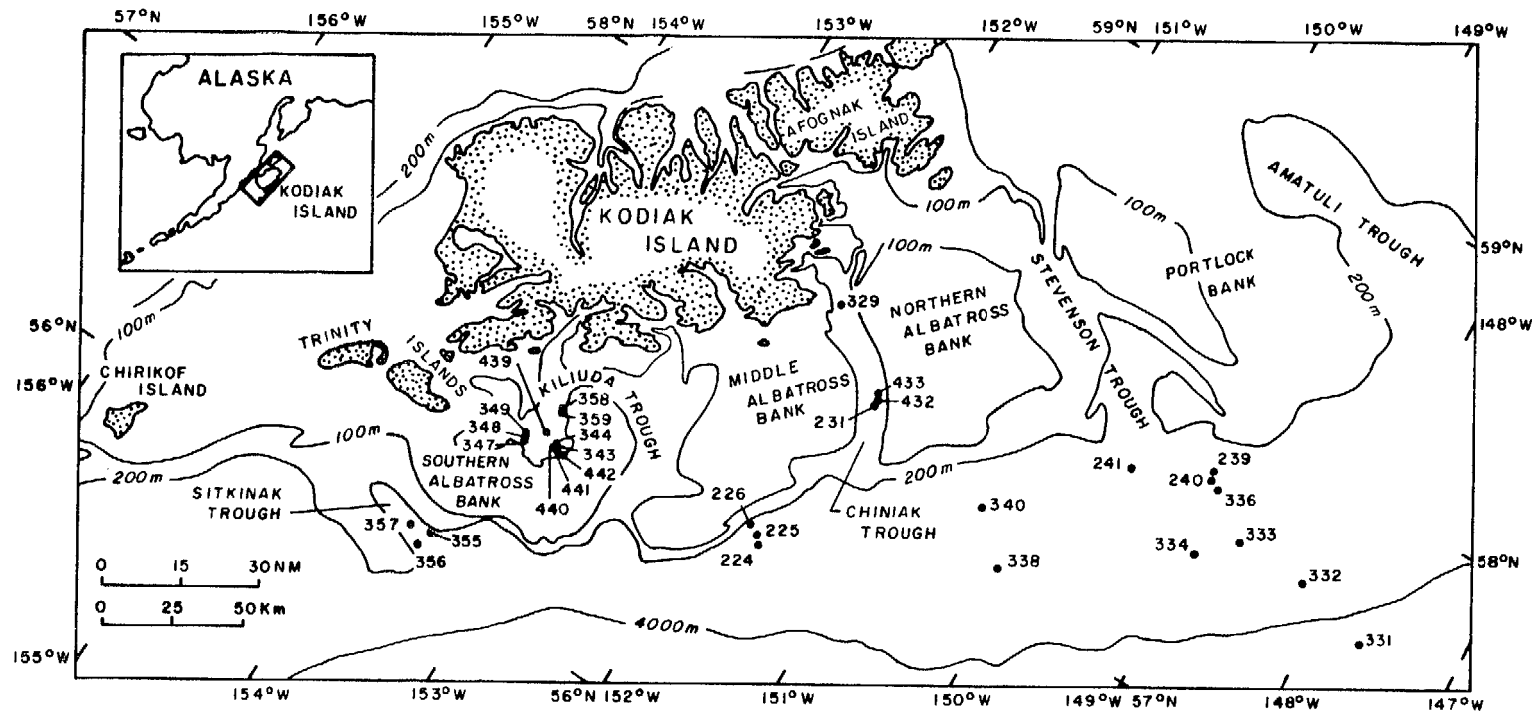


Fig. 23

LOG₁₀ CONCENTRATIONS OF C₁ IN μl/l OF INTERSTITIAL WATER

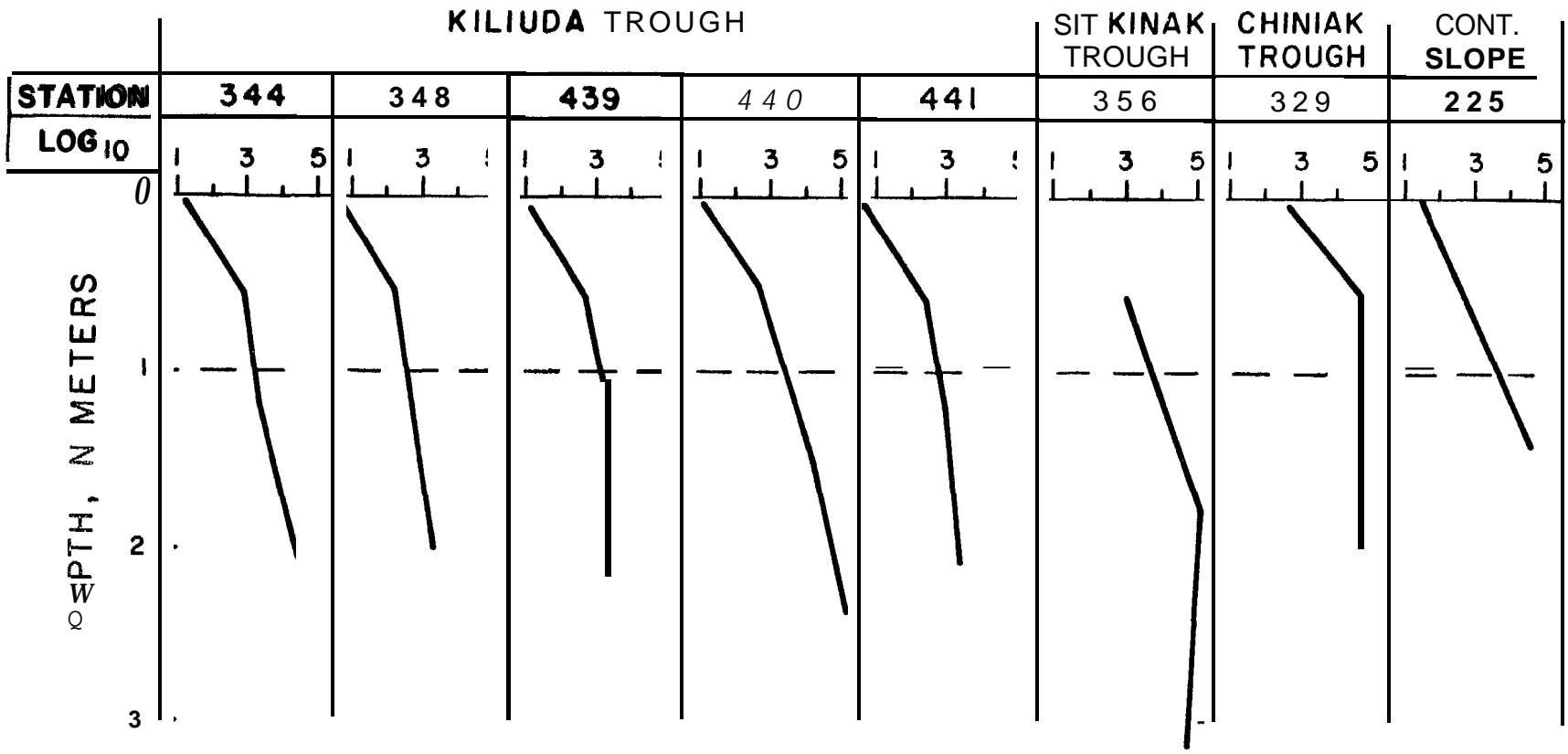


Fig. 24

65

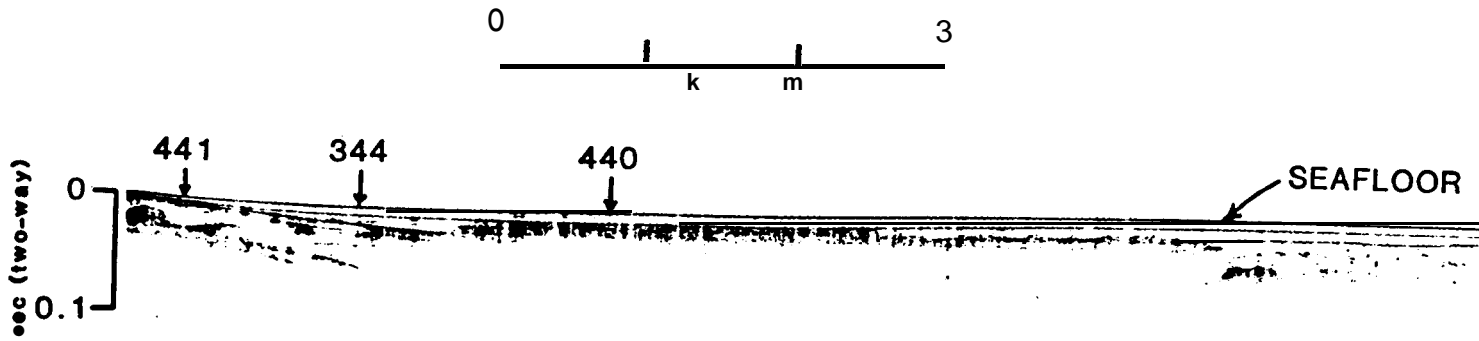


Fig. 26

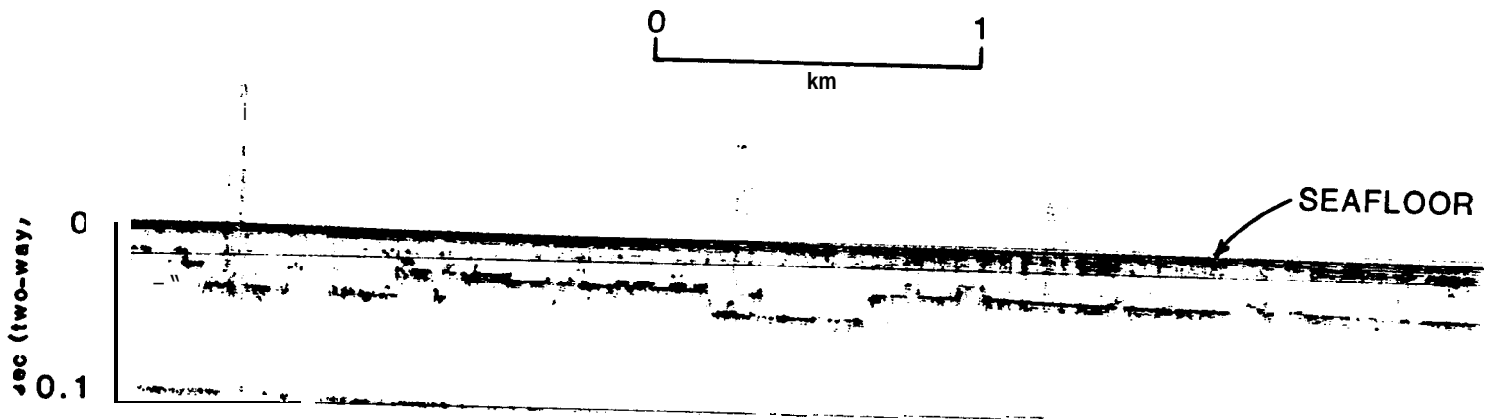


Fig. 27

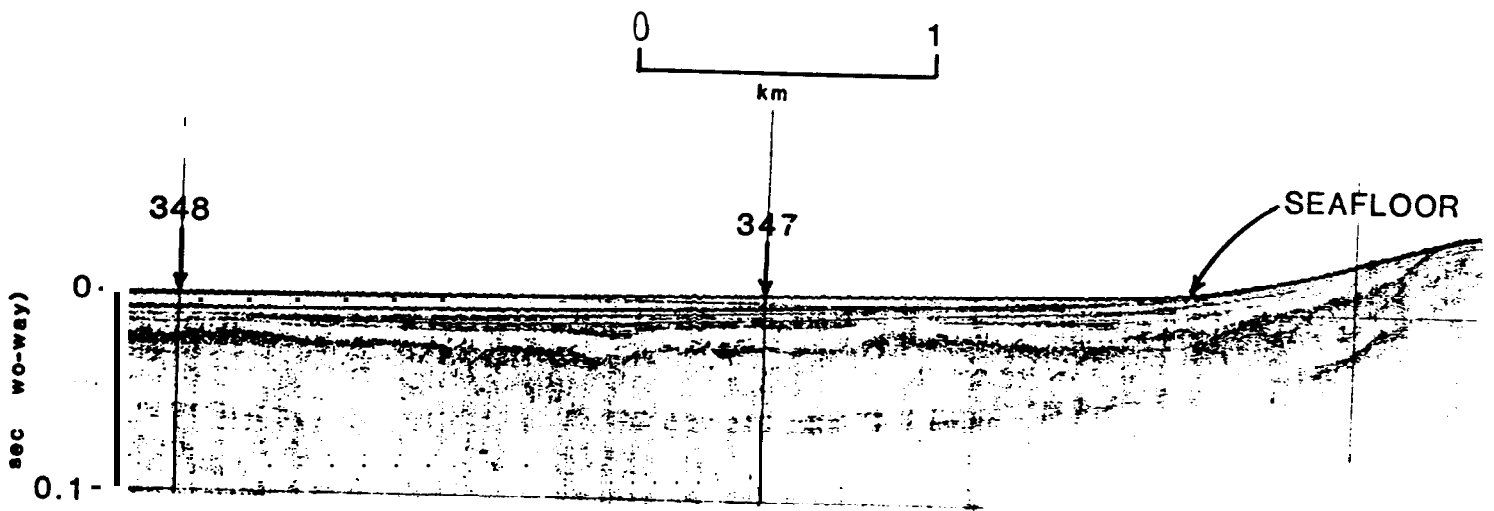


Fig. 28

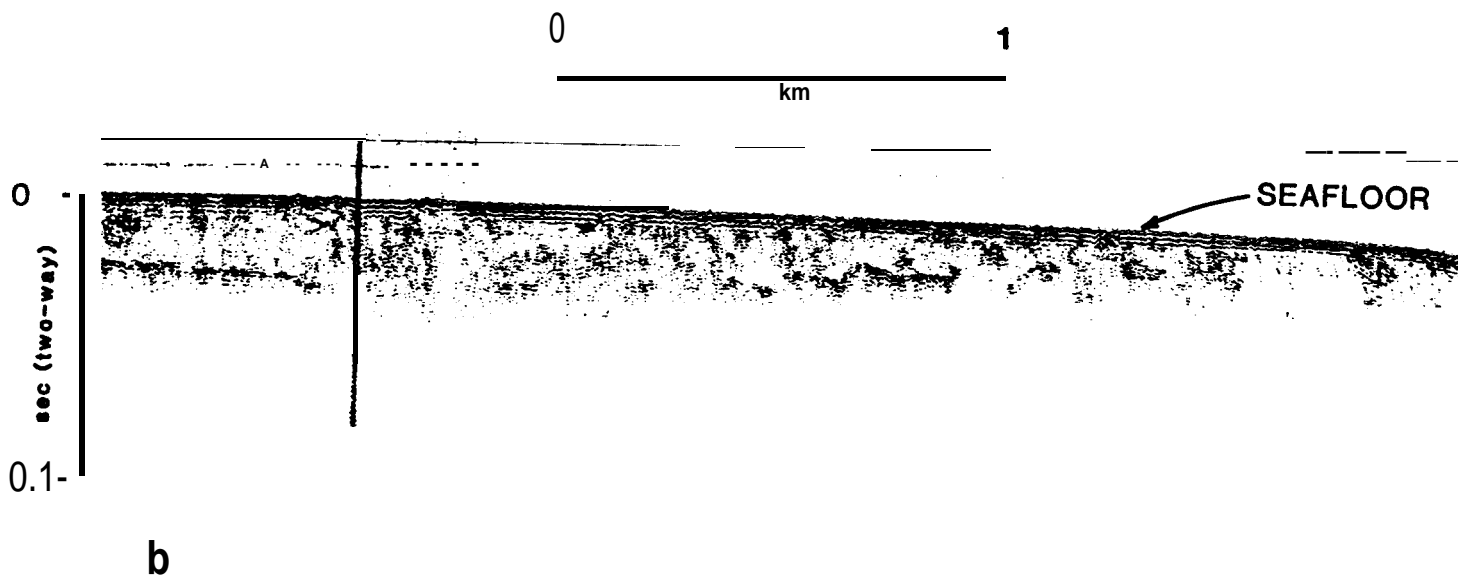
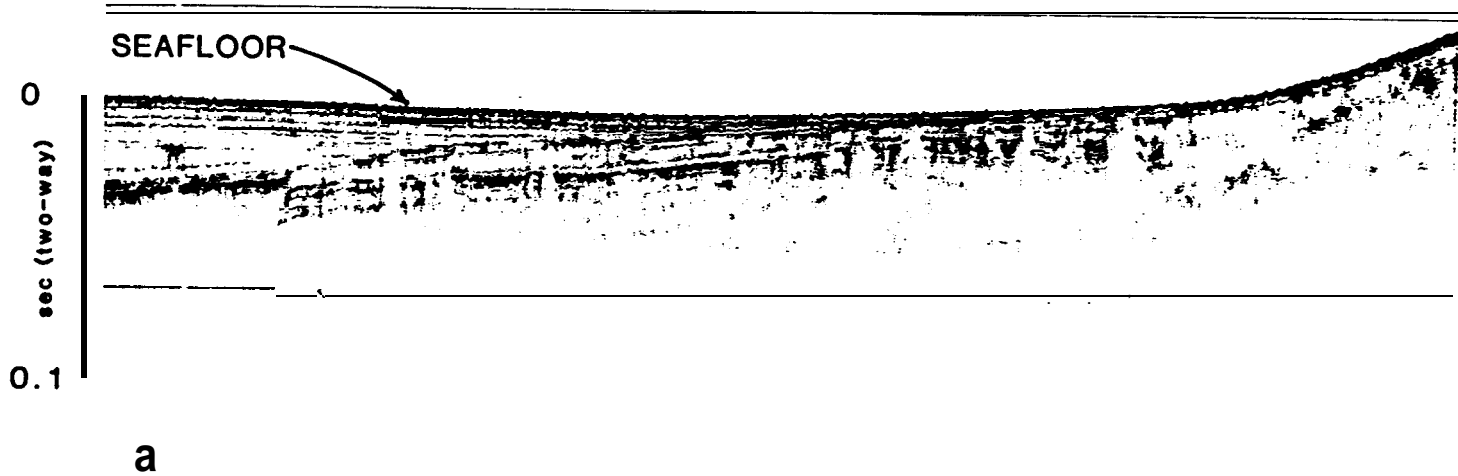
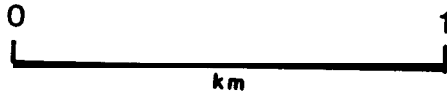
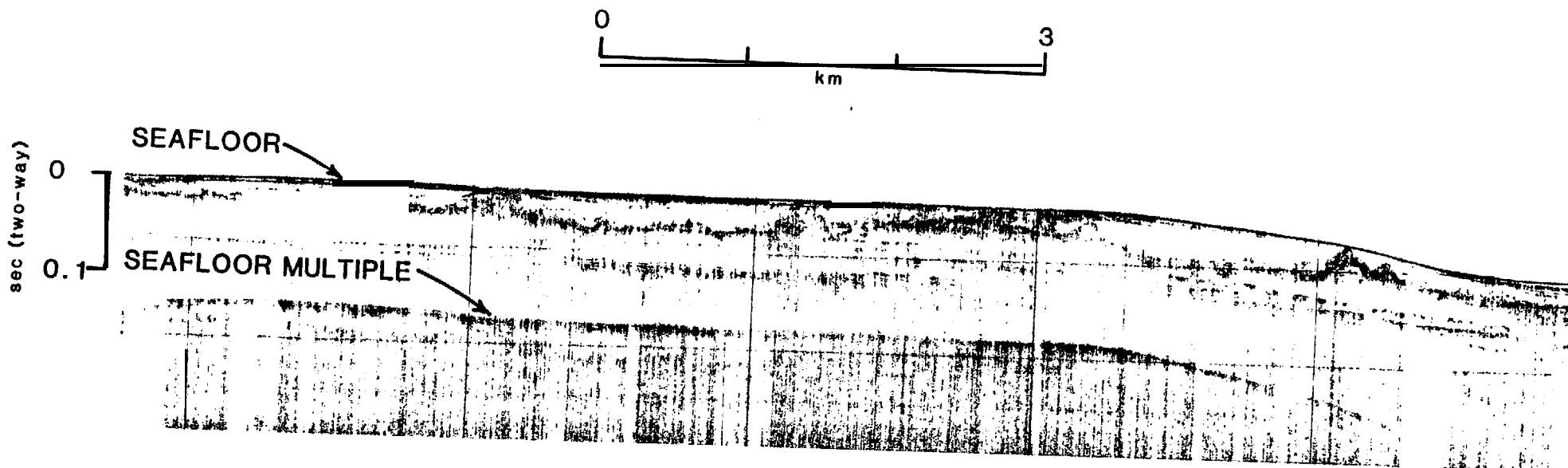


Fig. 29



69

Fig. 30

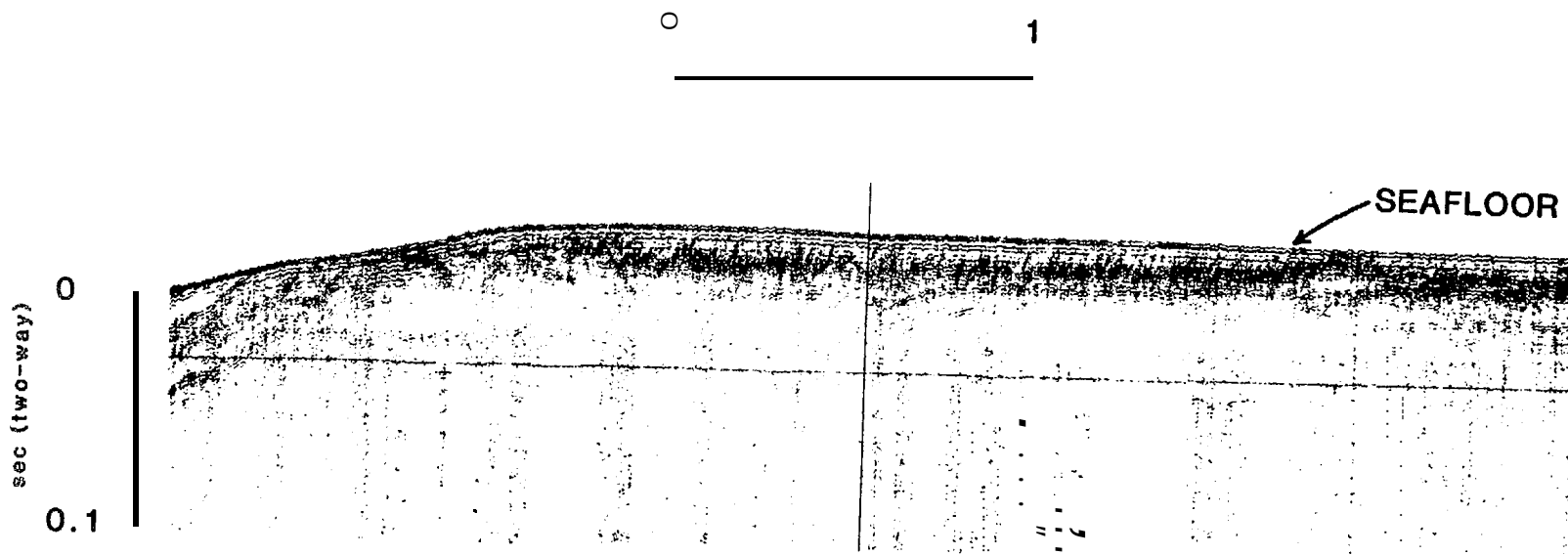


Fig. 31

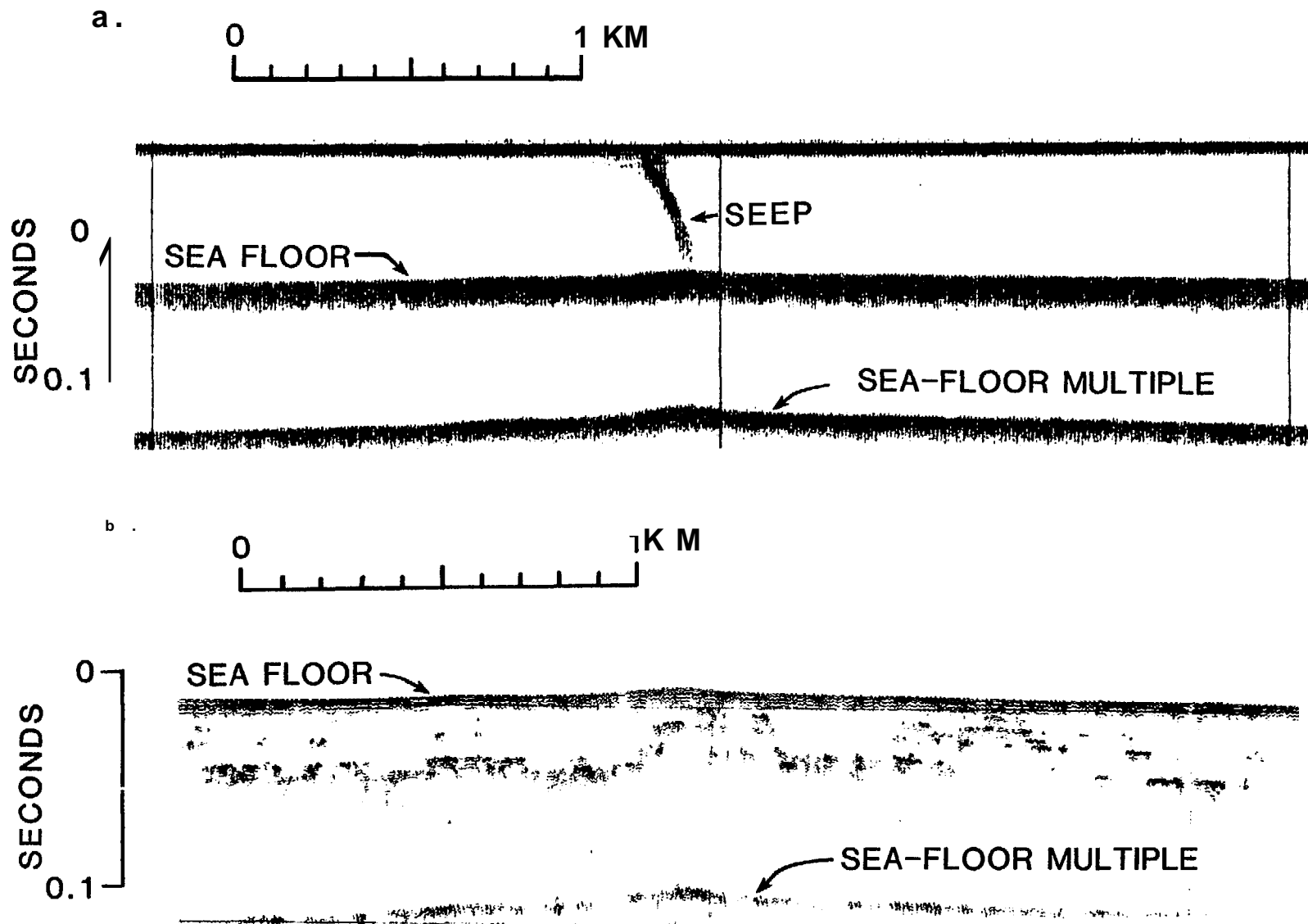


Fig. 32

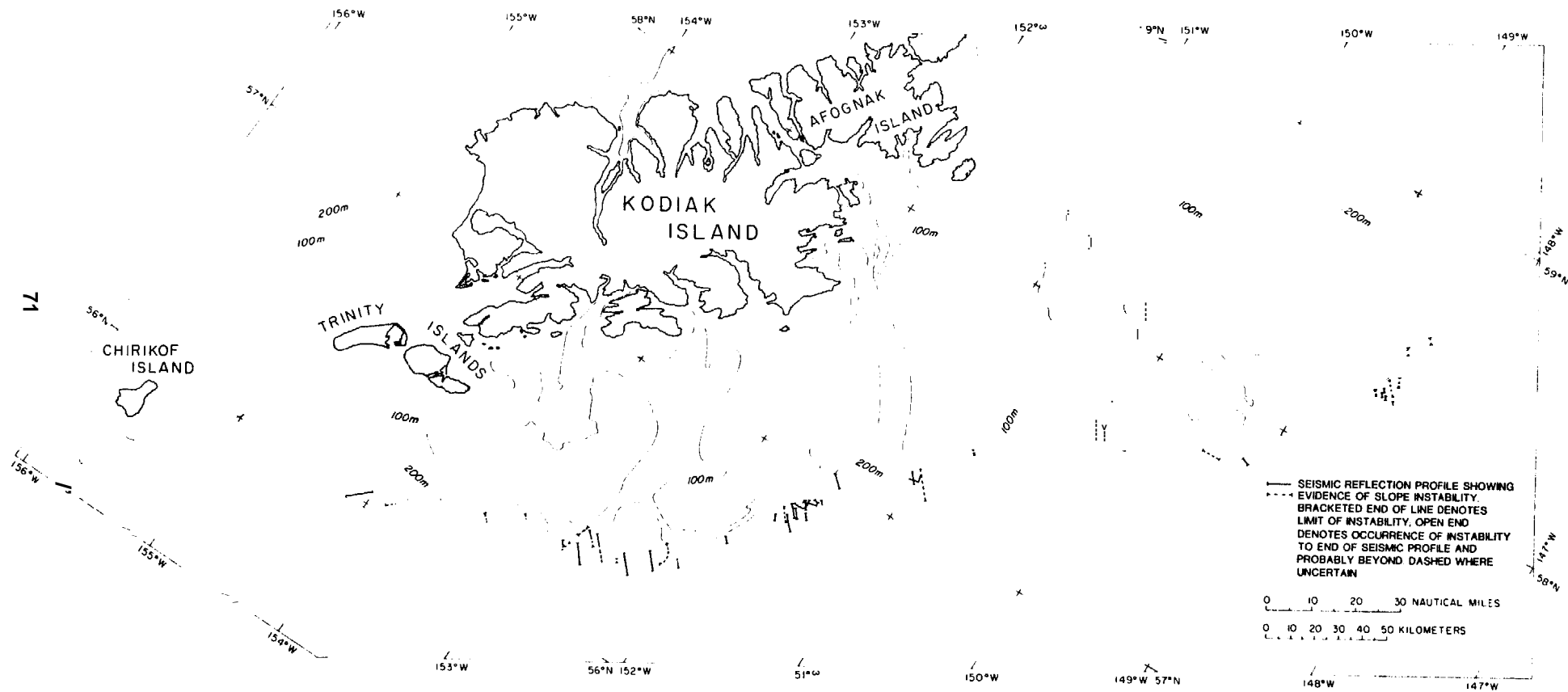


Fig. 33

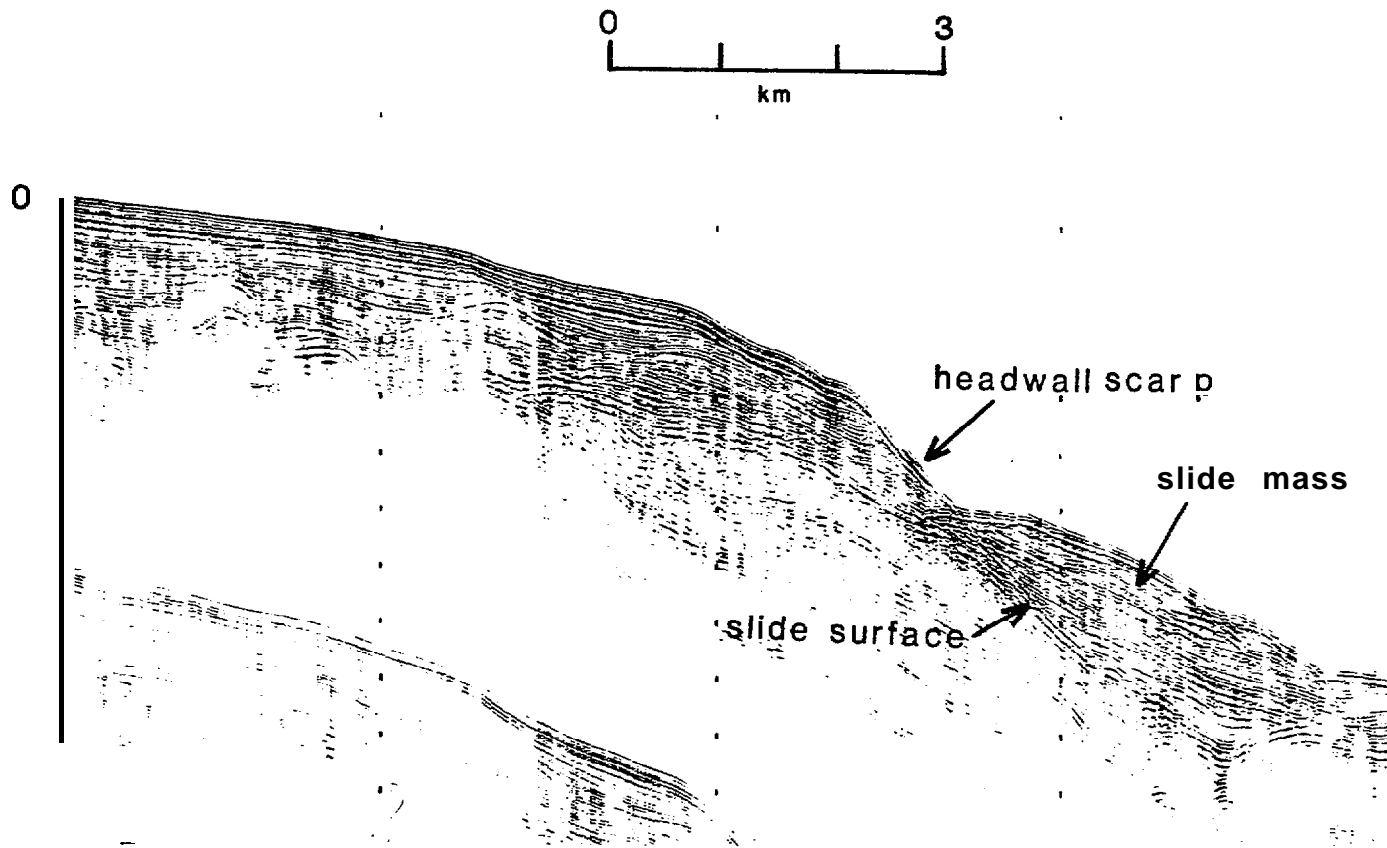


Fig. 34

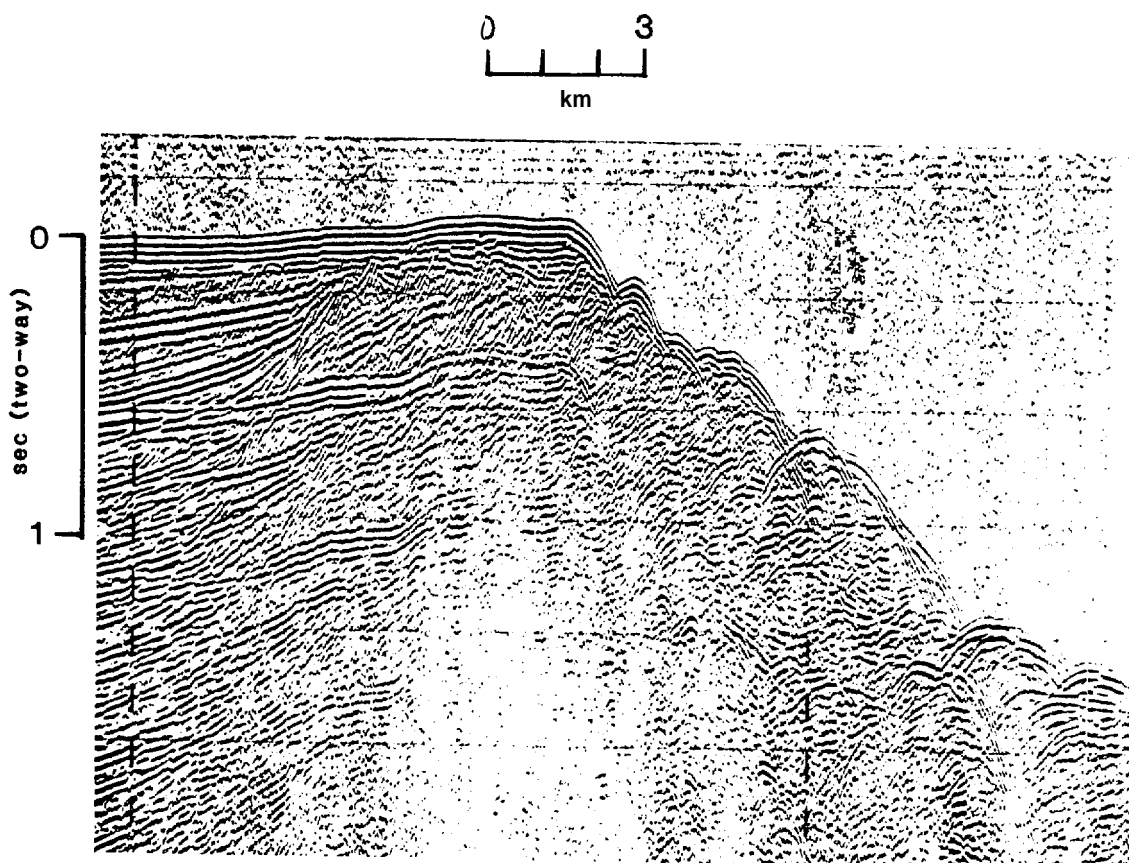


Fig. 35

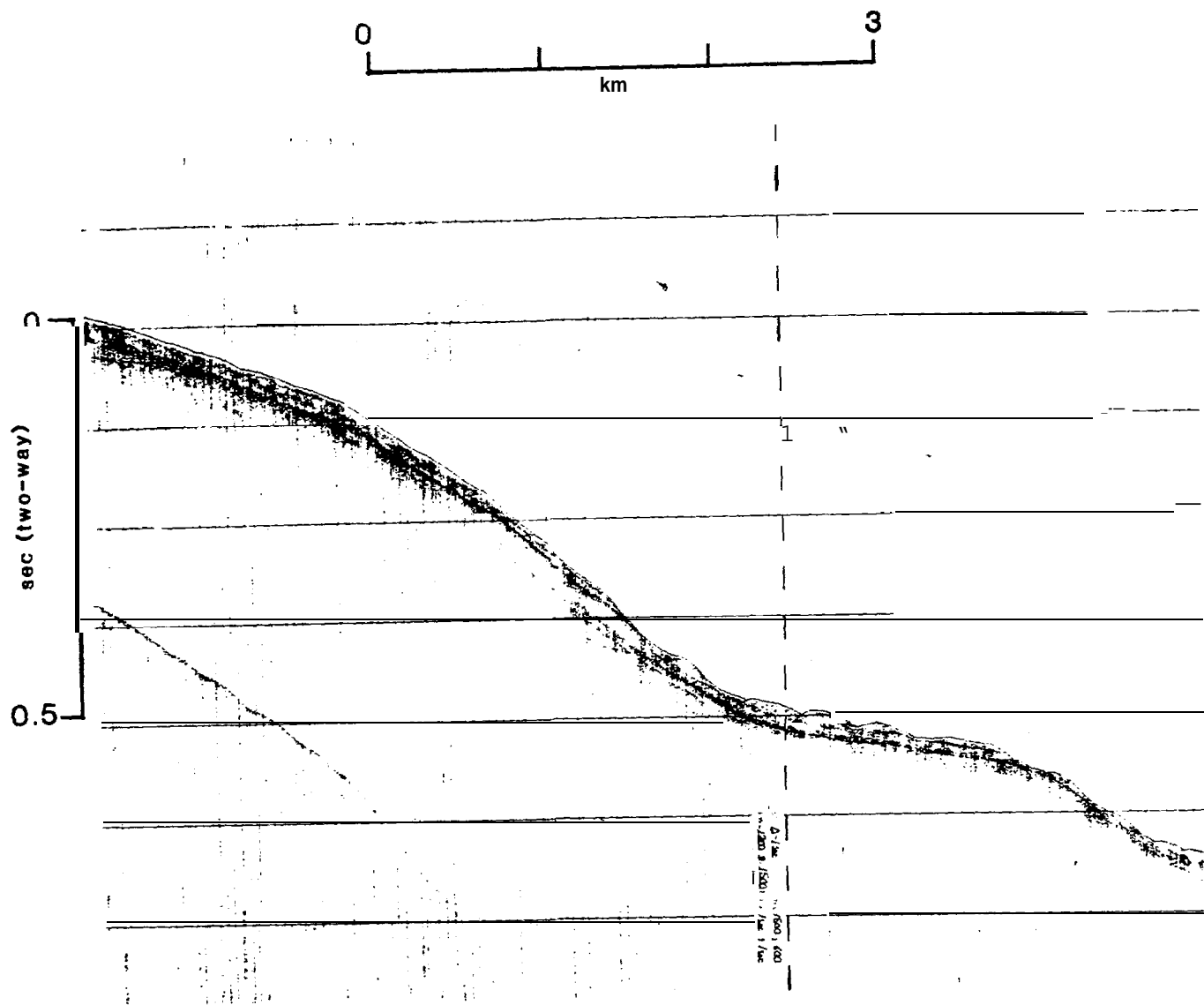
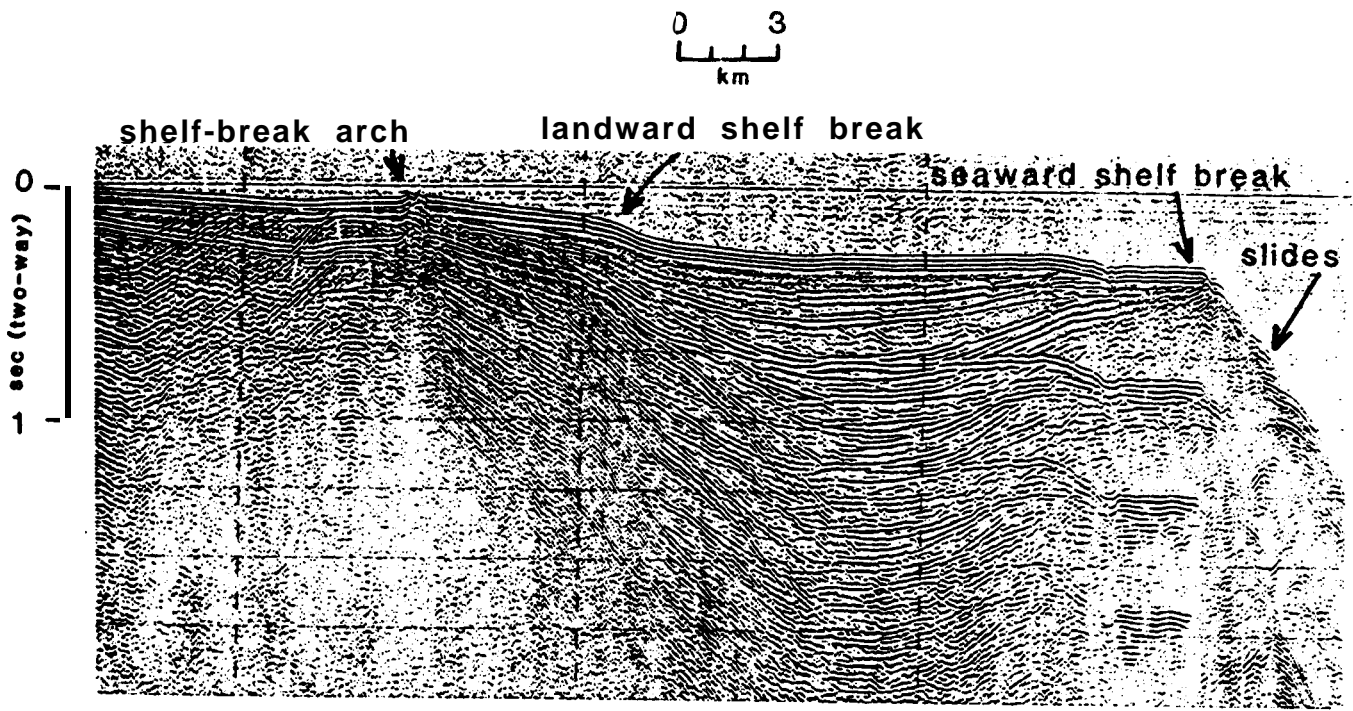


Fig. 36



a

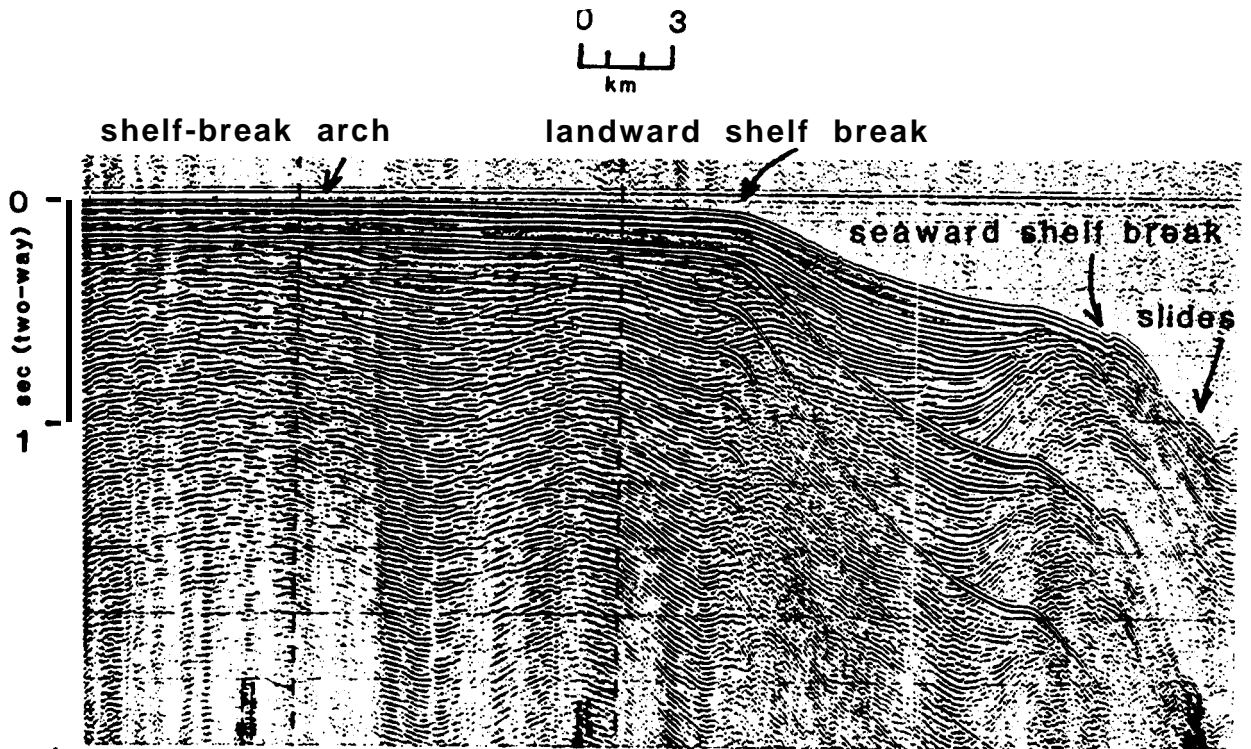


Fig. 57

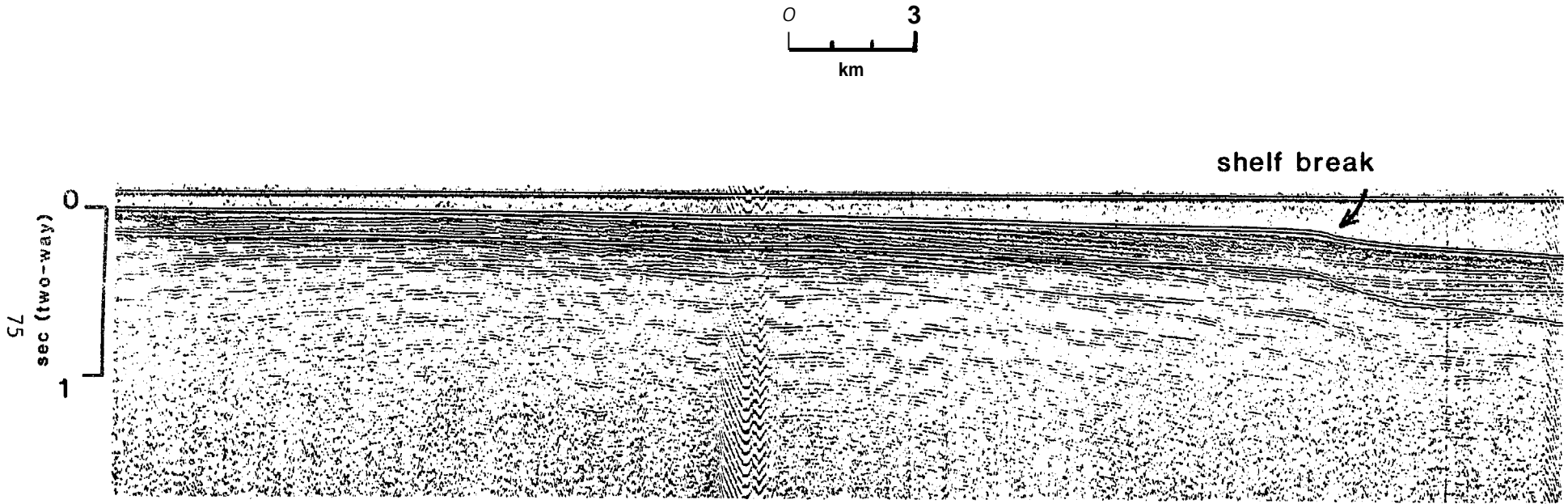


Fig. 38

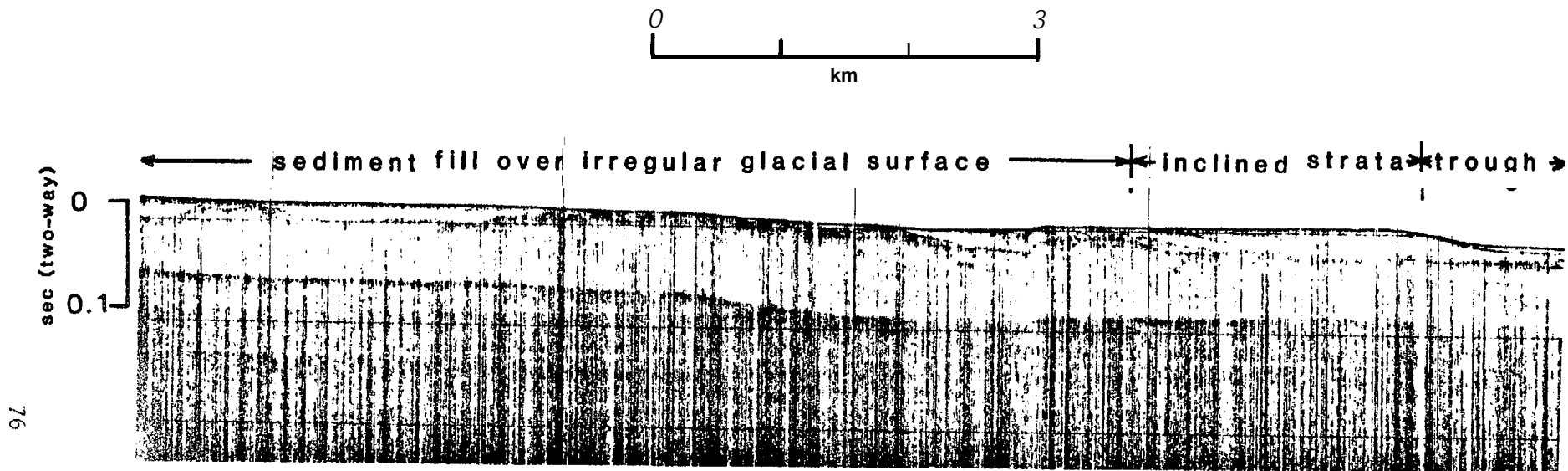


Fig. 39